Supplementary Information

Mitigating Future Respiratory Pandemics in Low-, Middle- and High-Income Countries: A Modelling Study of Health, Economic and Educational Losses

Patrick Doohan[1,*], Rob Johnson[1], Alessandra Løchen[1], Christian Morgenstern[1], David Haw[2], Alice Sabino[3], Edith Patouillard[4], Giovanni Forchini[1,5], and Katharina D. Hauck[1]

[1]MRC Centre for Global Infectious Disease Analysis, Jameel Institute, School of Public Health, Imperial College London, UK
[2]Department of Mathematical Sciences/Institute of Veterinary, Infection and Ecological Sciences, University of Liverpool
[3]Coalition for Epidemic Preparedness Innovations (CEPI), London, UK
[4]Department of Health Financing and Economics, World Health Organization, Geneva, Switzerland
[5]UBSE, Umeå Universitet, Umeå, Sweden
[*]Correspondence: patrick.doohan15@imperial.ac.uk

Contents

1 Background & Literature Review **2**

2 Model & Data **2**

2.1 Income-Group Archetypes . . . 3
2.2 Disease Epidemiology . . . 8
2.3 Mitigation Measures . . . 12
2.4 Closure Strategies . . . 26
2.5 Socioeconomic Loss . . . 33

3 Additional Figures **38**

4 Additional Tables **49**

5 Code & Future Work **62**

1 Background & Literature Review

The PubMed database was searched for studies that model the impacts of non-pharmaceutical interventions (NPIs) for mitigating hypothetical respiratory pandemics, using the search string model* AND ("future pandemic*" OR "pandemic influenza" OR "pandemic strain" OR "novel * outbreak*" OR "novel * pathogen*" OR "emerg* pathogen*") AND (strateg* OR mitigat* OR contain* OR intervention*), without language restriction and from database inception to 14th March 2025. The search yielded 46 original research studies, published between 2005 and 2024, and two secondary research studies: a systematic review of modelling studies of school closures[1] and a systematic review of modelling studies of combinations of mitigation measures[2]. The original research studies identified are very limited in scope: typically, influenza pandemics in high-income Anglosphere countries are considered, mitigated by fixed-duration NPIs that do not respond to the epidemic state, and the impacts quantified in terms of health losses alone. Only three studies identified are applied to low- or middle-income countries[3–5], only five studies consider diseases other than influenza[6–10] and only four quantify the economic losses of workplace closures in addition to the health impact[11–14], albeit in a simplistic manner that does not consider the underlying structure of the economy. No study was identified that considered any two of these three dimensions simultaneously, and no study was identified that quantified the long-term learning losses associated with school closures. Therefore, the pandemic planning research conducted to date is very narrow in focus and in the aftermath of the Covid-19 pandemic, there is a need for the health and socioeconomic assessments of NPIs for potential future pandemics across all country-income groups.

This modelling study quantifies and projects the joint health, economic and educational losses under alternative business- and school-closure mitigation strategies, with underlying NPIs and vaccination, for different respiratory pandemics and country-income groups. The closure strategies mimic those implemented during the Covid-19 pandemic and are fully responsive to the epidemic state for each simulation, and the model is parametrised by Covid-19 mitigation data. Here, a fully-integrated epidemiological-economic model is employed to project the socioeconomic losses of a given strategy, which captures the interdependence of disease transmission and economic activity, thus capitalising on recent developments in the field of economic epidemiology. Socioeconomic-loss-minimising strategies are identified for different diseases and country-income groups, considering the variability in underlying demographic, economic, mixing, and mitigation parameters. A cost-benefit analysis of switching between different closure strategies is performed. The study is a major update to the pandemic preparedness literature for the post-Covid era and provides insights into mitigating potential future pandemics, co-produced with global health policy partners. Furthermore, the model serves as a robust tool for the evaluation of the return-on-investment of pandemic prevention and preparedness measures considering the socioeconomic losses of pandemics beyond just health losses.

2 Model & Data

The model underlying the current study is daedalus, an integrated epidemiological-economic model that was originally developed in response to the Covid-19 pandemic to optimise economic sector closures in the UK[15], and subsequently employed to estimate the socioeconomic benefit of booster vaccinations in Indonesia[16] and deaths averted under various body-mass index distributions in Mexico[17]. The epidemiological component is a deterministic SEIR compartmental model with age and economic-sector heterogeneity, while the economic component is a deterministic partial-equilibrium aggregate production model with economic-sector heterogeneity. The component models are linked in a bi-directional manner, through economic-sector-dependent workplace transmission (impact of economy on epidemiology) and health-state-dependent labour supply (impact of epidemiology on economy). The mitigation measures considered include the full or partial differential closure of economic sectors (including education), home-working, distancing, case isolation, hospital capacity and vaccination, which may have combined health, economic and educational impacts. For example, economic sector closures reduce workplace transmission and health losses, but at the expense of reduced production and economic losses.

Here, the daedalus model is used to project the socioeconomic loss (see section 2.5) under various dynamic closure strategies (see section 2.4) imposed in conjunction with other mitigation measures (see section 2.3), for novel respiratory diseases (section 2.2) and country-income groups (section 2.1). The model is parametrised using income-group-specific demographic, economic and mixing data (see Figure S1), historic respiratory pandemic and pandemic-variant epidemiological data (see Table S1), and Covid-19 mitigation measure and closure data (see Figures S2 - S5 and Tables S3 - S2), which were assembled from numerous diverse sources and described in detail in the following sections. It must be emphasised that this is a projection study, not a model-fitting exercise. The objective is not to reconstruct historic outbreaks, but rather to investigate and compare the potential outcomes of hypothetical pandemics with realistic historically-inspired epidemiology, as a pandemic planning exercise. The code and data are available on GitHub[18].

2.1 Income-Group Archetypes

The analysis is stratified by country-income group, since there are fundamental differences in demography, mixing, economics and mitigation capability between low- and high-income countries, which will likely affect pandemic interventions and outcomes[19–21]. Three income-group 'archetypes' are considered, based on the World Bank classification[22], except for the low- and lower-middle-income countries which are combined due to lack of country-level data. Hence, the income-group archetypes and abbreviations are:

- LLMIC: low- and lower-middle-income countries
- UMIC: upper-middle-income countries
- HIC: high-income countries.

While it is technically feasible to stratify by country, this level of spatial resolution is problematic. It implies a degree of confidence in the underlying country-level data that is not well-suited to a projection study of this nature. Moreover, pandemic interventions and outcomes are influenced by numerous factors beyond those that can be adequately captured by a model, further limiting the appropriateness of such stratification.

Within each income-group archetype, 5000 'synthetic countries' are constructed by randomly sampling with replacement from the empirical distributions of the assembled country-level data for that income group, specifically the demographic, economic and mixing data. By generating a range of plausible synthetic countries, this approach accounts for uncertainty in the underlying data and allows for variability in model output. The generating process is described in more detail in subsequent paragraphs.

Demography

The total population of each synthetic country is fixed at 50 million, but the analysis is independent of population size given the deterministic nature of the model. The proportion of the total population in five-year age-bands is drawn from the empirical distribution for each country-income-group archetype (see Figure S1), obtained from the United Nations[23], and the resulting population by five-year age-band is denoted $\tilde{N}_a$. Remaining life-expectancy by five-year age-band, denoted $\tilde{l}_a$, is also drawn, with data sourced from the World Health Organization (WHO)[24].

However, the daedalus model employs a coarser disaggregation of the population into four age-groups:

- preschool-age: 0-4 years
- school-age: 5-19 years
- working-age: 20-64 years
- retired-age: 65+ years,

and so $\tilde{N}_a$ is aggregated into $\hat{N}_g$, where the index g represents the model age-groups listed above.

Economy

The economy of each synthetic country is disaggregated into 45 economic sectors, based on the 4^{th} revision of the International Standard Industrial Classification of All Economic Activities[25], which are listed in Table S3. The workforce by sector is conditional on the working-age population: the proportion of the working-age group working in each economic sector and not working at all is drawn from the empirical distribution for each country-income-group archetype (see Figure S1), estimated by dividing workforce data obtained from the Organisation for Economic Co-operation and Development (OECD)[26] and the International Labour Organization (ILO)[27] by the aforementioned working-age population data, and the resulting workforce by sector is denoted N_j for $j \in \{1, ..., 45\}$. Values of j exceeding 45 represent the non-working model age-groups (preschool-age, school-age, *non-working* working-age, retired-age), and so N_j denotes the population by economic sector and non-working age-group in general (henceforth termed model strata), such that:

$$\sum_{j=1}^{49} N_j = \sum_{g=1}^{4} \hat{N}_g = \sum_{a=1}^{21} \tilde{N}_a = 50,000,000.$$

It is assumed that the workforce by sector encompasses those in both the formal and informal sectors of the economy.

Annual gross value added (GVA) per worker by sector (a measure of worker productivity), denoted y_j, is also drawn from the empirical distribution estimated by dividing GVA data obtained from OECD input-output tables[28] by the aforementioned workforce data. Economic output is then measured in terms of Gross Domestic Product (GDP) in U.S. dollars ($) using a production approach, with linear production function

$$Y_0 = \sum_{1}^{45} y_j N_j,$$

where Y_0 is total annual pre-pandemic GDP. The economic model is stylised: neither sectoral interdependencies nor consumption are modelled, it is assumed that the goods/services market clears, and international trade is not modelled explicitly.

Mixing

Population mixing refers to the contact patterns between different population groups that facilitate disease transmission, a proportion of which are associated with economic activity. Contact patterns are encoded in contact matrices, which specify the mean number of contacts per day within and between each group in the population. Here, the total contact matrix of each synthetic country is denoted M, where element $M_{j,j'}$ represents the contacts experienced by model stratum j (economic sector or non-working age-group) from model stratum j'. Following a similar approach to the original daedalus model[15], the total contact matrix M is decomposed into community (A), worker-to-worker (B) and worker-to-consumer (C) contact matrices, where contact matrices B and C encode sector-specific workplace mixing heterogeneity, based on data synthesised from a French contact survey from 2012[29] mapped to the 45 economic sectors considered here. The community contact matrix A is further decomposed into household ($A^{(L)}$), other-location ($A^{(H)}$) and school ($A^{(S)}$) contact matrices, such that the total contact matrix at time t can be written as a sum across different locations:

$$M(t) = A^{(L)} + A^{(H)}(t) + A^{(S)}(t) + B(t) + C(t).$$

The time-dependence in this equation represents dynamic mitigation by economic sector closures (including education) and home-working, the specifics of which are described in detail below (see section 2.4). The extent to which sector j is open at time t is denoted $x_j(t)$, and the proportion of workers home-working denoted $q_j(t)$, therefore the total contact matrix can also be written $M(t) = M(x_j(t), q_j(t))$. The manner in which these mitigation measures reduce contact rates in different locations (if at all) is detailed in the following paragraphs.

The household, other-location and school contact matrices are drawn respectively from empirical distributions of 'home', 'other-location' and 'school' synthetic contact matrices for each country-income-group archetype, collated from work by Prem and colleagues[30,31], where the original 16-by-16 matrices for five-year age-bands are aggregated into four-by-four matrices for the model age-groups listed above. These are subsequently broadcasted to the 49 model strata, as described below. The worker-to-worker and consumer-to-worker contact matrices have fixed structure as specified in the original daedalus model, but these are rescaled such that the combined working-age-population-weighted-average workplace contact rate matches the value drawn from the empirical distribution calculated from the 'work' synthetic contact matrices (see Figure S1).

The household contact matrix $A^{(L)}$ represents intra- and inter-household contacts. Let $\hat{A}^{(L)}_{g,g'}$ denote the four-by-four matrix for model age-groups drawn from the empirical distribution of 'home' synthetic contact matrices. By broadcasting the four-by-four matrix in proportion to population by stratum, the household contact matrix is defined as

$$A^{(L)}_{j,j'} = \hat{A}^{(L)}_{g(j),g'(j')} \frac{N_{j'}}{\hat{N}_{g'(j')}},$$

where $N_{j'}$ is the population of stratum j' (economic sector or non-working age-group) and $\hat{N}_{g(j')}$ is the population of the model age-group g' that stratum j' belongs to. Household contacts are independent of economic sector closures and home-working (hence no t-dependence in the total contact matrix equation above).

The other-location contact matrix $A^{(H)}$ represents contacts in locations other than households, schools and workplaces - such as outdoors, modes of transport, hospitality venues and retail outlets. Let $\hat{A}^{(H)}_{g,g'}$ denote the four-by-four matrix for model age-groups drawn from the empirical distribution of 'other-location' synthetic contact matrices. As before, this four-by-four matrix is broadcasted to a 49-by-49 matrix in proportion to population by stratum. However, other-location contacts depend on the extent to which certain economic sectors are open - the hospitality sectors in particular. It is assumed that 45% of other-location contacts are made in hospitality venues, based on the proportion of 'leisure' contacts among 'other-location' contacts pooled across the countries of the POLYMOD study[32]. Therefore, the other-location contact matrix is defined as

$$A^{(H)}_{j,j'}(t) = \hat{A}^{(H)}_{g(j),g'(j')} \frac{N_{j'}}{\hat{N}_{g'(j')}} \left(0.55 + 0.45(x_{hosp}(t))^2\right),$$

where $x_{hosp}(t) = \sum_j x_j(t) N_j / \sum_j N_j$ for $j = 32, 43, 44$ (see Table 2.4) is the workforce-weighted-average extent to which the hospitality sectors are open. The scaling is quadratic in $x_{hosp}(t)$. Other-location contacts are independent of home-working.

The school contact matrix $A^{(S)}$ represents contacts in schools. Let $\hat{A}^{(S)}_{g,g'}$ denote the four-by-four matrix for model age-groups drawn from the empirical distribution of 'school' synthetic contact matrices. As before, this four-by-four matrix is broadcasted to a 49-by-49 matrix in proportion to population by stratum. School contacts depend on the extent to which the education sector is open, hence the school contact matrix is defined as

$$A^{(S)}_{j,j'}(t) = \hat{A}^{(S)}_{g(j),g'(j')} \frac{N_{j'}}{\hat{N}_{g'(j')}} \left(x_{edu}(t)\right)^{\mathbb{1}\{g(j),g'(j')\leq 2\}},$$

where $x_{edu}(t) = x_{41}(t)$ (see Table 2.4) is the extent to which the education sector is open and $\mathbb{1}$ is the indicator function, i.e. only intra- and inter- preschool- and school-age contacts are reduced. The scaling is quadratic in $x_{edu}(t)$. School contacts are independent of home-working.

The workplace contact matrices B and C represent worker-to-worker and consumer-to-worker contacts in workplaces respectively. In the original daedalus model[15], B is a diagonal matrix with diagonal elements b_j (pre-pandemic) and C is a square matrix with row-sums c_j (pre-pandemic) that are split column-wise in proportion to population by stratum, where b_j and c_j are the sector-specific values mapped from the French contact survey[29]. This implies that the combined working-age-population-weighted-average workplace contact rate is $w^{old} = \sum_{j:g(j)=3} (b_j + c_j) N_j / N_{g(j)}$, where $b_j = c_j = 0$ for $j > 45$, i.e. workplace contacts for non-working age-groups are zero. Here, the structure of the workplace contact matrices is preserved from the original daedalus model but the magnitude of workplace contacts is allowed to vary. Let w^{new} denote the workplace contact rate drawn from the empirical distribution calculated from 'work' synthetic contact matrices. Given that workplace contacts must also depend on the extent to which economics sectors are open and the proportion of workers home-working, the workplace contact matrices are defined as

$$\begin{aligned} B_{j,j}(t) &= b_j \frac{w^{new}}{w^{old}} \left(x_j(t)(1 - q_j(t))\right)^2 \\ C_{j,j'}(t) &= c_j \frac{N_{j'}}{\sum_{j'} N_{j'}} \frac{w^{new}}{w^{old}} x_j(t) \left(1 - q_j(t)\right), \end{aligned}$$

where the scaling in B is quadratic in $x_j(t)$ (worker-to-worker contacts) and $q_j(t)$ but the scaling in C is linear (consumer-to-worker contacts). The economic-sector heterogeneity of workplace transmission is encoded in b_j and c_j.

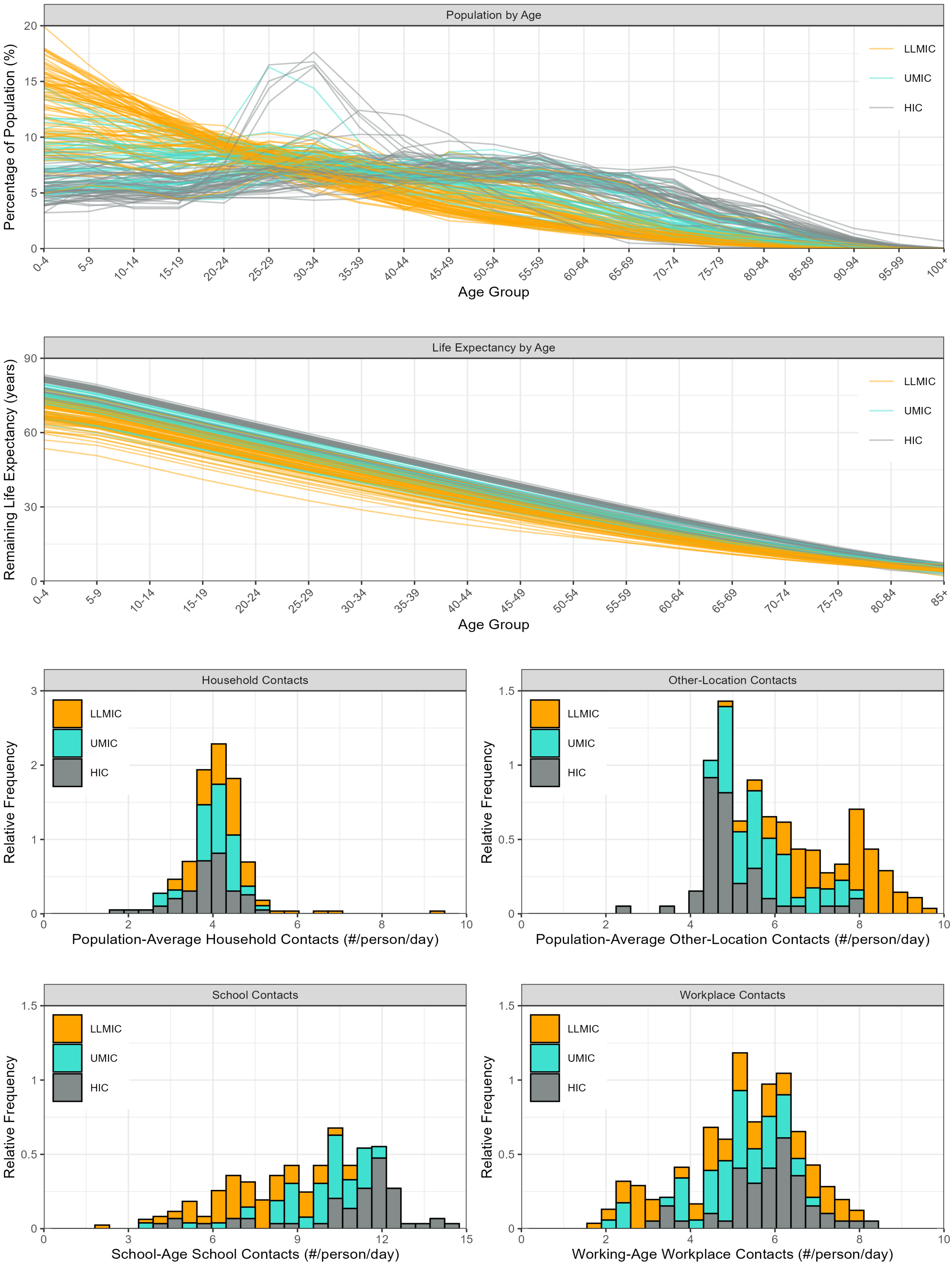

Figure S1: Continued on next page ...

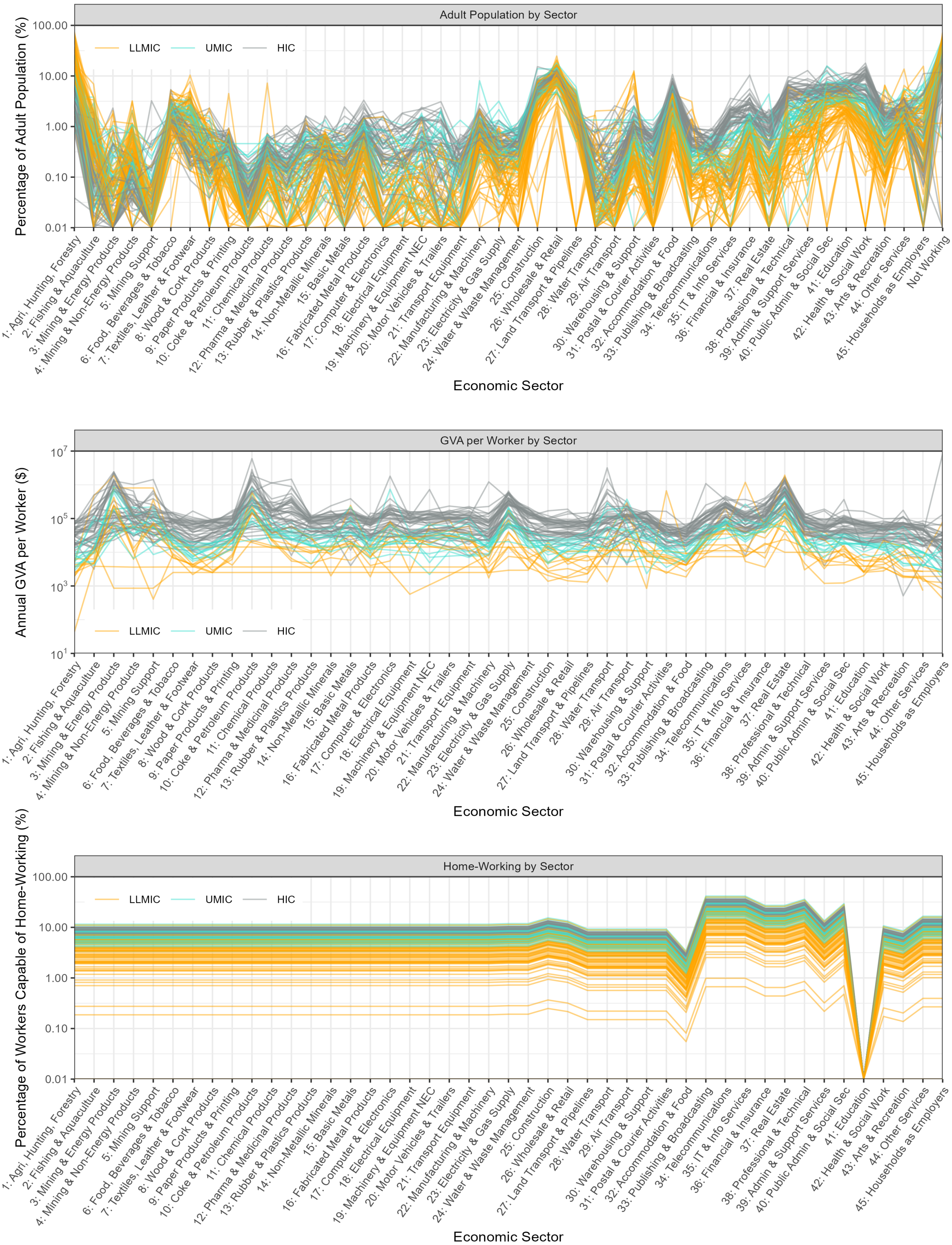

Figure S1: Demographic, mixing and economic data by country-income-group archetype (colours).

2.2 Disease Epidemiology

The original daedalus model and its subsequent applications[15–17] were developed in response to the Covid-19 pandemic, employing a compartmental epidemiological model with heterogeneity of age and economic-sector, and SEIR natural history. Here, the epidemiological component is generalised to model respiratory diseases with distinct epidemiological characteristics, defined in terms of transmissibility, delays and severity. Six diseases are considered, inspired by historic pandemics and pandemic variants caused by the Alphainfluenzavirus and Betacoronavirus viral genera:

- Influenza-2009-X
- Influenza-1957-X
- Influenza-1918-X
- Covid-Omicron-X
- Covid-Delta-X
- Covid-Wildtype-X.

The influenza diseases correspond to the pandemics of 2009 ('Swine flu'), 1957 ('Asian flu') and 1918 ('Spanish flu') respectively. The coronavirus diseases correspond to the Omicron and Delta variants of Covid-19, and the pre-Alpha-variant Covid-19 wild type. This set of diseases is epidemiologically diverse (see Table S1); with low-transmissibility low-severity Influenza-2009-X, low-transmissibility high-severity Influenza-1918-X, high-transmissibility low-severity Covid-Omicron-X, and high-transmissibility and high-severity Covid-Delta-X - and Influenza-1957-X and Covid-Wildtype-X in between. The transmission timescales also differ between the influenza and the coronavirus diseases, with the latter exhibiting longer generation times and hospital length of stay in general. Mimicking historic pandemics and pandemic variants ensures plausibility, given that the epidemiological parameter values have been realised in the past. However, it must be emphasised that the aim of this study is not to reconstruct historic outbreaks - this would require a much more tailored approach, the acquisition of appropriate epidemiological time series data (e.g., hospital admissions, deaths) and fitting the epidemiological model to these data - rather, each disease is considered in the hypothetical case. Furthermore, each disease is considered to be novel - it is assumed that there is no pre-existing natural- or vaccine-induced immunity, which would inhibit disease transmission and/or severity. For both of the above reasons, the suffix -X is appended to each disease name, in the spirit of WHO terminology[33].

In the epidemiological model, transmission and disease progression are described by the distribution of the population across different health states and the evolution of this distribution over time. The health states represent the natural history of disease and mitigation measures imposed in response to the outbreak: at time t, the population by stratum N_j is decomposed into susceptible $S_{j,v}$, exposed $E_{j,v}$, asymptomatic infectious $I^a_{j,v}$, symptomatic infectious $I^s_{j,v}$, recovered $R_{j,v}$, hospitalised $H_{j,v}$ and dead $D_{j,v}$ states, and following the imposition of mitigation measures (see section 2.3), isolating asymptomatic infectious $I^{ai}_{j,v}$, isolating symptomatic infectious $I^{si}_{j,v}$ and seroconverting (due to vaccination) $S^{c_u}_{j,v}$ states are included. The subscript v denotes vaccination status ($v = 0$ for unvaccinated and $v = 1$ for vaccinated), which duplicates the aforementioned health states, and vaccination status transitions occur due to seroconversion and waning of vaccine-induced immunity to infection. The system of ordinary differential equations (ODEs) describing the evolution in time of the distribution of the population across health states is

$$
\begin{aligned}
\frac{dS_{j,v}}{dt} &= \sum_{u=0}^{v-1} k^{12} S^{c_v}_{j,u} + \sum_{u=v+1}^{1} k^{13,r_v}_{u} S_{j,u} - \left(k^{1}_{j,v}(t) + \sum_{u=v+1}^{1} k^{11,c_u}_{j,v}(t) + \sum_{u=0}^{v-1} k^{13,r_u}_{v} \right) S_{j,v} \\
\frac{dS^{c_u}_{j,v}}{dt} &= k^{11,c_u}_{j,v}(t) S_{j,v} - \left(k^{1}_{j,v}(t) + k^{12} \right) S^{c_u}_{j,v} \\
\frac{dE_{j,v}}{dt} &= k^{1}_{j,v}(t) \left(S_{j,v} + \sum_{u=v+1}^{1} S^{c_u}_{j,v} \right) - \left(k^{2}(t) + k^{3}(t) + k^{4}(t) + k^{5}(t) \right) E_{j,v} \\
\frac{dI^{a}_{j,v}}{dt} &= k^{2}(t) E_{j,v} - k^{6} I^{a}_{j,v} \\
\frac{dI^{s}_{j,v}}{dt} &= k^{3}(t) E_{j,v} - \left(k^{7}_{j,v}(t) + k^{8}_{j,v}(t) \right) I^{s}_{j,v} \\
\frac{dI^{ai}_{j,v}}{dt} &= k^{4}(t) E_{j,v} - k^{6} I^{ai}_{j,v} \\
\frac{dI^{si}_{j,v}}{dt} &= k^{5}(t) E_{j,v} - \left(k^{7}_{j,v}(t) + k^{8}_{j,v}(t) \right) I^{si}_{j,v} \\
\frac{dR_{j,v}}{dt} &= k^{6} \left(I^{a}_{j,v} + I^{ai}_{j,v} \right) + k^{8}_{j,v}(t) \left(I^{s}_{j,v} + I^{si}_{j,v} \right) + k^{10}_{j}(t) H_{j,v} \\
\frac{dH_{j,v}}{dt} &= k^{7}_{j,v}(t) \left(I^{s}_{j,v} + I^{si}_{j,v} \right) - \left(k^{9}_{j}(t) + k^{10}_{j}(t) \right) H_{j,v} \\
\frac{dD_{j,v}}{dt} &= k^{9}_{j}(t) H_{j,v},
\end{aligned}
$$

where the set of health states and the flow structure are independent of disease. In particular, it is assumed that all asymptomatic infectious individuals recover and that death only occurs following symptomatic infection. Furthermore, viral evolution is not modelled and it is assumed that there is no waning of infection-induced immunity or vaccine-induced immunity to severe disease, at least over the timescales considered, but there is waning of vaccine-induced immunity to infection (see section 2.3).

The epidemiological dynamics are determined by the transition rates between health states, denoted k^n for $n \in \{1, ..., 13\}$ above, which are disease-dependent. The epidemiological parameters in Table S1 specify onward infectiousness (transmissibility), the time spent in each health state (delays) and the proportional split between complementary health states (severity), which are independent of country-income-group archetype, i.e. income-group-dependent population health or healthcare quality (below hospital capacity - see section 2.3) are not considered. However, synthetic country demography, economics and mixing introduces localised effects: transmission is a function of contacts between different economic sectors and non-working age-groups, and severity is a function of age. Therefore, for each disease, there is a local basic reproduction number and local population-average IHR and IFR in each synthetic country. Furthermore, almost all transition rates depend on mitigation measures (see section 2.3), and together these factors determine the overall intensity of an epidemic realisation. The dependence (or independence) of different transition rates on model stratum j (economic sector or non-working age-group), vaccination status u, v and time t are indicated in the system of ODEs above, and these are defined in full in the following section.

Parameter	Symbol	Influenza-2009-X	Influenza-1957-X	Influenza-1918-X	Covid-Omicron-X	Covid-Delta-X	Covid-Wildtype-X
Transmissibility							
Mean Basic Reproduction Number	$\bar{R}_0$	1.58 [34]	1.80 [35]	1.80 [36]	5.94 Calculated [37]	5.08 [38]	2.87 [39]
Transmission Probability from Symptomatic Contact	β	0.0426 Calculated [34]	0.0485 Calculated [35]	0.0674 Calculated [40]	0.1201 Calculated [37]	0.1026 Calculated [38]	0.0580 Calculated [39]
Relative Risk of Transmission from Asymptomatic Contact	ϵ	0.58 Assumed [41]	0.58 Assumed [41]	0.58 Assumed [41]	0.58 Assumed [41]	0.58 Assumed [41]	0.58 [41]
Delays							
Latent Period	$T^{E:I}$	1.1 [42]	1.1 Assumed [42]	1.1 Assumed [42]	4.0 Assumed [43]	4.0 [43]	4.6 [44]
Infectious Period for Asymptomatic Infection	$T^{I^a:R}$	2.5 [42]	2.5 Assumed [42]	2.5 Assumed [42]	2.1 Assumed [44]	2.1 Assumed [44]	2.1 [44]
Infectious Period for Symptomatic Infection	$T^{I^s:R}$	2.5 [42]	2.5 Assumed [42]	2.5 Assumed [42]	4.0 Assumed [44]	4.0 Assumed [44]	4.0 [44]
Time from Infectiousness to Hospital-Admission	$T^{I^s:H}$	2.5 [42]	2.5 Assumed [42]	2.5 Assumed [42]	4.0 Assumed [44]	4.0 Assumed [44]	4.0 [44]
Time from Hospital-Admission to Recovery	$T^{H:R}$	5.0 [45]	5.0 Assumed [45]	5.0 Assumed [45]	5.5 [46]	7.6 [46]	12.0 [47]
Time from Hospital-Admission to Death	$T^{H:D}$	5.0 [45]	5.0 Assumed [45]	5.0 Assumed [45]	5.5 [46]	7.6 [46]	12.0 [47]
Severity							
Symptomatic Infection Ratio	p^{I^s}	0.67 [48]	0.67 [48]	0.67 [48]	0.59 Assumed [49]	0.59 Assumed [49]	0.59 [49]
Infection Hospitalisation Ratio (IHR)	$\tilde{p}^{IHR}$						
0-4 years		0.0047	0.0009	0.1222	0.0000	0.0000	0.0000
5-9 years		0.0018	0.0009	0.0213	0.0000	0.0000	0.0000
10-14 years		0.0018	0.0009	0.0256	0.0006	0.0008	0.0004
15-19 years		0.0018	0.0009	0.0526	0.0006	0.0008	0.0004
20-24 years		0.0018	0.0009	0.0910	0.0083	0.0192	0.0104
25-29 years		0.0038	0.0009	0.1564	0.0083	0.0192	0.0104
30-34 years		0.0038	0.0009	0.1322	0.0197	0.0635	0.0343
35-39 years		0.0038	0.0009	0.1180	0.0197	0.0635	0.0343
40-44 years		0.0038	0.0009	0.0881	0.0157	0.0786	0.0425
45-49 years		0.0038	0.0226	0.0640	0.0157	0.0786	0.0425
50-54 years		0.0071	0.0226	0.0881	0.0211	0.1510	0.0816
55-59 years		0.0071	0.0226	0.0626	0.0211	0.1510	0.0816
60-64 years		0.0071	0.0226	0.1649	0.0306	0.2183	0.1180
65-69 years		0.0103	0.1806	0.2218	0.0306	0.2183	0.1180
70-74 years		0.0103	0.1806	0.2644	0.0614	0.3071	0.1660
75-79 years		0.0103	0.1806	0.2644	0.0614	0.3071	0.1660
80+ years		0.0103	0.1806	0.2644	0.1123	0.3404	0.1840
		Calculated [50]	Calculated [51]	Calculated [51]	Calculated [52]	Calculated [53]	[54]
Infection Fatality Ratio (IFR)	$\tilde{p}^{IFR}$						
0-4 years		0.0002	0.0001	0.0153	0.0000	0.0000	0.0000
5-9 years		0.0001	0.0001	0.0027	0.0000	0.0000	0.0000
10-14 years		0.0001	0.0001	0.0032	0.0001	0.0001	0.0001
15-19 years		0.0001	0.0001	0.0066	0.0001	0.0001	0.0001
20-24 years		0.0001	0.0001	0.0114	0.0002	0.0006	0.0003
25-29 years		0.0002	0.0001	0.0195	0.0002	0.0006	0.0003
30-34 years		0.0002	0.0001	0.0165	0.0005	0.0016	0.0008
35-39 years		0.0002	0.0001	0.0148	0.0005	0.0016	0.0008
40-44 years		0.0002	0.0001	0.0110	0.0006	0.0030	0.0016
45-49 years		0.0004	0.0017	0.0080	0.0006	0.0030	0.0016
50-54 years		0.0004	0.0017	0.0110	0.0015	0.0110	0.0060
55-59 years		0.0004	0.0017	0.0078	0.0015	0.0110	0.0060
60-64 years		0.0004	0.0017	0.0206	0.0050	0.0357	0.0193
65-69 years		0.0066	0.0134	0.0277	0.0050	0.0357	0.0193
70-74 years		0.0066	0.0134	0.0331	0.0158	0.0792	0.0428
75-79 years		0.0066	0.0134	0.0331	0.0158	0.0792	0.0428
80+ years		0.0066	0.0134	0.0331	0.0476	0.1443	0.0780
		Calculated [55]	Calculated [56]	Calculated [57]	Calculated [52]	Calculated [53]	[54]

Table S1: Epidemiological parameter values of the six diseases considered. Transmissibility parameters (excluding reproduction numbers) are reported as proportions, delay parameters in days and severity parameters as proportions. For each disease, the transmission probability from symptomatic contacts β is fixed and this defines a local basic reproduction number R_0 in each synthetic country, which is calculated using the next-generation method[58,59]. The values of β are calculated such that the mean reproduction number across all synthetic countries in all country-income-group archetypes $\bar{R}_0$ matches the prescribed value for each disease. In the absence of parameter estimates for a historic pandemic or pandemic variant, values were assumed based on similar diseases. Case hospitalisation and fatality ratios reported in the literature were interpreted to pertain to symptomatic infections only, and infection hospitalisation and fatality ratios $\tilde{p}^{IHR}$ and $\tilde{p}^{IFR}$ were calculated by multiplying by the associated symptomatic infection ratio p^{I^s}.

2.3 Mitigation Measures

In response to a disease outbreak in a synthetic country, four different mitigation measures are imposed: distancing, case isolation, hospital capacity and vaccination. The mitigation measures are modelled in an identical manner for each country-income-group archetype but the parametrisation is income-group-dependent, with parameters drawn from distributions fitted to Covid-19 data. To allow for interdependencies between mitigation parameters within each income group, a Gaussian copula approach is employed, where marginal distributions are fitted to parameter data separately (see Figure S2). Using the fitted marginal distributions, the observed data are transformed to z-scores and correlation coefficients are estimated for each pair of parameters in turn (see Figure S3). The mitigation parameters are most-strongly correlated in LLMICs, which encompasses countries with a wide range of response capabilities, where there are strong and significant associations between the testing rate and (earlier) vaccination administration start-time, administration rate and coverage, and between the vaccination administration rate and coverage. The significance of the association between the vaccination administration rate and coverage extends to UMICs and HICs, but with slightly and moderately weaker correlation coefficients, respectively. During simulations, samples are drawn from a multivariate normal distribution with income-group-specific correlation matrix, then independently transformed to the unit interval using the standard-normal cumulative density function and mapped back through the inverse marginal cumulative distribution functions to obtain parameter realisations. The implementation of mitigation measures over time for a sample of synthetic countries in each income-group archetype are shown in Figure S4 for illustrative purposes. Furthermore, the effectiveness of each mitigation measure is a function of time-dependent epidemiological output variables and thus endogenous to the local outbreak, as discussed below. Mitigation measures also encompass both government mandates and behavioural changes independent of mandates, such as adherence/compliance, although it is very difficult to disentangle the relative contributions of each factor in the Covid-19 data - however, this is not the objective of the current study. Each mitigation measure is discussed in detail below.

Distancing

Distancing as a mitigation measure refers to the physical and social distancing non-pharmaceutical interventions (NPIs) that reduce transmission (either the number of contacts or the probability of transmission given infectious contact), driven by the combined effects of government mandates and human behaviour (which are not disentangled), but do not incur an economic loss from a societal perspective. Examples include mask-wearing, personal hygiene, social bubbles and limits to social gatherings, and exclude case isolation, economic closures, school closures and home-working, each of which are modelled separately (see subsequent paragraphs and section 2.4). Distancing is modelled as a time-dependent multiplier within the force-of-infection term, denoted $k^1_{j,v}(t)$ in the system of ODEs above, which dampens transmission independent of location. Specifically, the force-of-infection term is written as

$$k^1_{j,v}(t) = \eta^E_v \rho(t) \beta \sum_{j'} M_{j,j'}(t) I_{j'}(t)/N_{j'},$$

where $M(t)$ is the time-dependent total contact matrix (see section 2.1), $I_{j'}(t)/N_{j'}$ is disease prevalence adjusted for infectiousness, β is the disease-dependent transmission probability given symptomatic contact (see Table S1), $\rho(t)$ is the distancing transmission multiplier and η^E_v is the relative risk of infection given vaccination status v (see subsequent paragraphs). The numerator of the disease prevalence term is $I_{j'}(t) = \sum_{v'} \eta^I_{v'} \left(\epsilon I^a_{j',v'}(t) + I^s_{j',v'}(t) + \epsilon \zeta^a(t) I^{ai}_{j',v'}(t) + \zeta^s_{j,v}(t) I^{si}_{j',v'}(t)\right)$, where ϵ is the relative risk of transmission given asymptomatic contact (see Table S1), $\zeta^a(t)$ and $\zeta^s_{j,v}(t)$ are the relative risk of transmission given isolating asymptomatic and symptomatic contacts respectively (see subsequent paragraphs), and $\eta^I_{v'}$ is the relative risk of transmission given vaccination status v (see subsequent paragraphs).

The distancing transmission multiplier is modelled using a logistic function of the form

$$\rho(t) = \left(\frac{1}{1 + \exp(c^0 + c^{death} \log_{10}(D^{new}(t)) - c^{time}(t - T^{res}))}\right)^{\mathbb{1}_{\{t \geq T^{res}\}}},$$

where T^{res} is the response time when distancing takes effect, c^0 is the intercept coefficient that controls the overall reduction in transmission independent of time, c^{death} is the death-sensitivity coefficient that controls the reduction in transmission as the number of daily deaths per 100k population $D^{new}(t) = \sum_{j,v} k^9_j(t) H_{j,v}(t)/(\sum_j N_j/10^5)$ increases and c^{time} is the time-decay coefficient that controls the speed at which transmission returns to pre-pandemic levels over time. This functional form was selected based on Covid-19 mobility data[60], which is used as a proxy for distancing: specifically, the percentage reduction in mobility averaged across retail and recreation, grocery and pharmacy, and transit stations is mapped linearly to the transmission multiplier on the unit interval, and this broadly decreases during Covid-19 waves due to infection avoidance and increases over time due to factors such as the relaxation of NPIs, reduced adherence to interventions and pandemic fatigue. Here, it is assumed that death is the epidemiological driver of the reduction in transmission, since this best generalises beyond Covid-19 to diseases with variable transmissibility and severity profiles. Therefore, distancing is fully endogenous to the local outbreak.

Data for the transmission multiplier parameters were generated on a country-by-country basis as follows. The response time T^{res} is defined to be the time delay from 1^{st} January 2020 until the day the Blavatnik stringency index[61] reaches a value of 20%, normalised by the (fixed) doubling time of Covid-19[62]. Without normalisation, the range of response times observed for Covid-19 may be entirely inappropriate for diseases with very different characteristics, and so the doubling time is used here as a scaling factor. The intercept coefficient c^0, the death-sensitivity coefficient c^{death} and the time-decay coefficient c^{time} are determined by fitting the logistic function above to the aforementioned mobility data, given the calculated response time T^{res} and daily death data for Covid-19[63] adjusted for under-reporting[64]. These country-level parameter data are stratified by country-income-group archetype and for each parameter, a set of candidate distributions are fitted with the `fitdist` package[65] using maximum likelihood estimation. The candidate distributions with lowest Akaike information criterion (AIC) values are identified, from which simulation parameters are drawn. The distancing parameter marginal distributions are shown in Figure S2 in light blue. In HICs, the mean response time is lowest and the mean time-decay coefficient is lowest, both of which result in reduced transmission and favourable outcomes. Since the response time is drawn in units of doubling times, it is converted to units of days by multiplication with the local doubling time of the synthetic country and disease in question before simulation. Illustrative values of the transmission multiplier for a sample of synthetic countries in each income-group archetype, as a function of daily deaths and time since the response time, are shown in Figure S4.

Case Isolation

Case isolation as a mitigation measures encompasses the detection and mandatory isolation of a proportion of the infectious, contingent on the operation of an effective testing and surveillance system, with the aim of reducing transmission - potentially to the point of suppression. Case detection is modelled in a stylised manner by the diversion of a proportion of the asymptomatic and symptomatic infectious to corresponding ‘isolating’ health states, controlled by time-dependent infection ascertainment ratios within the latent-to-infectious transition rates. Specifically, the latent-to-infectious transition rates are written as

$$\begin{aligned}
k^2(t) &= \frac{(1-\alpha^a(t))(1-p^{I^s})}{T^{E:I}} \\
k^3(t) &= \frac{(1-\alpha^s(t))p^{I^s}}{T^{E:I}} \\
k^4(t) &= \frac{\alpha^a(t)(1-p^{I^s})}{T^{E:I}} \\
k^5(t) &= \frac{\alpha^s(t)p^{I^s}}{T^{E:I}},
\end{aligned}$$

where $T^{E:I}$ is the latent period and p^{I^s} is the symptomatic infection ratio (see Table S1), and $\alpha^a(t)$ and $\alpha^s(t)$ are the infection ascertainment ratios (IARs) of the asymptomatic and symptomatic respectively.

The IARs are written

$$\begin{aligned}
\alpha^a(t) &= \mathbb{1}_{\{T^{test}\le t<T^{open}\}}\mathbb{1}_{\{I^{tot}(t)<I^{thresh}\}}\min\left(p^{asc},\left[\frac{a^{test}-H^{new}(t)}{I^{new}(t)}\right]^+\right) \\
\alpha^s(t) &= \mathbb{1}_{\{T^{test}\le t<T^{open}\}}\left[\mathbb{1}_{\{I^{tot}(t)<I^{thresh}\}}\min\left(p^{asc},\left[\frac{a^{test}-H^{new}(t)}{I^{new}(t)}\right]^+\right)\right. \\
&\quad \left.+\left(1-\mathbb{1}_{\{I^{tot}(t)<I^{thresh}\}}\right)\min\left(p^{asc},\left[\frac{a^{test}-H^{new}(t)}{I^{s,new}(t)}\right]^+\right)\right],
\end{aligned}$$

where T^{test} is the testing start-time when case isolation takes effect and T^{open} is the time when mandated sector closures and home-working are lifted and testing and case isolation end (see section 2.4), $I^{tot}(t) =$

$\sum_{j,v}\left(E_{j,v}(t)+I^{a}_{j,v}(t)+I^{s}_{j,v}(t)+I^{ai}_{j,v}(t)+I^{si}_{j,v}(t)+H_{j,v}(t)\right)$ is disease prevalence and $I^{thresh}=\sum_j N_j/10^7$ is a fixed prevalence threshold, p^{asc} is the maximum infection ascertainment ratio, a^{test} is the population-level testing rate, $H^{new}(t)=\sum_{j,v}k^{7}_{j,v}(t)\left(I^{s}_{j,v}(t)+I^{si}_{j,v}(t)\right)$ is daily hospital admissions, and $I^{new}(t)=\sum_{j,v}k^{1}_{j,v}(t)\left(S_{j,v}(t)+\sum_{u=v+1}^{1}S^{c_u}_{j,v}(t)\right)$ and $I^{s,new}(t)=p^{I^s}I^{new}(t)$ are total and symptomatic incidence, respectively. The functional form for the IARs relates case detection to testing, whereby ascertainment is zero in the absence of testing and only non-zero in the time interval $T^{test}\le t<T^{open}$, but also encodes an explicit dependence on disease prevalence and distinguishes two ascertainment régimes above and below the prevalence threshold: when $I(t)>I^{thresh}$, only the symptomatic infectious are detected up to a maximum of p^{asc}, but when $I(t)<I^{thresh}$, both the asymptomatic and symptomatic infectious are detected at the same level. The rationale behind this assumption is that the symptomatic infectious can be detected via either symptom-driven testing or contact tracing, while the asymptomatic infectious can only be detected via contact tracing, and it is unlikely that a substantial proportion of cases are detected via contact tracing unless prevalence is low and close to (local) extinction[66,67]. The IARs are also restricted by the testing rate, accounting for the 'pillar' of testing of those admitted to care,[68], where the upper bound is assumed to be the ratio of the extra-hospital testing rate to incidence (symptomatic and total incidence in the low- and high-ascertainment régimes, respectively).

However, ascertainment does not imply that the transmission risk from detected cases is zero, due to factors such as presymptomatic transmission, barriers to testing, testing turnaround times and contact tracing delays. Hence, the effectiveness of case isolation is modelled as time-dependent relative risks of transmission for the isolating within the force-of-infection term, with the underlying assumption that transmission risk is determined by the ratio of the 'effective' infectious period to the disease-dependent infectious period (see Table S1), where the effective infectious period is interpreted here to be the time from infectiousness to isolation. Specifically, the relative risk of transmission for the isolating asymptomatic and symptomatic infectious are

$$\zeta^{a}(t)=1+\mathbb{1}_{\{T^{\text{test}}\le t<T^{\text{open}}\}}\mathbb{1}_{\{I^{\text{tot}}(t)<I^{\text{thresh}}\}}\left(\frac{\min\left(T^{I:Iso,\bar{\alpha}},T^{I^a:R}\right)}{T^{I^a:R}}-1\right)$$

$$\begin{aligned}\zeta^{s}_{j,v}(t)=1+\mathbb{1}_{\{T^{\text{test}}\le t<T^{\text{open}}\}}\Bigg[&\mathbb{1}_{\{I^{\text{tot}}(t)<I^{\text{thresh}}\}}\left(\frac{\min\left(T^{I:Iso,\bar{\alpha}},T^{I^s}_{j,v}(t)\right)}{T^{I^s}_{j,v}(t)}-1\right)\\&+\left(1-\mathbb{1}_{\{I^{\text{tot}}(t)<I^{\text{thresh}}\}}\right)\left(\frac{\min\left(T^{I:Iso,\underline{\alpha}},T^{I^s}_{j,v}(t)\right)}{T^{I^s}_{j,v}(t)}-1\right)\Bigg]\end{aligned}$$

respectively, where $T^{I^a:R}$ is the infectious period for asymptomatic infection (see Table S1), $T^{I^s}_{j,v}(t)=T^{I^s:H}(p^{H}_{j,v}(t))+T^{I^s:R}(1-p^{H}_{j,v}(t))$ is the infectious period for symptomatic infection averaged across outcomes (see Table S1) with time-dependent symptomatic infection hospitalisation ratio $p^{H}_{j,v}(t)$ (see subsequent paragraphs), and $T^{I:Iso,\bar{\alpha}}$ and $T^{I:Iso,\underline{\alpha}}$ are the times from infectiousness to isolation for the high- and low-ascertainment régimes described above. These delays are defined in turn as the difference between the times from infection to isolation and the time from infection to infectiousness, i.e., the latent period. Here, it is assumed that the times from infection to isolation for both the high- and low-ascertainment régimes are fixed values that are disease-independent, reflecting the operation of a testing and surveillance system and the corresponding delays associated with testing turnaround, notification and contact-tracing, irrespective of the disease in question. Summing estimates of the Covid-19 incubation period of 5.8 days[69] and symptom-onset to isolation delay for traced-cases of -0.8[70] and general cases of 2.4[71], the times from infection to isolation for the high- and low-ascertainment régimes are calculated to be 5 days and 8.2 days respectively, and thus the times from infectiousness to isolation are defined as $T^{I:Iso,\bar{\alpha}}=\left[5-T^{E:I}\right]^{+}$ and $T^{I:Iso,\underline{\alpha}}=\left[8.2-T^{E:I}\right]^{+}$, scaling linearly with the disease-dependent latent period $T^{E:I}$. Substituting the parameter values in Table S1 into the above equations yields disease- and ascertainment régime-dependent values of $\zeta^{a}(t)$ and $\zeta^{s}_{j,v}(t)$: for the influenza diseases, there is no reduction in transmission for the isolating asymptomatic or symptomatic infectious in either régime since both latent and infectious periods are very short, hence case isolation as a mitigation measure is ineffective; for the coronavirus diseases, there is little reduction in transmission in the low-ascertainment régime, but in the high-ascertainment régime there is a more substantial reduction in transmission with relative risks ranging from 0.19-0.48 for the asymptomatic infectious and 0.1-0.25 for the symptomatic infectious. Though stylised, the scaling of the effectiveness of case isolation with latent and infectious periods is consistent with previous work on outbreak control, case isolation and contact-tracing[72–74]. The set-up is also generalisable to diseases with variable transmissibility, delays and severity: the symptomatic infection ratio determines whether the asymptomatic or symptomatic IAR and relative transmission risk applies, model-endogenous disease prevalence dictates the ascertainment régime that applies, and the latent and infectious periods control the relative risk of transmission for the isolating infectious (see S1). Therefore, case isolation is also fully endogenous to the local outbreak.

Testing data were generated on a country-by-country basis by fitting a ramp function to Covid-19 testing data[75], specifically the time series of cumulative tests normalised by population. The testing start-time T^{test} is defined to be the time delay from 1^{st} January 2020 normalised by the (fixed) doubling time of Covid-19[62], as for the response time. The testing rate a^{test} is assumed to be disease-independent. Ascertainment data were generated by averaging Covid-19 symptomatic infection ascertainment ratios for various countries over time 76, which are also assumed to be disease-independent. As before, these country-level parameter data are stratified by country-income-group archetype and a set of candidate distributions are fitted with the `fitdist` package[65] using maximum likelihood estimation. The candidate distributions with lowest Akaike information criterion (AIC) values are identified, from which simulation parameters are drawn. The case isolation parameter marginal distributions are shown in Figure S2 in light green. The mean testing start-time is largest in LLMICs and smallest in HICs, while the mean testing rate is lowest in LLMICs and highest in HICs, reflecting existing testing and surveillance system vulnerabilities in lower-income countries. Since the testing start-time is drawn in units of doubling times, it is converted to units of days by multiplication with the local doubling time of the synthetic country and disease in question before simulation. The testing rate is drawn per capita and multiplied by the local population before simulation. Illustrative values of the maximum infection ascertainment ratio for a sample of synthetic countries in each income-group archetype, as a function of time since the outbreak, are shown in Figure S4. Note that it is the maximum IAR that is plotted here, rather than the prevalence-dependent asymptomatic and symptomatic IARs, for ease of exposition.

Hospital Capacity

Hospital capacity as a mitigation measure refers to the ability of the health system to cater to pandemic patients, including the availability of hospital beds, equipment, therapeutics and healthcare workers. In particular, the IFRs displayed in Table S1 are interpreted to reflect patient outcomes given the appropriate level of care. But if the health system is not resilient and the healthcare demand induced by the pandemic exceeds the available supply, then patient outcomes will deteriorate due to overutilisation. Hence, healthcare provision is modelled as a time-dependent hospitalisation fatality ratio (HFR) in the hospital outcome transition rates, denoted $k_j^9(t)$ and $k_j^{10}(t)$ in the system of ODEs above, which increases when hospital occupancy exceeds the fixed spare hospital beds threshold. Specifically, the complementary hospital outcome transition rates are written as

$$k_j^9(t) = \frac{p_j^D(t)}{T_j^H(t)}$$
$$k_j^{10}(t) = \frac{1 - p_j^D(t)}{T_j^H(t)},$$

where $p_j^D(t)$ is the time-dependent HFR and $T_j^H(t) = T^{H:D}(p_j^D(t)) + T^{H:R}(1 - p_j^D(t))$ is the length-of-stay averaged across outcomes (see Table S1).

The HFR is modelled as a linear function of hospital occupancy and is written

$$p_j^D(t) = \left(1 + 1.87\left[\frac{H^{tot}(t) - H^{max}}{H^{max}}\right]^+\right)\hat{p}_{g(j)}^D,$$

where $\hat{p}_{g(j)}^D$ is the baseline HFR, $H^{tot}(t) = \sum_{j,v} H_{j,v}(t)$ is current hospital occupancy and H^{max} is the number of spare hospital beds. Below capacity, the HFR is identical to the baseline value, but beyond this threshold, the HFR increases with occupancy. The scaling factor of 1.87, referred to as the hospital surge HFR, was estimated from a similar model applied to the Covid-19 pandemic in Indonesia[16] and it is assumed that this same value applies to other diseases. The baseline HFR is disease-dependent and is mapped from five-year age-bands to the model age-groups weighting by population and IHR, specifically

$$\hat{p}_g^D = \sum_{a \in g} \frac{\tilde{p}_a^{IFR}}{\tilde{p}_a^{IHR}} \frac{\tilde{p}_a^{IHR}\tilde{N}_a}{\sum_{a' \in g}\tilde{p}_{a'}^{IHR}\tilde{N}_{a'}}.$$

Therefore, healthcare provision is endogenous to the local outbreak. Factors relating to healthcare-seeking behaviour are not modelled, nor are barriers to care beyond the supply of hospital beds.

Data for spare hospital beds were generated on a country-by-country basis: total hospital bed data were sourced from the World Bank[77] and bed occupancy rate (BOR) data from the WHO[78]. Spare hospital beds H^{max} (per capita) is then defined as the product of total hospital beds per 100k population and the complement of the BOR;

if BOR data were unavailable, a value of 85% was assumed[79]. As before, these country-level parameter data are stratified by country-income-group archetype and a set of candidate distributions are fitted with the `fitdist` package[65] using maximum likelihood estimation. The candidate distributions with lowest Akaike information criterion (AIC) values are identified, from which simulation parameters are drawn. The hospital capacity parameter marginal distributions are shown in Figure S2 in purple. The mean hospital capacity is lowest in LLMICs and highest in HICs, reflecting existing health system vulnerabilities in lower-income countries. Since the number of spare hospital beds is drawn per capita, it is multiplied by the local population before simulation. Illustrative values of the number of spare hospital beds for a sample of synthetic countries in each income-group archetype are also shown in Figure S4, where it is noted that these are time-independent.

Vaccination

Vaccination as a mitigation measure refers to the administration of a strain-specific but imperfect vaccine to a proportion of the population (determined by the combined effects of government mandates and human behaviour, which again are not disentangled) a period of time after the outbreak begins. The protective effects of the vaccine not only reduce transmission and adverse outcomes among the vaccinated population, but also reduce transmission among the unvaccinated population due to the positive externalities of vaccination. Vaccination is modelled as a duplication of the health states in the system of ODEs above, indexed by the subscript v where $v = 0$ represents the unvaccinated and $v = 1$ the vaccinated, and vaccination confers partial protection against infection, hospitalisation/severe disease and onward transmission. Vaccination status transitions occur due to vaccine administration and seroconversion ($v = 0 \to v = 1$), depending on the administration start-time, administration rate and coverage, and waning of vaccine-induced immunity to infection over time ($v = 1 \to v = 0$). Here, 'vaccinated' is interpreted to be the completion of a two-dose schedule, and only full and not partial vaccination is modelled. In particular, the protective effects of vaccination do not apply to the seroconverting health state $S^{c_u}_{j,v}$.

The vaccine administration transition rate, denoted $k^{11,c_u}_{j,v}(t)$ in the system of ODEs above, is written as

$$k^{11,c_1}_{j,v=0}(t) = \frac{\psi_j(t)}{S_{j,v=0}(t) + E_{j,v=0}(t) + I^a_{j,v=0}(t) + I^s_{j,v=0}(t) + I^{ai}_{j,v=0}(t) + I^{si}_{j,v=0}(t) + R_{j,v=0}(t) + H_{j,v=0}(t) + D_{j,v=0}(t)},$$

where the numerator $\psi_j(t)$ is the total number of vaccines administered per day to stratum j at time t that are distributed uniformly among all unvaccinated health states in the denominator, reflecting vaccine wastage due to immunological redundancy. Here,

$$\psi_j(t) = \mathbb{1}_{\{T^{vax}_{\pi^{-1}(g(j))} \leq t < T^{vax}_{\pi^{-1}(g(j))+1}\}} \frac{a^{vax} N_j}{\hat{N}_{g(j)}},$$

where a^{vax} is the population-level vaccine administration rate and

$$T^{vax}_h = T^{vax} + \sum_{s=1}^{h-1} \frac{\hat{N}_{\pi(s)} \hat{p}^{vax}_{\pi(s)}}{a^{vax}}$$

represents the time of vaccine rollout to priority group h, given initial vaccine administration start-time T^{vax}, population-level vaccine coverage p^{vax} and permutation function $\pi : h \to g$ that assigns priority group order h to model age-group g. Note that T^{vax}_5 represents the vaccine administration end-time.

The seroconversion transition rate, denoted k^{12} in the system of ODEs above, is written as

$$k^{12} = \frac{1}{T^c},$$

where T^c is the time from vaccination to seroconversion/development of immunity (see Table S2). Compared to the unvaccinated, the vaccinated have reduced relative risk of infection η^E_v in the force-of-infection term above, reduced relative risk of hospitalisation for symptomatic infection η^H_v to be discussed below, and reduced relative risk of transmission η^I_v in the force-of-infection term above (see Table S2). The waning transition rate, denoted $k^{13,\bullet}_\bullet$ in the system of ODEs above, is written as

$$k^{13,\bullet}_\bullet = \frac{1}{T^r},$$

326 where T^r is the time from seroconversion to waning/loss of immunity to infection (see Table S2).

Given that vaccine-induced immunity to infection wanes but vaccine-induced immunity to severe disease does not, the hospitalisation and recovery transition rates must be defined carefully. The recovery transition rate for the asymptomatic infectious, denoted k^6 in the system of ODEs above, is independent of vaccination but for completeness is defined here as

$$k^6 = \frac{1}{T^{I^a:R}},$$

where $T^{I^a:R}$ is the infectious period for asymptomatic infection (see Table S1). The hospitalisation and recovery transition rates for the symptomatic infectious, denoted $k^7_{j,v}(t)$ and $k^8_{j,v}(t)$ in the system of ODEs above, are written as

$$\begin{aligned} k^7_{j,v}(t) &= \frac{p^H_{j,v}(t)}{T^{I^s}_{j,v}(t)} \\ k^8_{j,v}(t) &= \frac{1 - p^H_{j,v}(t)}{T^{I^s}_{j,v}(t)}, \end{aligned}$$

where $p^H_{j,v}(t)$ is the time-dependent symptomatic infection hospitalisation ratio (SHR) and $T^{I^s}_{j,v}(t) = T^{I^s:H}(p^H_{j,v}(t)) + T^{I^s:R}(1 - p^H_{j,v}(t))$ is the infectious period for symptomatic infection averaged across outcomes (see Table S1). Specifically, the SHR is written as

$$p^H_{j,v}(t) = \left(\frac{S^n_j(t) + \eta^E_v \eta^H_v (S_{j,v=0}(t) - S^n_j(t)))}{S_{j,v=0}(t)} \right)^{\mathbb{1}\{v=0\}} \eta^H_v \hat{p}^H_{g(j)},$$

where $\hat{p}^H_{g(j)}$ is the baseline SHR, η^H_v is the relative risk of hospitalisation for symptomatic infection mentioned above (see Table S2) and $S^n_j(t)$ is an auxiliary health state representing the fully-naive susceptible (never infected nor vaccinated), which is the solution of the auxiliary equation $\frac{dS^n_j}{dt} = -\left(k^1_{j,v}(t) + \sum_{u=v+1}^{1} k^{11,c_u}_{j,v}(t)\right) S^n_j$. This multiplier decays over time from an initial value of 1, when $S_{j,v=0}(t) = S^n_j(t)$ (i.e., the entire population is fully-naive susceptible), and approaches a value of $\eta^E_{v=1}\eta^H_{v=1}$ as vaccine-induced immunity to infection wanes, representing the retention of vaccine-induced immunity to severe disease. The baseline SHR is disease-dependent and is mapped from five-year age-bands to the model age-groups weighting by population, specifically

$$\hat{p}^H_g = \sum_{a \in g} \frac{\tilde{p}^{IHR}_a}{p^{I^s}} \frac{\tilde{N}_a}{\sum_{a' \in g} \tilde{N}_{a'}}.$$

327 Therefore, the effectiveness of vaccination is fully endogenous to the local outbreak.

The vaccine efficacy parameters η^E_v, η^H_v, η^I_v and vaccine delay parameters T^c, T^r are fixed (see Table S2), and it is assumed that these are independent of country-income-group archetype and disease. Factors such as the affordability of higher-efficacy vaccines for different countries are not considered (e.g., Covid-19 mRNA vaccines). However, the variability in vaccine administration and coverage parameters is modelled, reflecting the inequitable vaccine access, differences in immunisation infrastructure and logistics, and population willingness to vaccinate[80]. Data for these vaccination parameters were generated on a country-by-country basis as follows. The vaccine administration start-time T^{vax} and the vaccine administration rate a^{vax} (per capita) are determined by fitting a ramp function to Covid-19 vaccination data[81], specifically the time series of fully-vaccinated individuals normalised by population. The start-time is defined in days from from 1^{st} January 2020 and unlike previous delay parameters, it is not normalised by the doubling time, under the assumption that the delay is dominated by the disease-independent timescales of vaccine development and deployment rather than the timescales of disease detection. The administration rate is defined as the number of individuals completing a two-dose schedule per 100k population per day, consistent with the fact that only full and not partial vaccination is modelled. The vaccine coverage p^{vax} is extracted from the same data, defined as the maximum (and final) value attained, which is assumed to be disease-independent. As before, these country-level parameter data are stratified by income-group archetype and a set of candidate distributions are fitted with the `fitdist` package[65] using maximum likelihood estimation. The candidate distributions with lowest Akaike information criterion (AIC) values are identified, from which simulation parameters are drawn. The vaccination parameter marginal distributions are shown in Figure S2 in orange. The mean administration start-time is longest in LLMICs and shortest in HICs, while mean administration rate and coverage are lowest in LLMICs and highest in HICs, reflecting the income group inequities mentioned above. Since the administration rate is drawn per capita, it is multiplied by the local population before simulation. Illustrative values of population-level vaccination coverage for a sample of synthetic countries in each income-group archetype, as a function of time since the outbreak, are shown in Figure S4. Finally, for all diseases except for Influenza-1918-X, vaccine prioritisation follows an age-descending order with reversal permutation function

$$\pi = \begin{pmatrix} 1 & 2 & 3 & 4 \\ 4 & 3 & 2 & 1 \end{pmatrix},$$

whereas for Influenza-1918-X the working-age group is prioritised above the retired-age group due to the comparable IFR in both age-groups (see Table S1), with permutation function

$$\pi = \begin{pmatrix} 1 & 2 & 3 & 4 \\ 3 & 4 & 2 & 1 \end{pmatrix}.$$

Of course, vaccine prioritisation is inherently an optimisation problem in its own right and will depend on country- and disease-specific factors[82]; however, this is not the objective of the current study.

Parameter	**Symbol**	**Value**
Time from Vaccination to Seroconversion	T^c	21 Assumed
Relative Risk of Infection	$\eta^E_{v=1}$	0.30 Assumed
Relative Risk of Hospitalisation for Symptomatic Infection	$\eta^H_{v=1}$	0.33 Assumed
Relative Risk of Transmission	$\eta^I_{v=1}$	0.70 Assumed
Time from Seroconversion to Waning	T^r	365 Assumed

Table S2: Vaccine parameter values. Delays are reported in days. The relative risks correspond to vaccine efficacies of 70% against infection, 90% against hospitalisation/severe disease (complement of the product of the relative risk of infection and the relative risk of hospitalisation for symptomatic infection) and 30% against onward transmission. The corresponding relative risks for for the unvaccinated are $\eta^E_{v=0} = \eta^H_{v=0} = \eta^I_{v=0} = 1$. Waning refers to the loss of vaccine-induced immunity to infection but not severe disease.

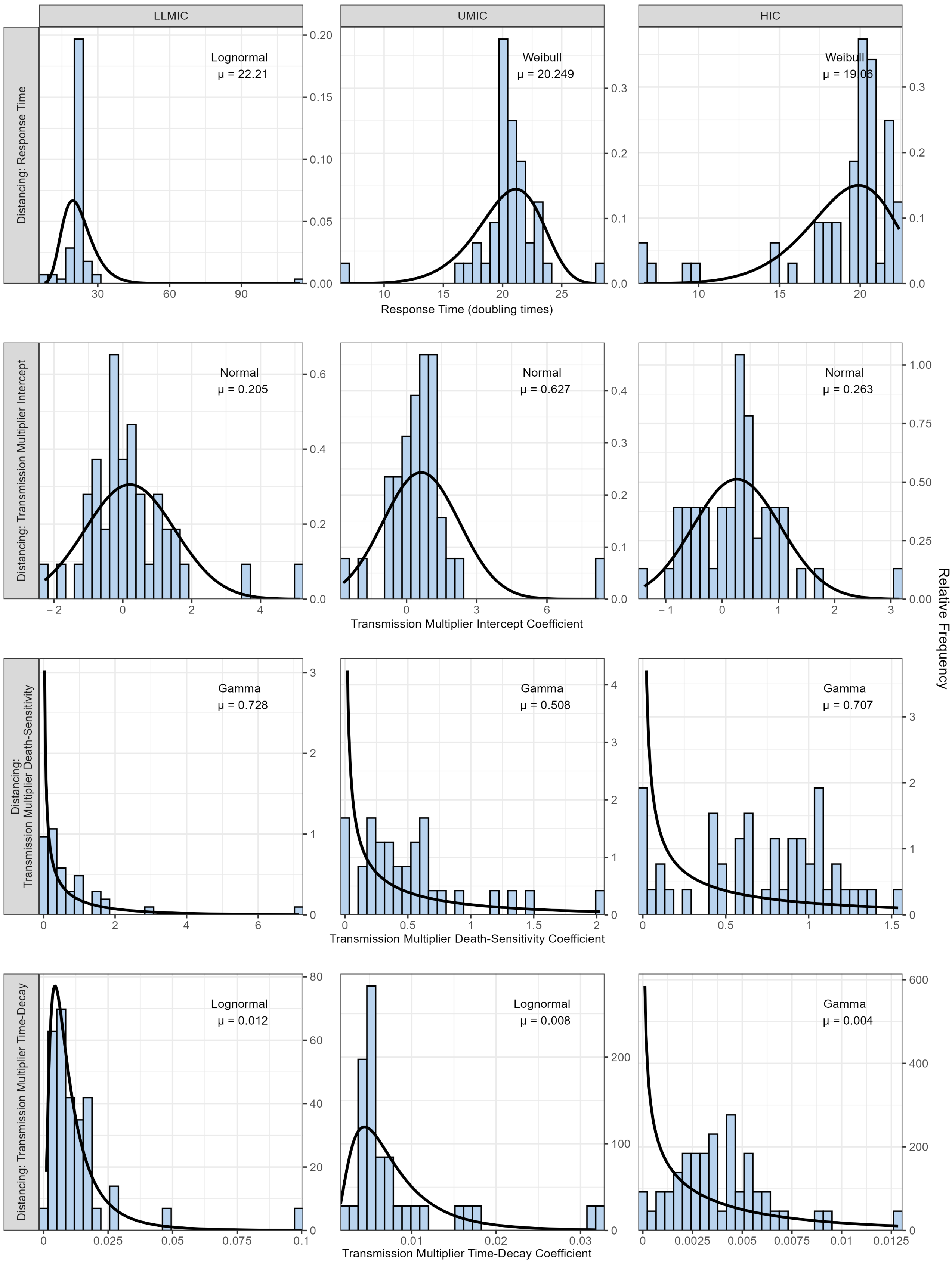

Figure S2: Continued on next page ...

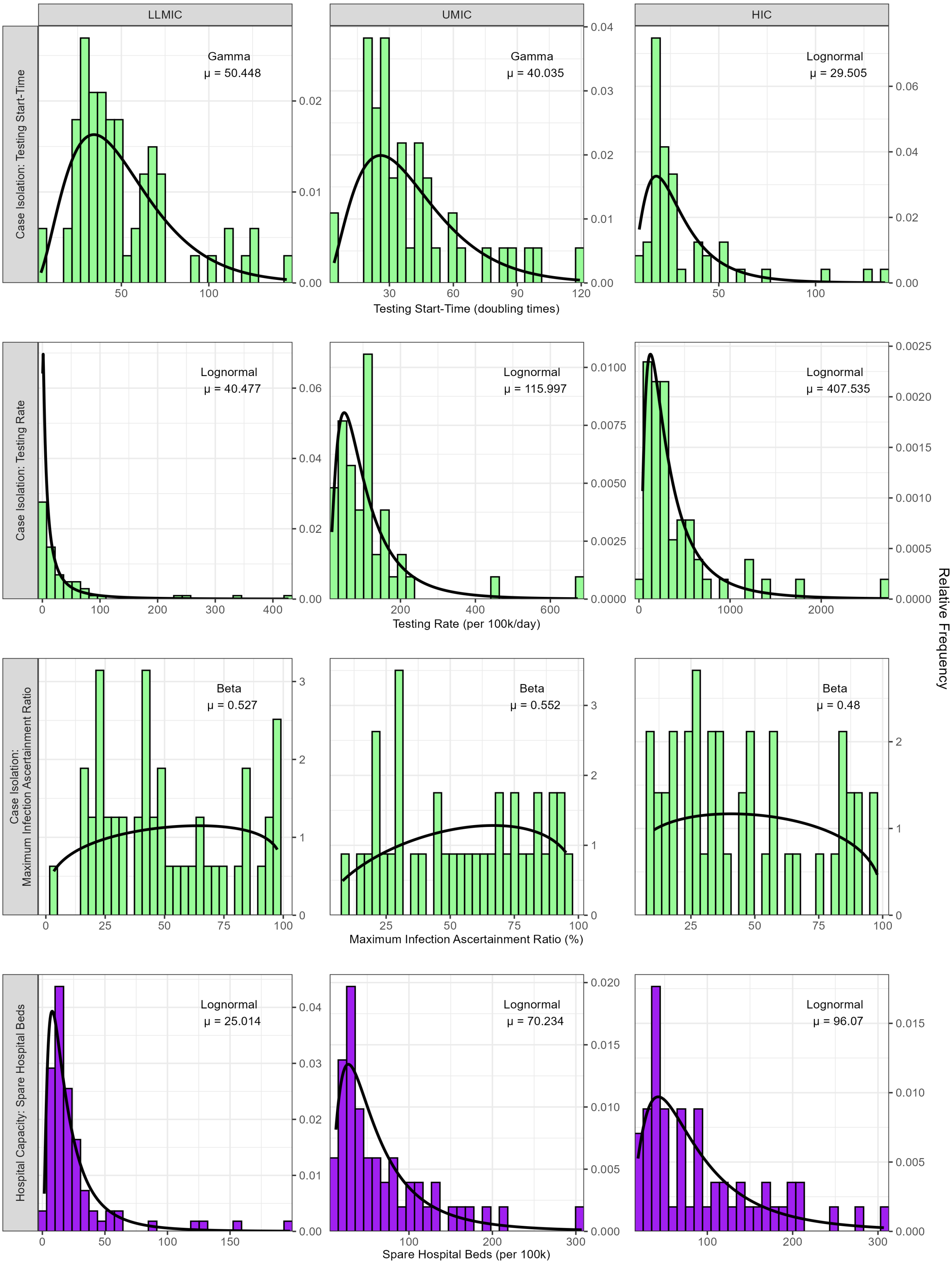

Figure S2: Continued on next page ...

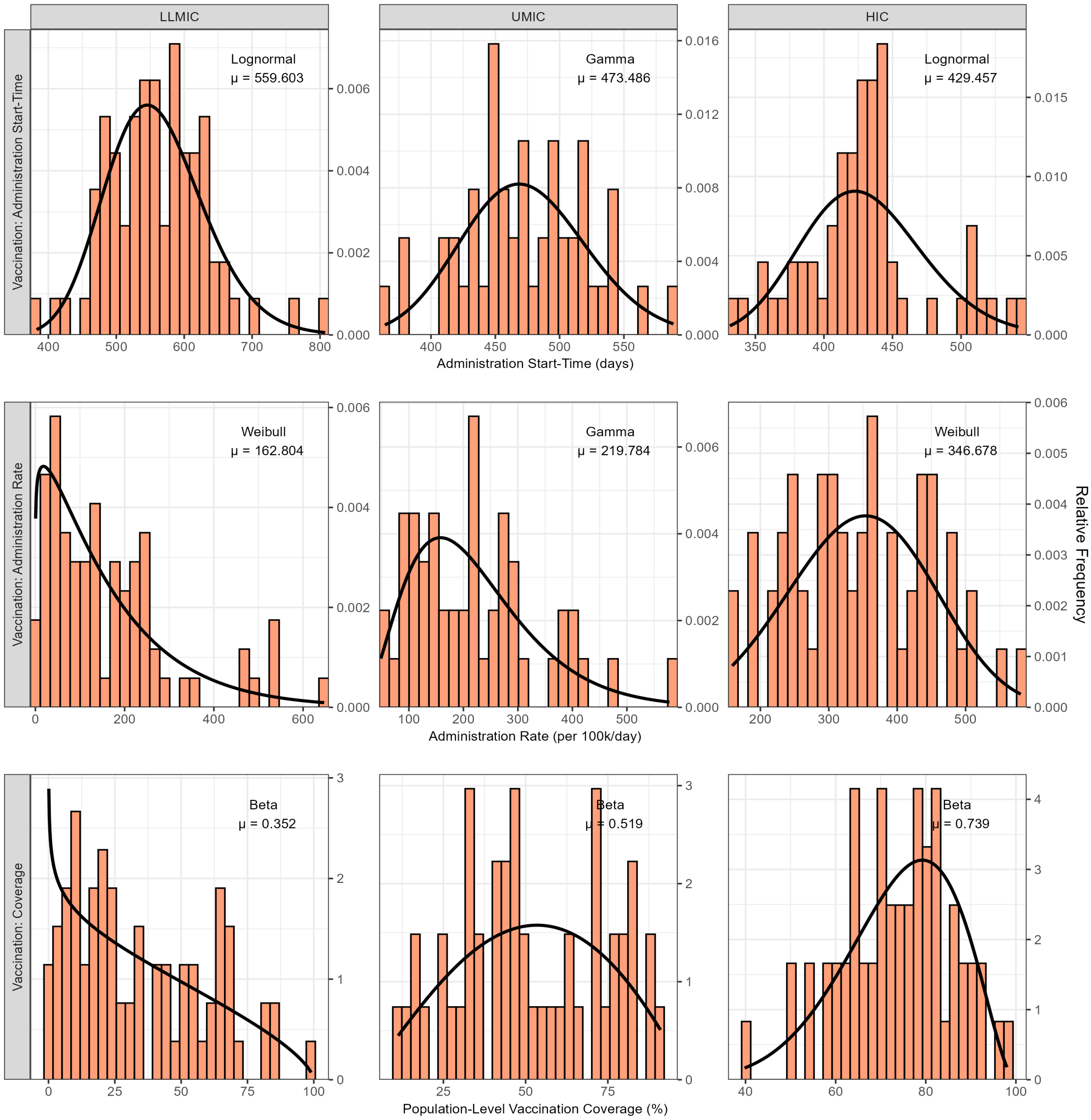

Figure S2: Mitigation measure data and fitted marginal distributions by country-income-group archetype. The mitigation measures are distancing, case isolation, hospital capacity and vaccination (colours), each with underlying parameters. The fitted marginal distribution is that with lowest AIC among a set of candidate distributions, and the resulting distribution type and its mean are displayed in each panel.

Figure S3: Continued on next page ...

Figure S3: Continued on next page ...

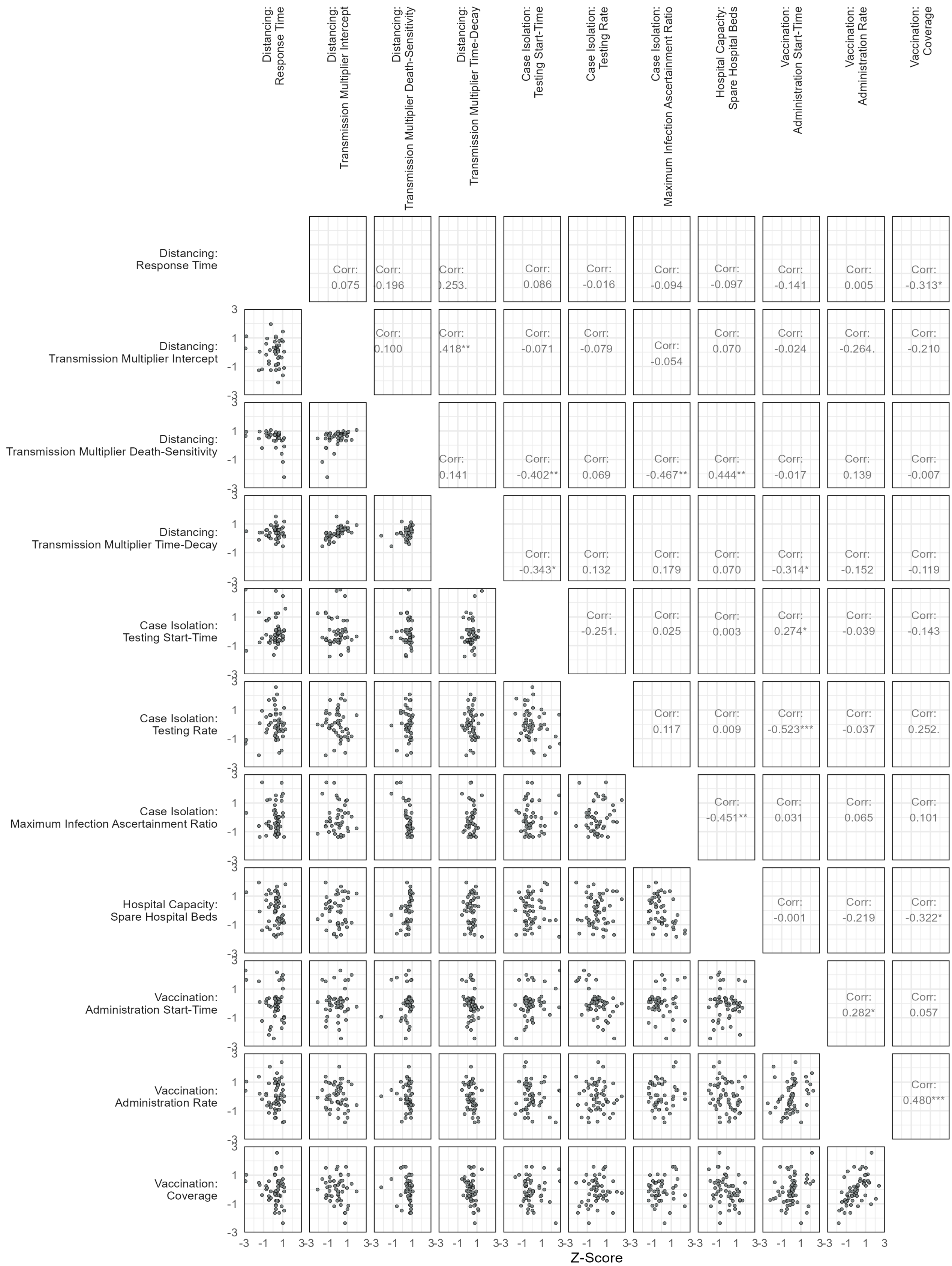

Figure S3: Pairwise z-score scatterplots and associated correlation coefficients of mitigation measure data by country-income-group archetype. The z-scores are calculated for the observed data using the fitted marginal distributions in Figure S2 above, for each income-group archetype (colours).

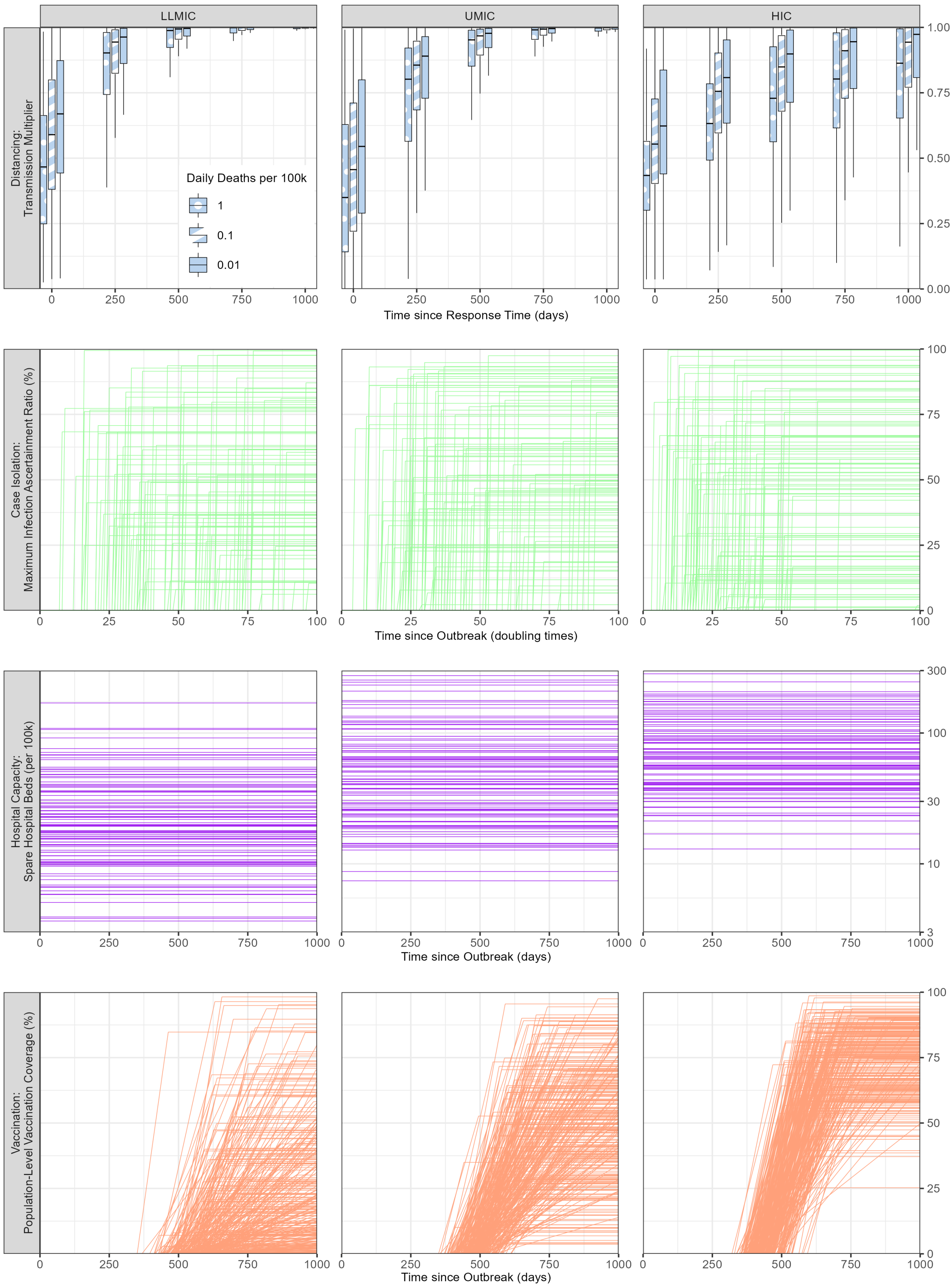

Figure S4: Mitigation measure implementation, as a function of time, for sample synthetic countries by country-income-group archetype. The mitigation measures (colours) are distancing via a time- and death-dependent transmission multiplier (parametrised by the response time, intercept coefficient, death-sensitivity coefficient and time-decay coefficient), case isolation via a time- and prevalence-dependent infection ascertainment ratio (parametrised by the testing start-time, testing rate and maximum infection ascertainment ratio), hospital capacity via time-independent spare hospital beds, and vaccination via the time-dependent rollout of vaccines (parametrised by administration start-time, rate and population-level coverage).

2.4 Closure Strategies

For more transmissible and/or severe disease outbreaks, the imposition of the aforementioned mitigation measures may not yield adequate control. As illustrated by the Covid-19 pandemic, the mandated closure of businesses and schools may be required in addition to distancing and case isolation in order to hold hospital occupancy below capacity, especially prior to vaccine availability [83]. In the daedalus model, it is assumed that decision-makers have the ability to mandate the partial- or full-closure of any sector of the economy and the extent to which economic sector j is open at time t is denoted $x_j(t)$, where the closure of the education sector $x_{edu}(t) = x_{41}(t)$ also corresponds to school closure. Home-working may also be mandated and the proportion of workers home-working is denoted $q_j(t)$. The purpose of sector closures is to reduce transmission, driven by decreased mixing in workplaces, schools and other-locations encoded in the contact matrices (see section 2.1), where the proportional closure of a sector is assumed to be equal to the proportional reduction in the workforce of that sector and a corresponding reduction in contacts. However, sector closures also incur both short- and long-term losses (see section 2.5), the magnitude of which depends on closure extent and timing. Indeed, the daedalus model was originally developed to project the health and economic impacts of different sector closure policies for Covid-19 in the UK, in order to quantify the lives vs. livelihoods trade-off, and to identify GDP-maximising policies subject to hospital occupancy constraints in particular [15].

Here, pre-defined dynamic closure strategies are modelled instead of an optimisation-based approach. Four distinct closure strategies may be pursued in response to a disease outbreak in a synthetic country, inspired by strategies implemented during the Covid-19 pandemic [84]. Namely, the set of closure strategies comprises:

- Elimination, inspired by 'aggressive containment' Covid-zero strategies, e.g. New Zealand [85], Singapore [86]
- Reactive-Business/Reactive-School Closures, inspired by 'suppression' reactive business/school closure strategies, e.g. EU countries [87], UK [88]
- Reactive-Business/Sustained-School Closures, inspired by 'suppression' reactive business closure strategies with long-term school closures, e.g. Bangladesh [89], Philippines [90]
- No Closures, inspired by 'mitigation' herd-immunity strategies, e.g. Zambia [91],

which range from laissez-faire to very stringent. Each strategy is defined in detail below but broadly speaking, the Elimination strategy alternates between heavy and light sector closures in response to the effective reproduction number, the Reactive-Business/Reactive-School Closures strategy alternates between heavy and light sector closures in response to hospital occupancy, the Reactive-Business/Sustained-School Closures strategy alternates between heavy and light sector closures in response to hospital occupancy but keeps the education sector and schools closed for the duration of the outbreak, and the No Closures strategy refrains from any sector closures. The distancing, case isolation, hospital capacity and vaccination mitigation measures described above are imposed irrespective of the strategy pursued, hence no entirely unmitigated scenario is considered. Each closure strategy is defined as a set of discrete economic configurations and specific rules for switching between them. Here, an economic configuration is a vector that defines the extent to which the entire economy (including the education sector and schools) is open at a given time, expressed as a proportion; for example, the fully-open configuration $x_j(t) = 1$. The set of economic configurations for each strategy are displayed in Table S3 and the associated reductions in transmission is shown in Figure S5 for each disease and country-income-group archetype (excluding distancing). The rules for switching between configurations are also strategy-dependent and these are described in detail below; examples include reaching the response time T^{res}, hospital occupancy $H^{tot}(t)$ nearing hospital capacity H^{max}, the value of the effective reproduction number R_t, and reaching the vaccine administration end-time T_5^{vax}. Critically, the closure strategies are dynamic, since configuration switching is model-endogenous and depends on both the epidemiological model health states (see section 2.2) and the mitigation measure parameters (see Figure S2), which in turn depend on disease epidemiological parameters (see Table S1) and income-group-dependent synthetic country characteristics (see Figure S1). As a result, for each strategy, the extent of sector closures is fixed as per the economic configurations, but the timing will vary in terms of occurrence, duration and frequency.

Every closure strategy begins (and ends) with the fully-open configuration $x_j(t) = 1$ and no mandated home-working $q_j(t) = 0$. This continues until the response time is reached, at which point distancing takes effect (see section 2.3) and the strategies diverge. Whether sector closures are imposed at the response time depends on the strategy and the strategy-specific switching rules (see subsequent paragraphs). Irrespective of the strategy, it is assumed that any imposed closures coincide with mandated home-working (note that home-working without closures is not modelled due to conflicting evidence regarding the associated productivity losses/gains [92]), where the proportion of workers capable of home-working depends on the income-group archetype and economic sector (see Figure S1). Furthermore, during periods with the heavy-closure configuration (which may be imposed under any strategy except for No Closures - see Table S3), the distancing transmission multiplier is restricted from exceeding its value at the time of imposition of heavy closures, i.e. no decay of distancing (due to factors such as reduced adherence and pandemic fatigue) is modelled during periods of heavy closures. The penultimate rule for lifting all sector closures and mandated home-working (as well as case isolation - see section 2.3) and switching back to the fully-open configuration is also strategy-independent, and is defined to be the first occurrence of any of three events: the effective reproduction number is subcritical without any closures, home-working or case isolation; reaching the vaccine administration end-time; or 2.5 years after the response time. Though the switching rule is strategy-independent, the time of occurrence, denoted T^{open}, is strategy-dependent. Likewise, the strategy-independent rule for ending the simulation following T^{open} is reaching the post-outbreak disease-free equilibrium with hospital occupancy lower than one per million population and subcritical effective reproduction number, simultaneously, and the time of occurrence is denoted T^{end}. The strategy-specific switching rules are described in the following paragraphs.

No Closures

Under the No Closures strategy, the first switching rule is reaching the response time (as for all closure strategies), at which point distancing takes effect via the aforementioned transmission multiplier (see section 2.3) and illustrative transmission-reduction values are shown in Figure S4, as a function of daily deaths and time since the response time. No mandated sector closures or home-working are ever imposed and the fully-open configuration is maintained throughout, regardless of epidemiology, i.e. $x_j(t) = 1$ and $q_j(t) = 0 \; \forall \; j, t$. As well as distancing, the case isolation, hospital capacity and vaccination mitigation measures are modelled in the same manner as for the other strategies, hence it is not identical to an entirely unmitigated outbreak. However, this will depend on the values of the mitigation measure parameters drawn (see Figure S2): if the parameter values are unfavourable (e.g., little distancing, low ascertainment, few spare hospital beds, slow vaccination), then the No Closures strategy may be similar to an 'approximately' unmitigated outbreak [91], but if the parameter values are favourable, then it may be similar to the successful implementation of a Covid-19 'mitigation' strategy. Case isolation ceases upon reaching T^{open}.

Reactive-Business/Sustained-School Closures

Under the Reactive-Business/Sustained-School Closures strategy, the first switching rule is reaching the response time, at which point distancing takes effect but the fully-open configuration is maintained (initially) according to a 'wait-and-see' approach. The second rule for switching to the heavy-closure configuration is defined to be hospital occupancy nearing hospital capacity; specifically, the event $H^{tot}(t) = 0.95H^{max}$ (i.e., occupancy reaching a fixed threshold of 95% of capacity) is used if the instantaneous occupancy growth rate ($r(t) = \dot{H}^{tot}(t)/H^{tot}(t)$) is low (less than 0.025 - determined empirically), but the event $H^{tot}(t) = \exp\left(-r\frac{T^{E:I}+T^{I^s:H}}{2}\right)H^{max}$ (i.e., occupancy reaching a dynamic threshold that depends on the occupancy growth rate and time from exposure to hospital-admission) is used otherwise, in order to prevent large capacity breaches. However, if neither event occurs, sector closures will not be triggered, for example, for less transmissible and/or severe diseases or if the spare hospital capacity is large. In this case, the fully-open configuration is maintained throughout and the Reactive-Business/Sustained-School Closures strategy is indistinguishable from the No Closures strategy - this situation is termed 'Untriggered Closures'. Otherwise, if either event occurs, there is a switch to the heavy-closure configuration (see Table S3), which includes school closure. The third rule is for switching from the heavy-closure to the light-closure configuration, if there is a sufficient reduction in transmission, and it is defined to be hospital occupancy falling to the fixed threshold of 25% of capacity, $H^{tot}(t) = 0.25H^{max}$. The light-closure configuration involves broadly less-stringent sector closures for businesses, but school closures are sustained, replicating the long-term school closures observed in several middle-income countries during the Covid-19 pandemic [89,90]. The relative reductions in R_0 for both heavy- and light-closure configurations are shown in Figure S5, where it is apparent that there is less of a difference in transmission between the two configurations when compared to other closure strategies due to the sustenance of school closures. The strategy alternates between the light- and heavy-closure configurations depending on hospital occupancy via the aforementioned switching rules, until all mandated sector closures and home-working are lifted, and case isolation ceases, at T^{open}.

Reactive-Business/Reactive-School Closures

Under the Reactive-Business/Reactive-School Closures strategy, the switching rules are identical to the Reactive-Business/Sustained-School Closures strategy: distancing takes effect at the response time albeit with the fully-open configuration, the heavy-closure configuration is imposed if hospital occupancy nears hospital capacity as per the same event definitions, and the light-closure configuration is imposed subsequently conditional on a sufficient reduction in occupancy, as above. However, the difference between the Reactive-Business/Reactive-School and Reactive-Business/Sustained-School Closures strategies is the economic configurations employed (see Table S3). In particular, the heavy-closure configuration involves broadly more-stringent sector closures for businesses compared to the heavy-closure configuration for the Reactive-Business/Sustained-School Closures strategy, with the same level of school closure, but the light-closure configuration allows schools to reopen unlike the light-closure configuration for the Reactive-Business/Sustained-School Closures strategy. Accordingly, the relative reductions in R_0 in Figure S5 are more different between the heavy- and light-closure configurations, and flank the distributions of both the heavy- and light-closure configurations of the Reactive-Business/Sustained-School Closures strategy above. Therefore, the strategy alternates between light- and heavy- simultaneous school- and business-closures depending on hospital occupancy, replicating the reactive suppression strategies observed during the Covid-19 pandemic[87,88], until all mandated sector closures and home-working are lifted, and case isolation ceases, at T^{open}.

Elimination

Under the Elimination strategy, the first switching rule is reaching the response time with the activation of distancing, as for the other strategies, but now the heavy-closure configuration is imposed immediately. Here, the heavy-closure configuration is identical to that of the Reactive-Business/Reactive-School Closures strategy, with stringent sector closures of both businesses and schools, with the aim of reducing prevalence to the extent that case isolation substitutes the need for stringent business and school closures. Since the IARs increase in the high-ascertainment régime at low prevalence, this substitution is possible even for more transmissible diseases provided that there is a sufficiently high level of ascertainment and isolation effectiveness (see section 2.3), and if the reduction in transmission under the heavy-closures configuration is sufficient to cross the prevalence threshold. The second rule for switching to the light-closure configuration is if the effective reproduction number conditional on switching to the light-closure configuration is subcritical, i.e. $R_t(M(x_{j,\text{light}}, q_j)) < 1$, for total contact matrix $M(x_j(t), q_j(t))$, light-closure configuration $x_{j,\text{light}}$ and the proportion of workers home-working q_j (see section 2.1). The light-closure configuration involves broadly less-stringent sector closures for businesses compared to the light-closure configuration for either the Reactive-Business/Sustained-School or Reactive-Business/Reactive-School Closures strategies, and also allows schools to reopen (see Table S3), replicating the Covid-zero strategies that allowed for an open domestic economy when successful[85,86]. The relative reduction in R_0 for the light-closure configuration in the high-ascertainment régime of case isolation is shown in Figure S5, accounting for the variability in isolation effectiveness between diseases and ascertainment between income groups. The third rule is for switching back to the heavy-closure configuration if there is an increase in transmission that threatens containment, defined to be an instantaneous effective reproduction number $R_t > 1.2$, for example due to the waning of vaccine-induced immunity to infection. The strategy alternates between the light- and heavy-closure configurations depending on the conditional and instantaneous effective reproduction numbers via the aforementioned switching rules until all mandated sector closures and home-working are lifted, and case isolation ceases, at T^{open}. Since this is an elimination strategy and not an eradication strategy[93], it is possible that there is an 'exit wave' after T^{open}, depending on the vaccine rollout and the vaccination parameters drawn.

Each closure strategy - its economic configurations and switching rules - is implemented in the same manner for each synthetic country within each income-group archetype. However, the reduction in transmission under a given economic configuration depends on several underlying parameters, including the number of workers in each economic sector, the magnitude of workplace contacts and the proportion of workers capable of home-working (see Figure S1). The rules for switching between configurations are also inherently linked to the mitigation measure parameters, including the response time, maximum infection ascertainment ratio, spare hospital beds, and vaccination administration start-time and rate (see Figure S2). Therefore, it is expected that any systematic differences in parameters between different income-group archetypes as seen in Figures S1 and S2, will manifest in terms of the occurrence, duration and frequency of sector closures, and the associated short- and long-term losses (see section 2.5). A realisation of each closure strategy is plotted in Figure S6.

The economic configurations for every closure strategy are shown in Table S3, the values of which were calculated based on the ratio of GVA observed during the Covid-19 pandemic to the corresponding pre-pandemic values by economic sector, where data for the Reactive-Business/Sustained-School Closures strategy were obtained from Indonesia[94], data for the Reactive-Business/Reactive-School Closures strategy from the UK[95] and data for the Elimination strategy from the UK[95] and Australia[96] for the heavy and light configurations respectively. The dichotomous values for the education sector (0.10 or 1) are assumed to correspond to school closure and openness respectively, rather than calculated from GVA data. Home-working data were generated on a country-by-country basis: UK data on the proportion of workers home-working by sector were sourced from the ONS[97] and mapped to different countries, using country-level estimates of the total proportion of the workforce home-working[98] combined with the aforementioned workforce data from the OECD[26] and the ILO[27].

Economic Sector	No Closures	Reactive-Business/ Sustained-School Closures		Reactive-Business/ Reactive-School Closures		Elimination	
		Heavy	Light	Heavy	Light	Heavy	Light
1: Agriculture, Hunting, Forestry	1	1	1	0.86	0.88	0.86	1
2: Fishing and Aquaculture	1	1	1	0.86	0.88	0.86	1
3: Mining and Quarrying, Energy Producing Products	1	0.67	0.79	0.90	0.91	0.90	1
4: Mining and Quarrying, Non-Energy Producing Products	1	1	1	0.90	0.91	0.90	1
5: Mining Support Service Activities	1	1	1	0.90	0.91	0.90	1
6: Food Products, Beverages and Tobacco	1	1	1	0.70	0.94	0.70	1
7: Textiles, Textile Products, Leather and Footwear	1	0.89	0.92	0.70	0.94	0.70	0.98
8: Wood and Products of Wood and Cork	1	1	0.95	0.70	0.94	0.70	0.98
9: Paper Products and Printing	1	1	0.98	0.70	0.94	0.70	0.98
10: Coke and Refined Petroleum Products	1	0.87	0.88	0.70	0.94	0.70	0.88
11: Chemical and Chemical Products	1	1	1	0.70	0.94	0.70	0.88
12: Pharmaceuticals, Medicinal Chemical and Botanical Products	1	1	1	0.70	0.94	0.70	0.88
13: Rubber and Plastics Products	1	0.87	1	0.70	0.94	0.70	0.88
14: Other Non-Metallic Mineral Products	1	0.92	0.89	0.70	0.94	0.70	0.88
15: Basic Metals	1	1	1	0.70	0.94	0.70	1
16: Fabricated Metal Products	1	0.90	1	0.70	0.94	0.70	1
17: Computer, Electronic and Optical Equipment	1	0.90	1	0.70	0.94	0.70	1
18: Electrical Equipment	1	0.90	1	0.70	0.94	0.70	1
19: Machinery and Equipment, NEC	1	0.89	0.95	0.70	0.94	0.70	1
20: Motor Vehicles, Trailers and Semi-Trailers	1	0.66	0.82	0.70	0.94	0.70	1
21: Other Transport Equipment	1	0.66	0.82	0.70	0.94	0.70	1
22: Manufacturing NEC; Repair and Installation of Machinery and Equipment	1	0.98	1	0.70	0.94	0.70	0.98
23: Electricity, Gas, Steam and Air Conditioning Supply	1	0.94	0.94	0.89	1	0.89	0.97
24: Water Supply, Sewerage, Waste Management and Remediation Activities	1	1	1	0.92	0.98	0.92	0.97

continued on next page

continued from previous page

Economic Sector	**No Closures**	**Reactive-Business/ Sustained-School Closures**		**Reactive-Business/ Reactive-School Closures**		**Elimination**	
25: Construction	1	0.95	0.95	0.56	0.92	0.56	0.94
26: Wholesale and Retail Trade, Repair of Motor Vehicles	1	0.92	0.97	0.65	1	0.65	1
27: Land Transport and Transport via Pipelines	1	0.83	1	0.63	0.82	0.63	1
28: Water Transport	1	0.81	0.98	0.63	0.82	0.63	1
29: Air Transport	1	0.16	0.42	0.63	0.82	0.63	0.18
30: Warehousing and Support Activities for Transportation	1	0.64	0.91	0.63	0.82	0.63	0.91
31: Postal and Courier Activities	1	0.64	0.91	0.63	0.82	0.63	0.91
32: Accommodation and Food Service Activities	1	0.77	0.91	0.10	0.85	0.10	0.92
33: Publishing, Audiovisual and Broadcasting Activities	1	1	1	0.88	0.91	0.88	1
34: Telecommunications	1	1	1	0.88	0.91	0.88	1
35: IT and Other Information Services	1	1	1	0.88	0.91	0.88	1
36: Financial and Insurance Activities	1	1	1	0.95	0.96	0.95	1
37: Real Estate Activities	1	1	1	0.98	0.99	0.98	1
38: Professional, Scientific and Technical Activities	1	0.90	0.95	0.85	0.92	0.85	1
39: Administrative and Support Services	1	0.90	0.95	0.66	0.80	0.66	0.90
40: Public Administration and Defence, Compulsory Social Security	1	0.96	1	1	1	1	1
41: Education	1	0.10	0.10	0.10	1	0.10	1
42: Human Health and Social Work Activities	1	1	1	0.75	0.92	0.75	1
43: Arts, Entertainment and Recreation	1	0.90	0.96	0.55	0.71	0.55	0.94
44: Other Service Activities	1	0.90	0.96	0.54	0.83	0.54	0.94
45: Activities of Households as Employers, Undifferentiated Goods- and Services-Producing Activities of Households for Own Use	1	0.90	0.96	0.49	0.53	0.49	0.94
	Assumed	Calculated [94]	Calculated [94]	Calculated [95]	Calculated [95]	Calculated [95]	Calculated [96]

Table S3: Economic configurations for different closure strategies: the extent to which each economic sector is open during times of heavy and light closures, denoted $x_j(t)$, expressed as a proportion. Each closure strategy begins and ends with the fully-open configuration $x_j(t) = 1$.

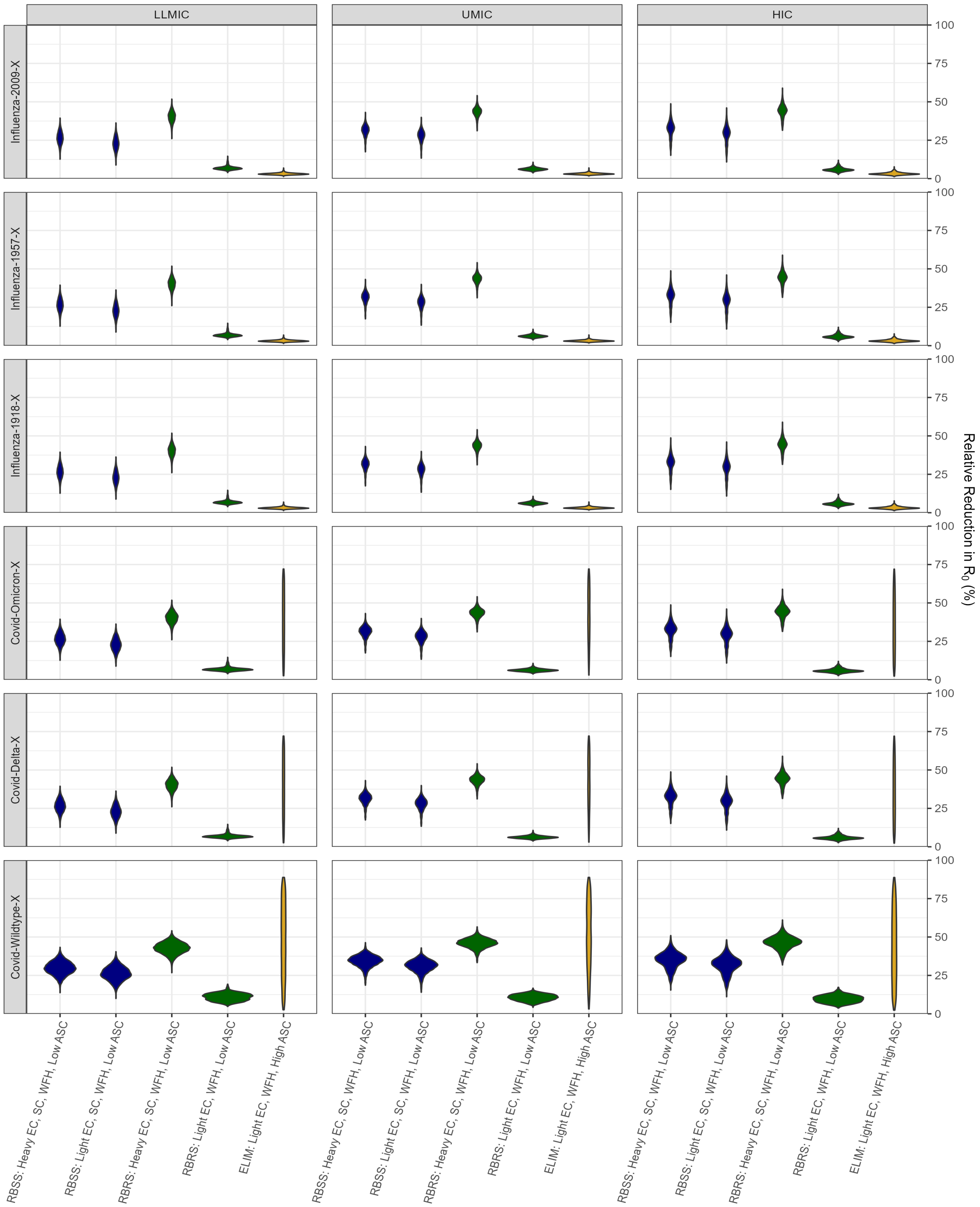

Figure S5: Distributions of the relative reduction in R_0 under different closure strategy configurations and corresponding ascertainment régimes, for each disease and country-income-group archetype. The closure strategies (colours) include Reactive-Business/Sustained-School Closures (RBRS), Reactive-Business/Reactive-School Closures (RBRS) and Elimination (ELIM), and the light- and heavy-closure configurations encompass economic closures (EC), school closures (SC) and working-from-home (WFH), as indicated on the plot axis. The Elimination strategy heavy-closure configuration is identical to that of the Reactive-Business/Reactive-School Closures strategy (see Table 2.4) and hence not plotted, nor is the No Closures strategy shown, since there is no mandated closures nor working-from-home. The distributions exclude the additional reduction in transmission associated with distancing (see Figure S4), but include the reduction in transmission associated with case isolation in the low- and high-ascertainment régimes (see section 2.3), where it is noted that the Elimination strategy light-closure configuration is only likely to be entered in the high-ascertainment régime at low prevalence.

2.5 Socioeconomic Loss

In order to compare outcomes under different closure strategies, the health, economic and educational losses are quantified from a societal perspective[99]. Following a similar method to recent work by Johnson and colleagues[16], the total socioeconomic loss (TSL) is defined as the sum of the value of life-years lost (VLYL), GDP loss (GDPL) and the value of school-years lost (VSYL):

$$\begin{aligned}
\text{TSL} &= \text{VLYL} &+& \quad \text{GDPL} &+& \quad \text{VSYL} \\
&= \text{LYL} \cdot \text{VLY} &+& \left(\tfrac{T^{end}}{365} Y_0 - Y\right) &+& \quad \text{SYL} \cdot \text{VSY},
\end{aligned}$$

where LYL is the number of life-years lost, Y is actual GDP relative to annual pre-pandemic GDP Y_0 and SYL is the number of school-years lost (see subsequent paragraphs). VLY is the monetary value of a life-year and VSY is the monetary value of a school-year, used to convert the losses to common units, which allows for the comparison of scenarios with potential trade-offs between competing objectives. Discounting is not applied; therefore, these values represent unweighted monetary losses at the time of pandemic occurrence, rather than the present value. See 16 for more details on the losses that are included and excluded. In this study, the TSL and its components are normalised by annual pre-pandemic GDP, i.e. TSL/Y_0, VLYL/Y_0, GDPL/Y_0 and VSYL/Y_0, to also allow for comparison of losses between different income-group archetypes.

Health Loss: Value of Life-Years Lost

The VLYL is the product of the number of life-years lost LYL and the value of a life-year VLY, where the valuation of life is based on the intrinsic rather than the instrumental interpretation[100], i.e. an individual's willingness to pay for reductions in their own mortality risk. The number of life-years lost is defined as

$$\text{LYL} = \sum_{j,v} D_{j,v}(T^{end}) \hat{l}_{g(j)}^{(death)},$$

where $\sum_{j,v} D_{j,v}(T^{end})$ is the cumulative number of deaths by the end of the simulation T^{end} and

$$\hat{l}_g^{(death)} = \sum_{a \in g} \tilde{l}_a \frac{\tilde{p}_a^{IFR} \tilde{N}_a}{\sum_{a' \in g} \tilde{p}_{a'}^{IFR} \tilde{N}_{a'}}$$

is the aforementioned remaining life-expectancy mapped from five-year age-bands to the model age-groups weighting by population and IFR. The value of a life-year is defined as

$$\text{VLY} = \frac{\text{VSL}}{\left(\frac{\sum_g \hat{l}_g^{(life)} \hat{N}_g}{\sum_g \hat{N}_g}\right)}$$

where VSL is the value of a statistical life and

$$\hat{l}_g^{(life)} = \sum_{a \in g} \tilde{l}_a \frac{\tilde{N}_a}{\sum_{a' \in g} \tilde{N}_{a'}}$$

is the aforementioned remaining life-expectancy mapped from five-year age-bands to the model age-groups weighting by population only. Here, the VSL is interpreted to be the population- and remaining-life-expectancy-weighted-average VLY, where each year has equal value[101,102]. The VSL itself is calculated according to the Masterman-Viscusi model[103] extrapolating from values for the USA, specifically

$$\text{VSL} = \begin{cases} \text{VSL}^{\text{USA}} \left(\dfrac{\text{GDP}_{pc}}{\$8809}\right) \left(\dfrac{\$8809}{\text{GDP}_{pc}^{\text{USA}}}\right)^{0.85} & \text{if } \text{GDP}_{pc} < \$8809, \\ \text{VSL}^{\text{USA}} \left(\dfrac{\text{GDP}_{pc}}{\text{GDP}_{pc}^{\text{USA}}}\right)^{0.85} & \text{otherwise;} \end{cases}$$

where $\text{VSL}^{\text{USA}} = \$10,900,000$ is the VSL of the USA[104], $\text{GDP}_{pc}^{\text{USA}} = \$60,362$ is the GDP per capita of the USA[28], and $\text{GDP}_{pc} = Y_0 / \sum_j N_j$ is GDP per capita of the synthetic country in question, given annual pre-pandemic GDP Y_0.

Economic Loss: GDP Loss

The GDPL is the deviation of the actual GDP Y from a counterfactual scenario with $\frac{T^{end}}{365}$ years of annual pre-pandemic GDP Y_0, which is a measure of the short-term loss of GDP induced by reduced labour supply due to the disease itself (worker illness and death) and due to mitigation (economic sector closures and worker isolation). Here, actual GDP is defined as

$$Y = \sum_{j \neq edu}^{45} \frac{y_j}{365} \int_{t=0}^{T^{end}} x_j(t)(N_j - N_j^{abs}(t))dt \; + \; \frac{y_{edu}}{365} N_{edu} T^{end},$$

where y_j is annual GVA per worker in sector j, $N_j - N_j^{abs}(t)$ is the available workforce given $N_j^{abs}(t)$ worker absences due to illness, death and isolation, and $x_j(t)$ is the extent to which each sector is open at time t (see section 2.4). Note that the education sector is treated separately (see subsequent paragraphs). The assumption underlying this equation is that the production of each economic sector scales linearly with both the extent to which it is open and the effective labour supply available to it, at a given time. In particular, the number of worker absences in sector j at time t is defined as

$$N_j^{abs}(t) = \sum_v \left(I^s_{j,v}(t) + H_{j,v}(t) + D_{j,v}(t) + I^{ai}_{j,v}(t) \frac{T^{iso}}{T^{I^a:R}} (1 - q_j(t)) + I^{si}_{j,v}(t) \frac{T^{iso}(1 - p^H_{j,v}(t)) + T^{I^s}_{j,v}(t) p^H_{j,v}(t)}{T^{I^s}_{j,v}(t)} \right),$$

where the number of isolating asymptomatic infectious $I^a j, v(t)$ and isolating symptomatic infectious $I^s j, v(t)$ are scaled by the mandatory isolation period T^{iso} relative to the corresponding infectious periods (see sections 2.2 and 2.3), and $T^{iso} = T^{E:I} + \max(T^{I^a:R}, T^{I^s:R}, T^{I^s:H})$. It is assumed that the isolating asymptomatic infectious are also capable of home-working, even if isolating, and so $I^a j, v(t)$ is also scaled by the complement of the proportion of workers home-working $q_j(t)$. Here, the economic impact is measured solely in terms of reduced labour supply, but other factors such as behavioural changes regarding the supply of labour or consumption, changes in capital, or price dynamics are not considered.

Educational Loss: Value of School-Years Lost

The VSYL is the product of the number of school-years lost SYL and the value of a school-year VSY, which is a measure of the impact of lost education on long-term worker productivity and economic growth [16]. The number of school-years lost is defined as

$$\text{SYL} = \frac{1}{365} \int_{t=0}^{T^{end}} \left(N^{abs}_{stu}(t) + (N_{stu} - N^{abs}_{stu}(t))(1 - x_{edu}(t))(1 - 1/3) \right) dt,$$

where $N_{stu} = N_{47}$ is the school-age population, $N^{abs}_{stu}(t)$ is the number of student absences due to illness, death and isolation, and $x_{edu}(t) = x_{41}(t)$ is the extent to which the education sector is open. This equation encodes education lost due to the disease itself (student illness and death) and due to mitigation (school closures and student isolation), but accounts for the effect of remote teaching in alleviating the education lost due to school closures specifically, assuming relative effectiveness of remote teaching of 1/3 [105,106]. In particular, the number of student absences at time t is defined as

$$N^{abs}_{stu}(t) = \sum_v \left(I^s_{47,v}(t) + H_{47,v}(t) + D_{47,v}(t) + I^{ai}_{47,v}(t) \frac{T^{iso}}{T^{I^a:R}} + I^{si}_{47,v}(t) \frac{T^{iso}(1 - p^H_{47,v}(t)) + T^{I^s}_{47,v}(t) p^H_{47,v}(t)}{T^{I^s}_{47,v}(t)} \right),$$

analogous to worker absences above, except for the home-working scaling factor. The value of a school-year (per student) is defined as

$$\text{VSY} = \frac{p^{GDP} Y_0}{N_{stu}},$$

where

$$p^{GDP} = \begin{cases} 1.07 & \text{for LLMICs,} \\ 0.67 & \text{for UMICs,} \\ 0.27 & \text{for HICs;} \end{cases}$$

is the income-group-dependent proportion of annual pre-pandemic GDP lost (in the long-term but discounted to present-day) under one year of school closures, calculated from Psacharopoulos et al. [107]. It is assumed that each VSY has equal value in time, applied equally to the number of school-years lost, meaning that any potential 'catch-up' in lost education following the reopening of schools is not considered[108,109].

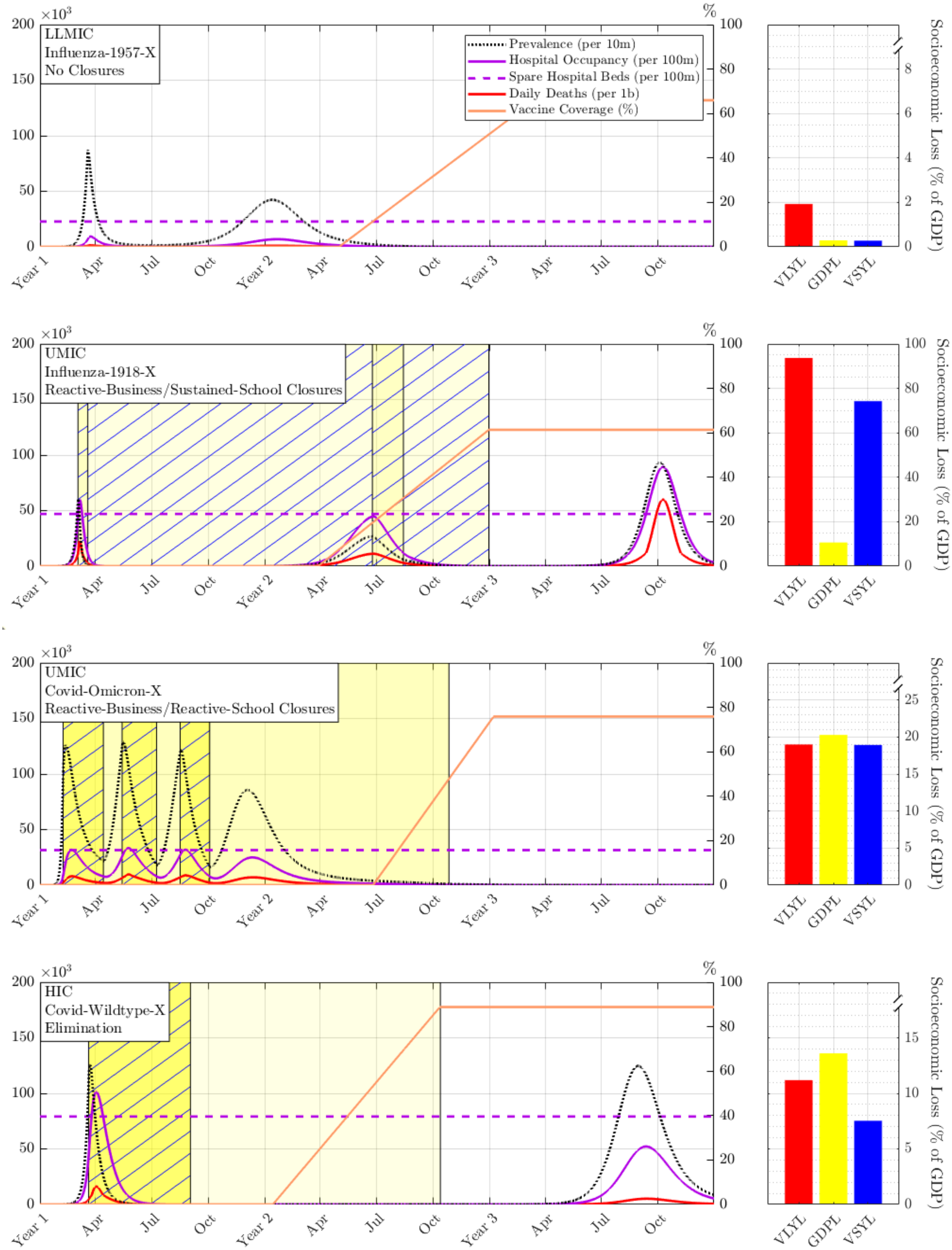

Figure S6: A realisation of each closure strategy and the resulting socioeconomic losses (expressed as a percentage of annual GDP) broken down into VLYL, GDPL and VSYL, for various diseases and country-income groups. The yellow shading represents the average extent of economic closures for businesses imposed at a given time and the blue diagonal lines represent whether school closures are imposed, under a given strategy.

Data	Source	Year	Reference
Population by Age	United Nations	2019	23
Life-Expectancy by Age	WHO	2025	24
Workforce by Sector	OECD, ILO	2021, 2025	26, 27
GVA by Sector	OECD	2021	28
Contact Matrices by Age and Setting	Prem et al. (2017), (2021)	2017, 2021	30, 31
Google Mobility Trends by Setting	Our World in Data	2020	60
Covid-19 Stringency Index	Our World in Data	2021	61
Covid-19 Deaths	Our World in Data	2020	63
Covid-19 Excess Mortality	Wang et al. (2022)	2022	64
Covid-19 Testing	Our World in Data	2020	75
Covid-19 Ascertainment	Russell et al.	2020	76
Hospital Beds	World Bank	2021	77
Hospital Bed Occupancy Rate	WHO	2024	78
Covid-19 Vaccinations	Our World in Data	2020	81
Working-from-Home	Gottlieb et al. (2021)	2021	98

Table S4: Overview of country-level data employed in the analysis, sources and references.

3 Additional Figures

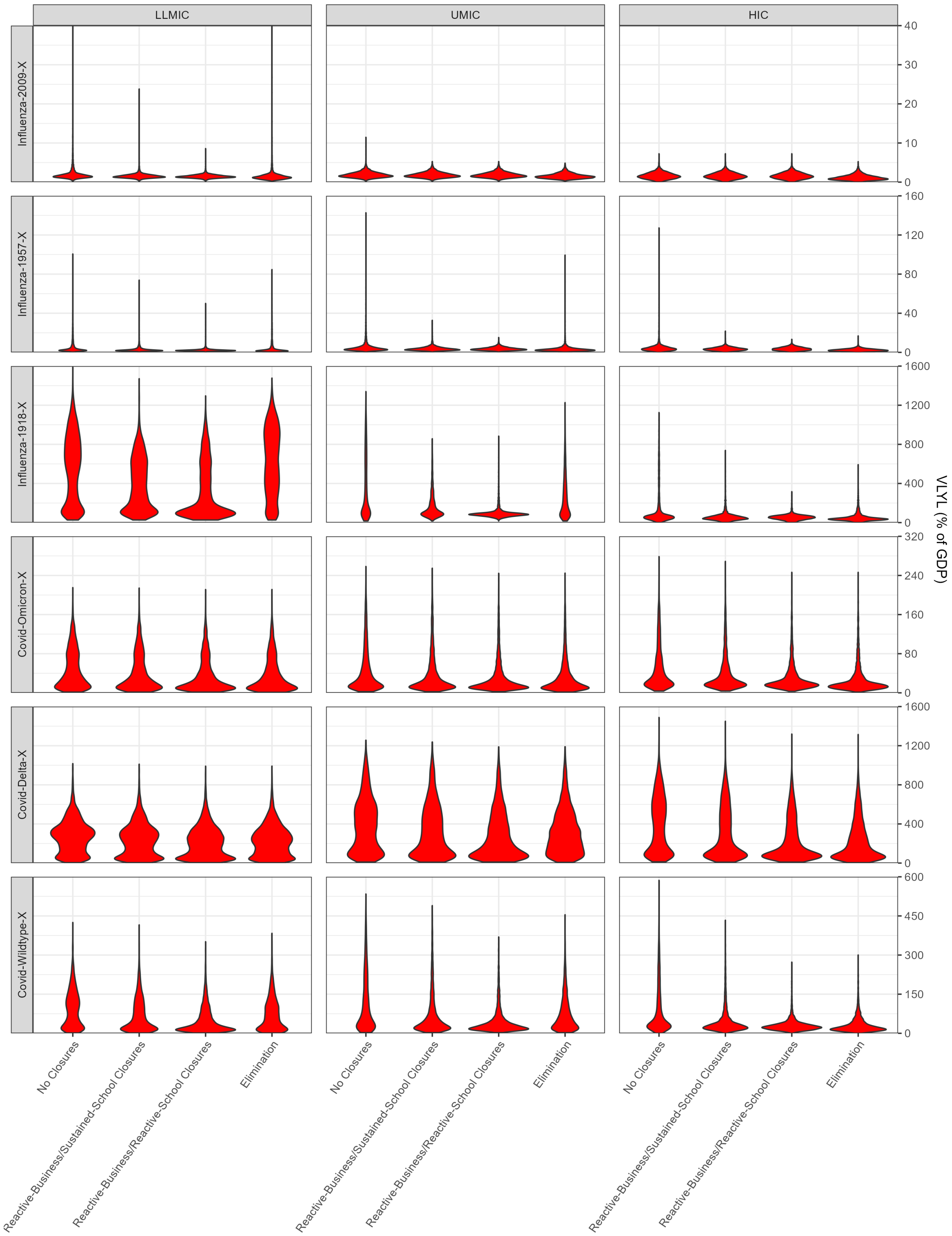

Figure S7: Distributions of projected VLYL (expressed as a percentage of annual GDP) under different closure strategies, for each disease and country-income group. Summary statistics are shown in Table S6.

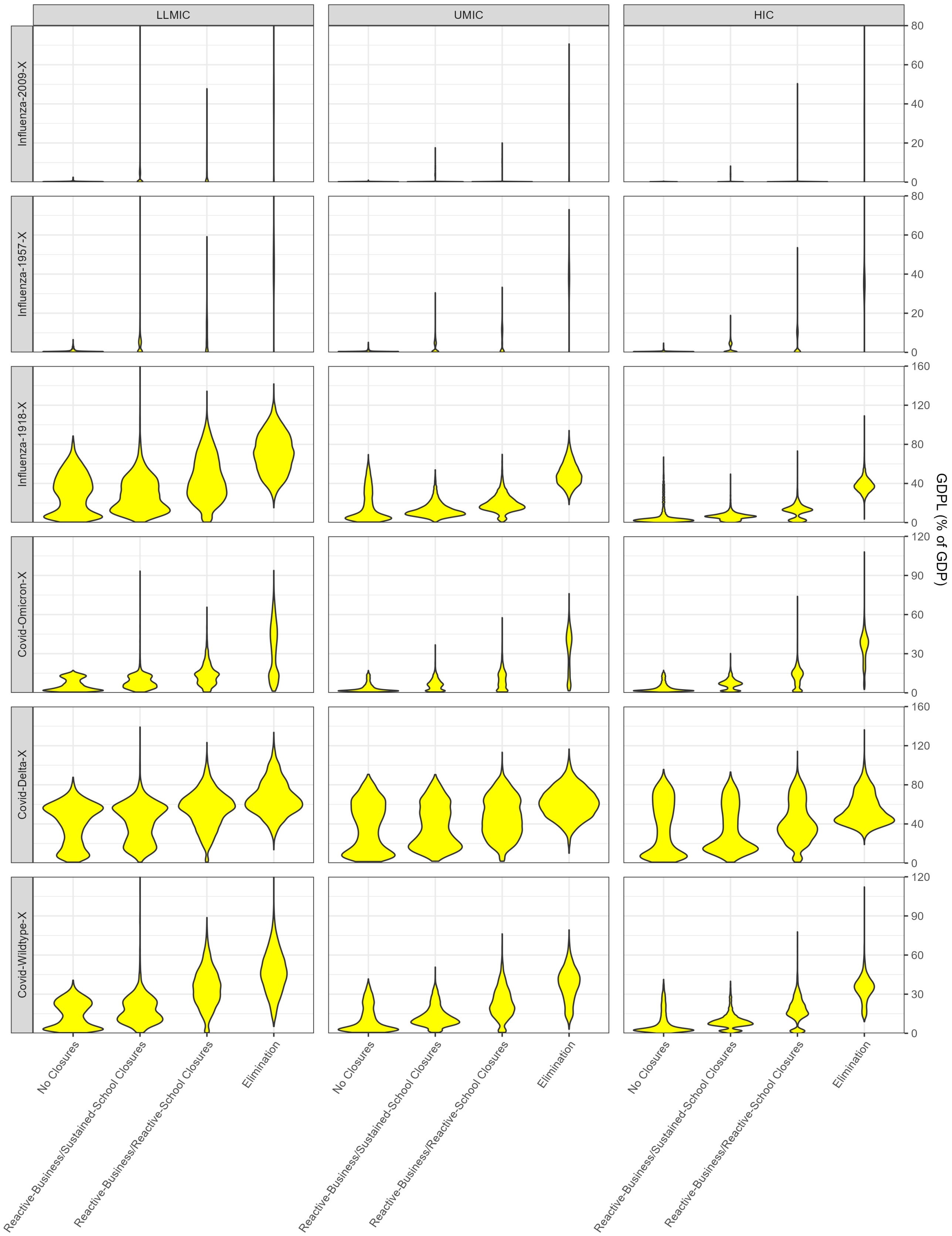

Figure S8: Distributions of projected GDPL (expressed as a percentage of annual GDP) under different closure strategies, for each disease and country-income group. Summary statistics are shown in Table S7.

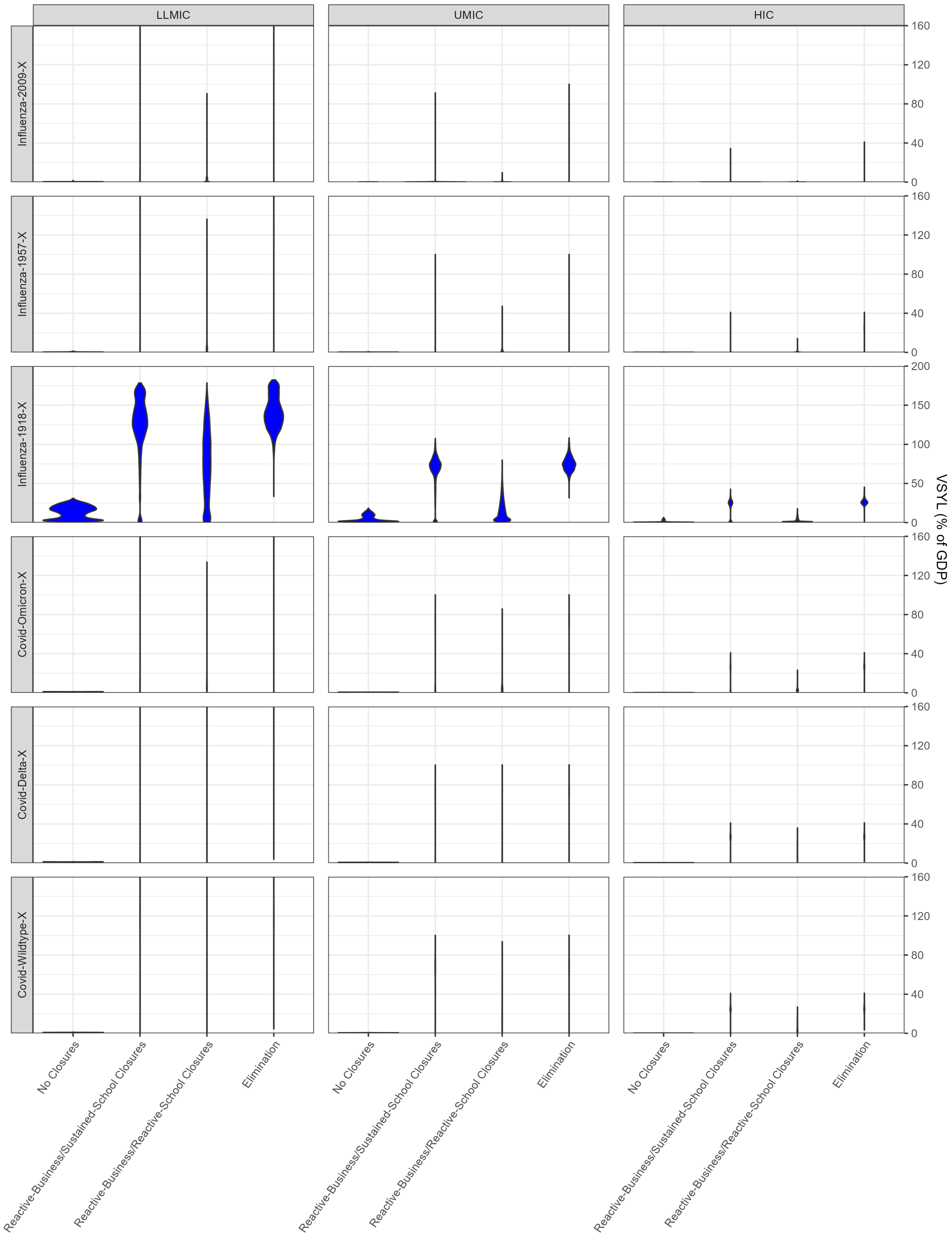

Figure S9: Distributions of projected VSYL (expressed as a percentage of annual GDP) under different closure strategies, for each disease and country-income group. Summary statistics are shown in Table S8.

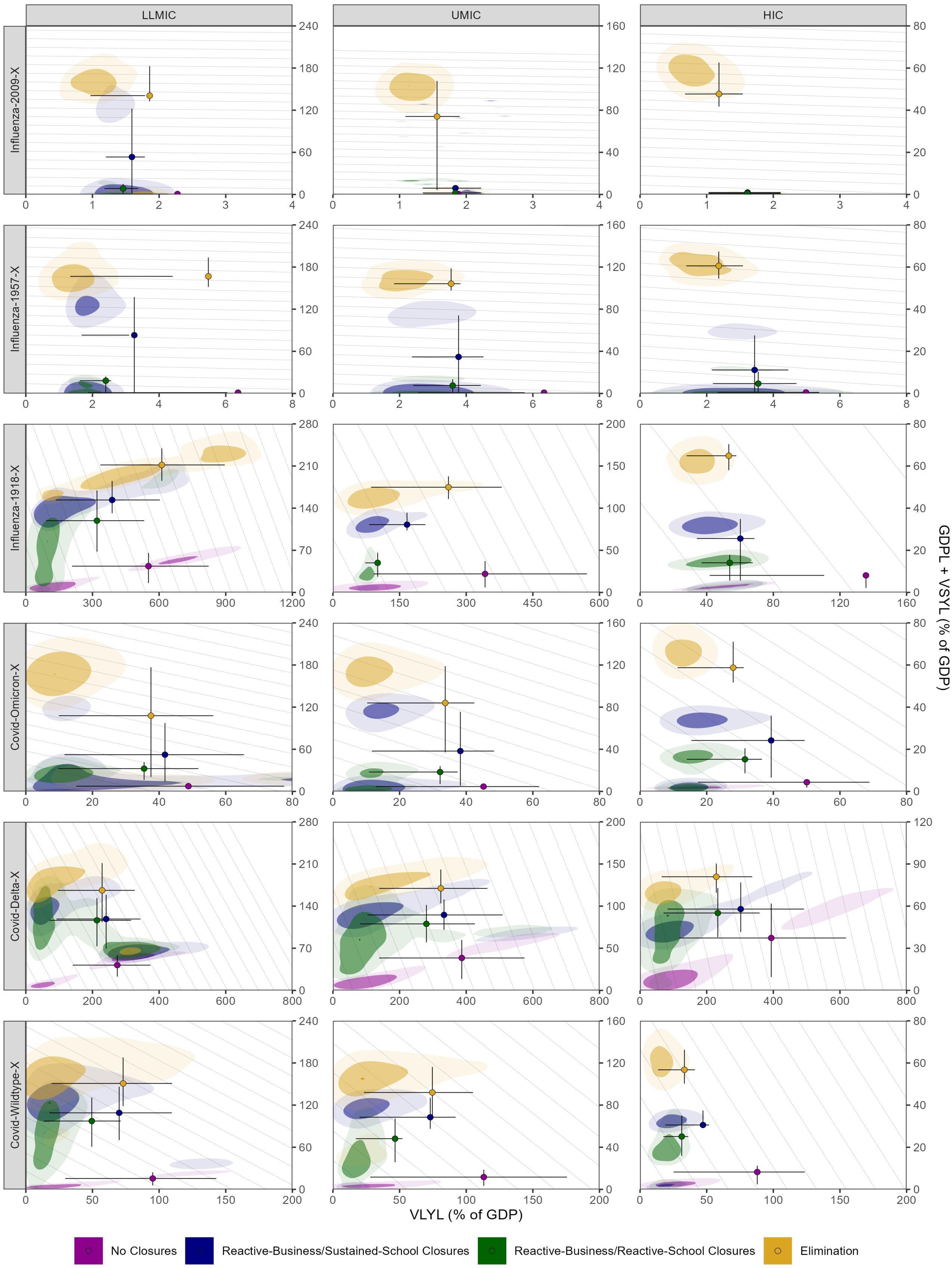

Figure S10: Joint distributions of projected VLYL and GDPL + VSYL (expressed as a percentage of annual GDP) under different closure strategies, for each disease and country-income group. The mean VLYL and GDPL + VSYL (circles), and inter-quartile range (errorbars) are plotted for each closure strategy (colours). Summary statistics are shown in SI Tables S6-S8.

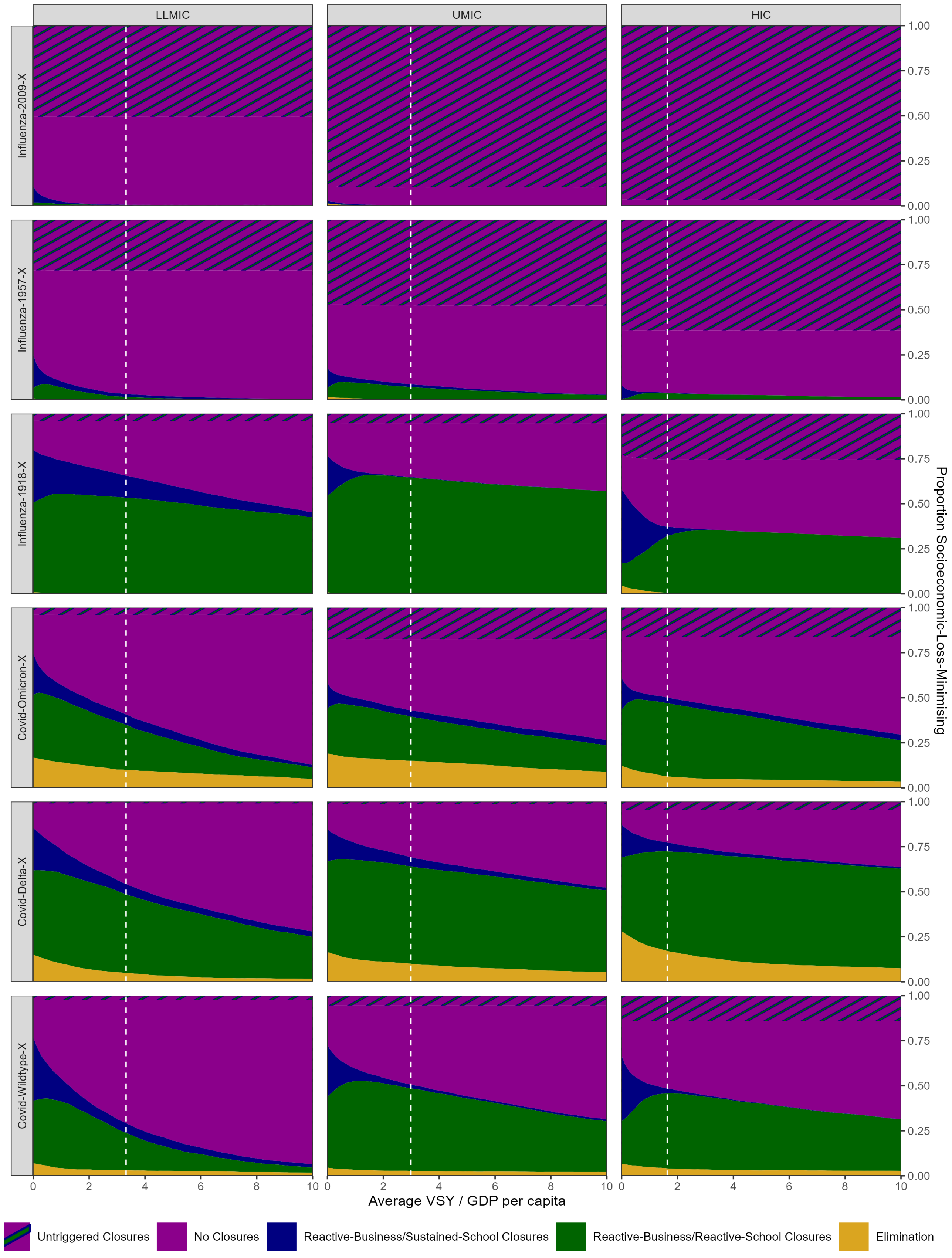

Figure S11: Proportion of synthetic countries for which each closure strategy is socioeconomic-loss-minimising, as a function of average VSY (expressed as a multiple of GDP per capita), for each disease and country-income group. Untriggered Closures is not a distinct closure strategy (colours), but instead refers to the situation where closures are not triggered under the Reactive-Business/Sustained-School or Reactive-Business/Reactive-School Closures strategies, resulting in socioeconomic loss equal to that of the No Closures strategy. The vertical dashed line represents the income-group-average VSY at baseline.

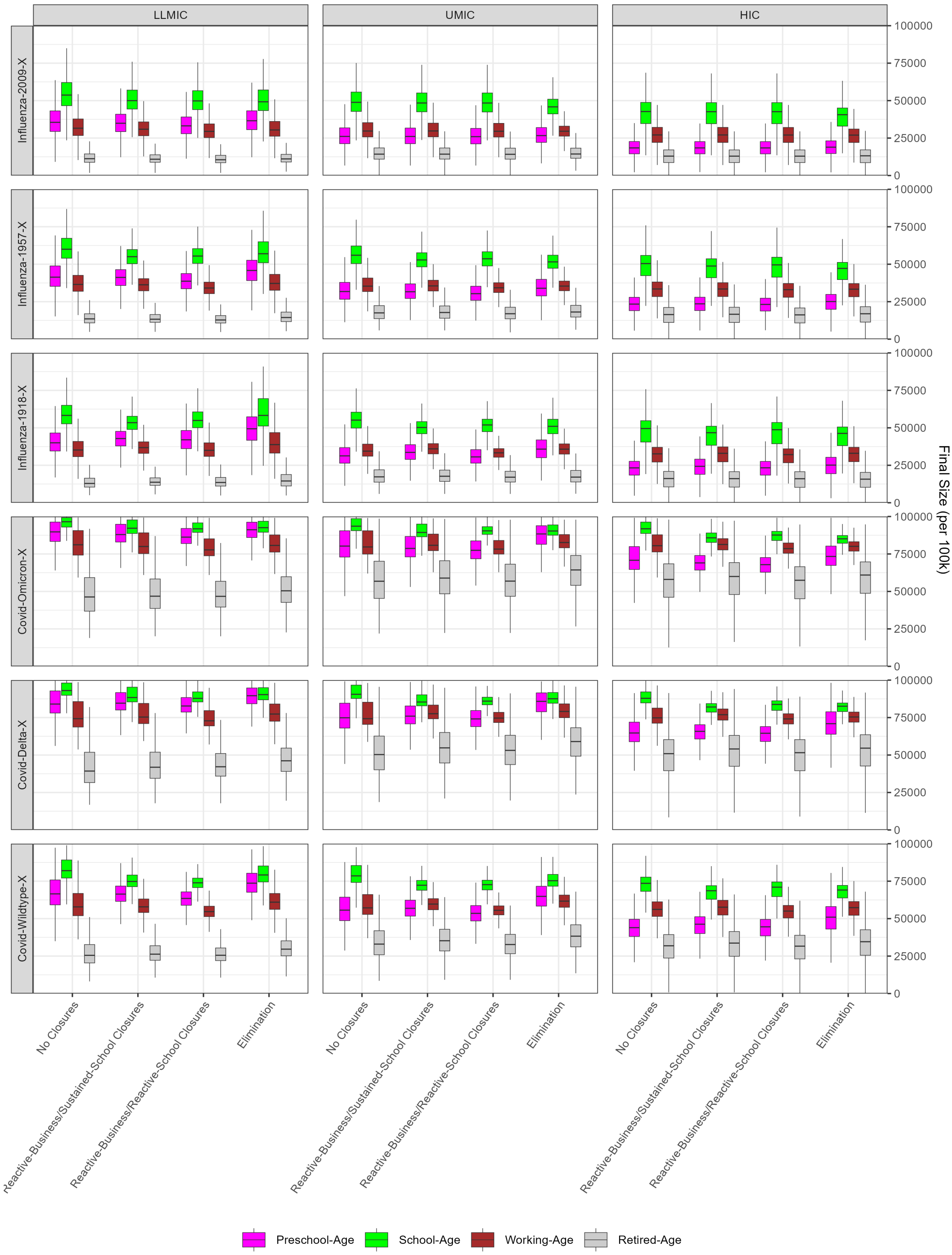

Figure S12: Distributional effects: distributions of projected epidemic final size by age-group (per 100k population) under different closure strategies, for each respiratory disease and country-income group.

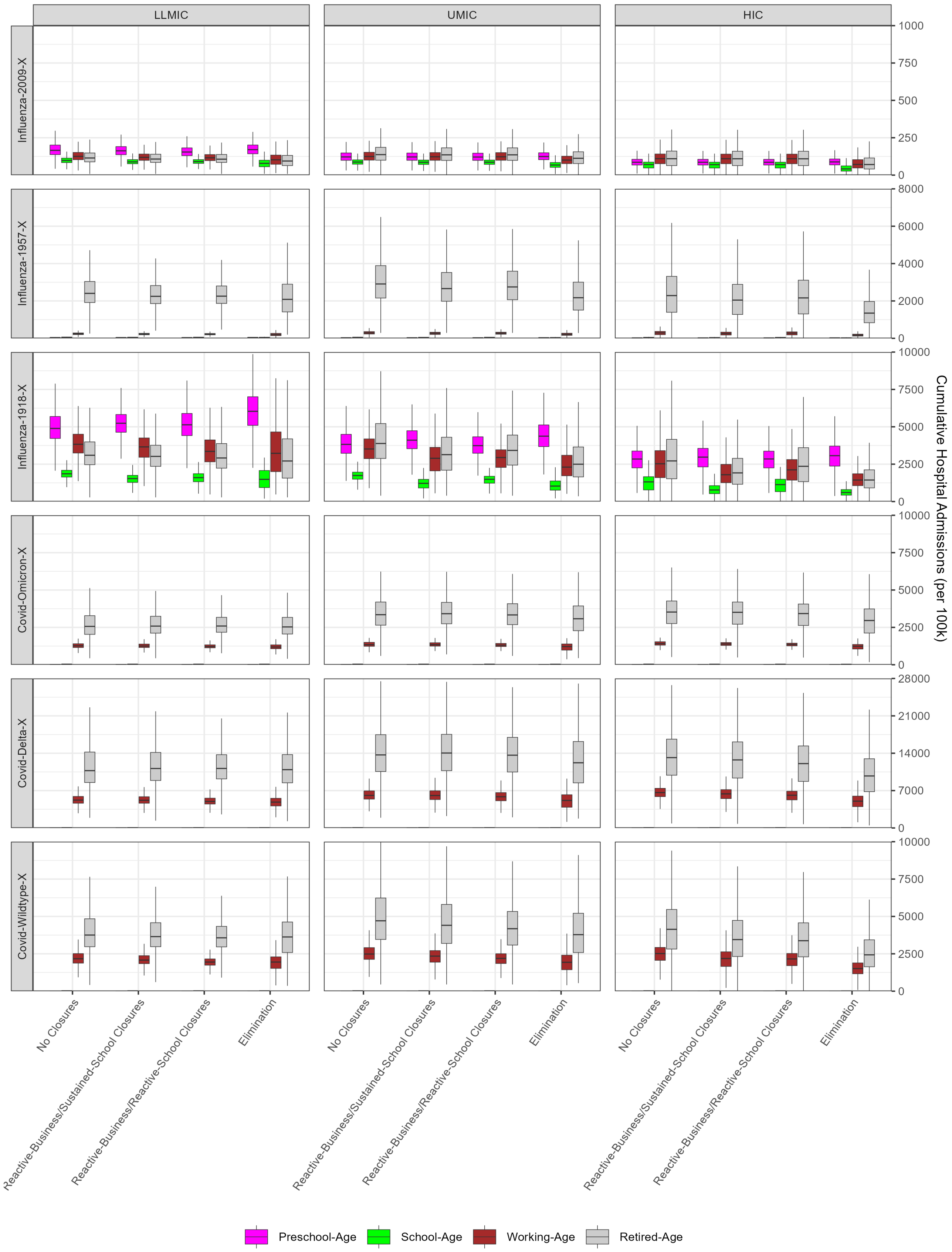

Figure S13: Distributional effects: distributions of projected cumulative hospital admissions by age-group (per 100k population) under different closure strategies, for each respiratory disease and country-income group.

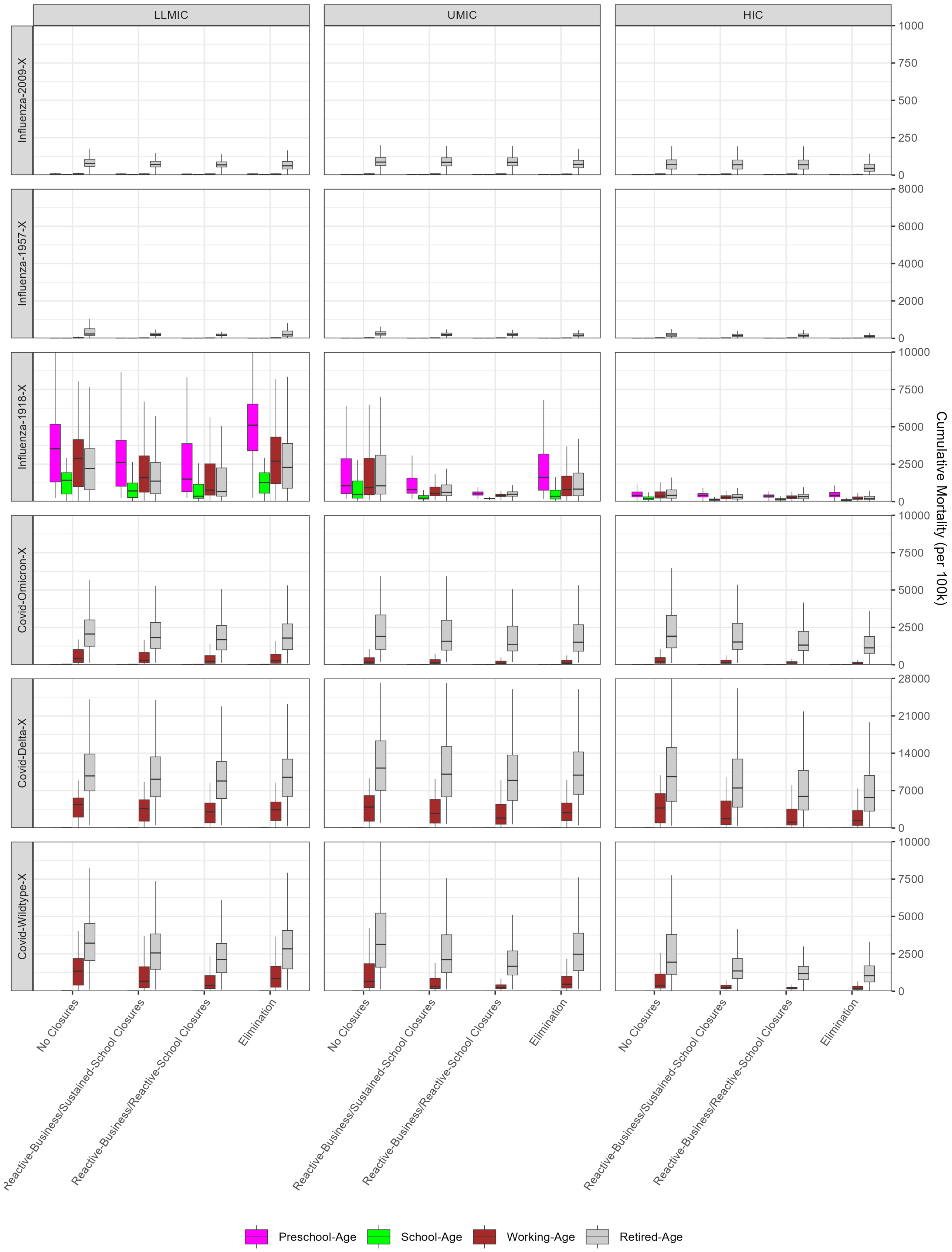

Figure S14: Distributional effects: distributions of projected mortality by age-group (per 100k population) under different closure strategies, for each respiratory disease and country-income group.

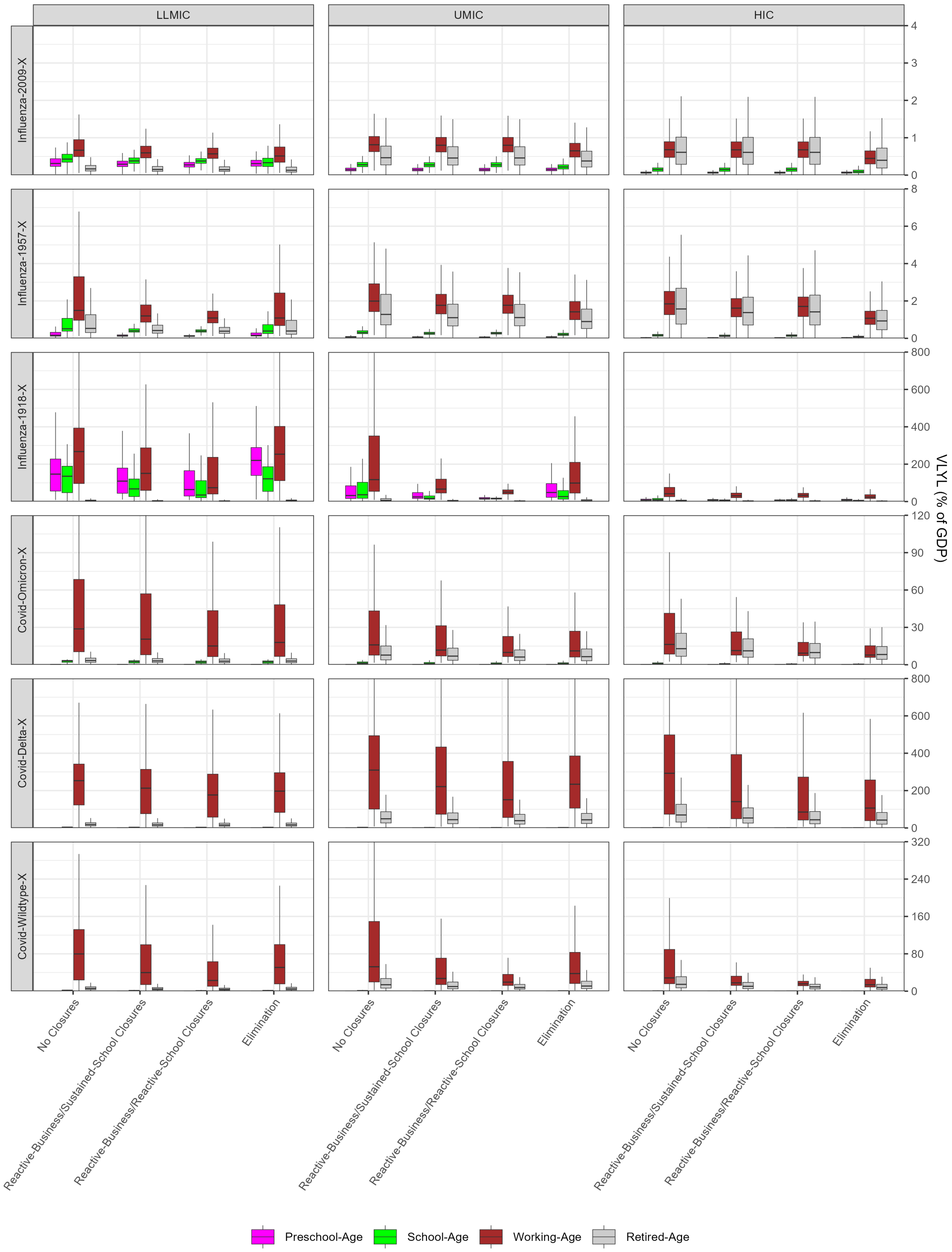

Figure S15: Distributional effects: distributions of projected value of life-years lost (VLYL) by age-group (expressed as a percentage of annual GDP) under different closure strategies, for each respiratory disease and country-income group. Summary statistics are shown in Table S10.

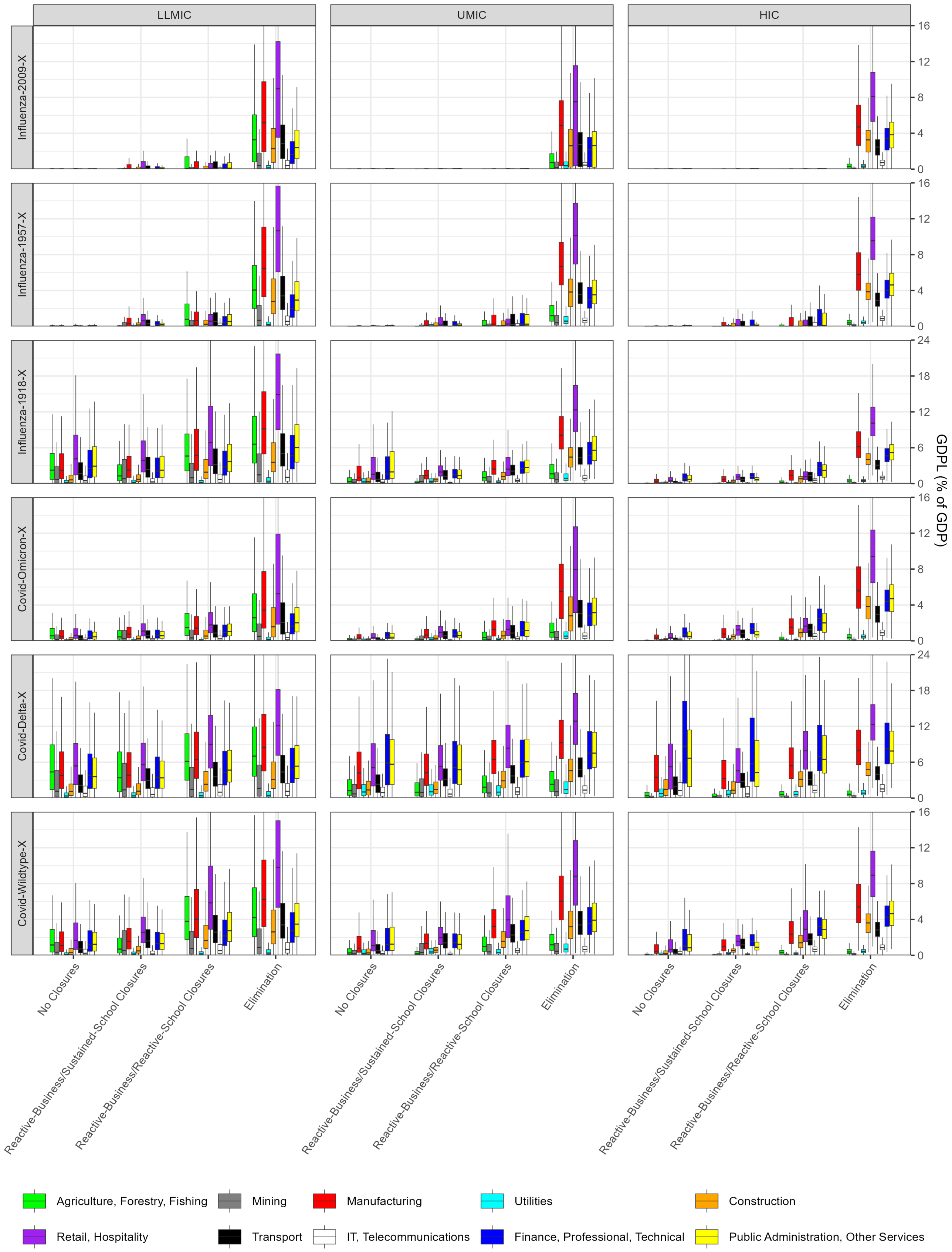

Figure S16: Distributional effects: distributions of projected GDP loss (GDPL) by aggregate economic sector (expressed as a percentage of annual GDP) under different closure strategies, for each disease and country-income group. Summary statistics are shown in Table S11.

4 Additional Tables

Income Group / Disease	Closure Strategy	Mean	SD	Q_1	Q_2	Q_3
LLMIC						
Influenza-2009-X	**No Closures***†	2.9	3.0	1.8	2.2	2.8
	Reactive-Business/Sustained-School Closures	55.0	66.0	2.0	3.0	123.5
	Reactive-Business/Reactive-School Closures	9.9	11.0	2.0	3.1	16.2
	Elimination	142.6	68.1	134.1	160.3	184.7
Influenza-1957-X	**No Closures***†	7.6	10.3	2.6	3.5	7.2
	Reactive-Business/Sustained-School Closures	86.3	66.7	3.3	112.5	140.8
	Reactive-Business/Reactive-School Closures	20.6	21.8	3.3	15.7	26.6
	Elimination	172.2	48.2	154.9	175.4	200.9
Influenza-1918-X	No Closures	595.8	367.8	224.4	630.6	890.2
	Reactive-Business/Sustained-School Closures	542.2	294.2	274.5	503.5	788.9
	Reactive-Business/Reactive-School Closures*†	439.5	331.0	166.4	297.9	700.7
	Elimination	824.1	363.6	527.1	828.4	1134.4
Covid-Omicron-X	**No Closures***†	56.2	44.2	18.1	42.0	89.9
	Reactive-Business/Sustained-School Closures	94.1	55.7	48.3	90.5	132.0
	Reactive-Business/Reactive-School Closures	68.0	41.5	36.7	58.4	93.0
	Elimination	145.4	71.7	88.2	150.3	196.9
Covid-Delta-X	**No Closures**	316.5	185.0	166.1	326.1	431.2
	Reactive-Business/Sustained-School Closures	359.6	163.7	227.2	356.2	456.1
	Reactive-Business/Reactive-School Closures*†	329.9	163.1	205.4	320.7	429.2
	Elimination	395.1	155.3	276.1	377.1	488.2
Covid-Wildtype-X	**No Closures***†	110.8	81.6	35.0	104.7	167.4
	Reactive-Business/Sustained-School Closures	179.0	73.0	133.6	171.9	222.5
	Reactive-Business/Reactive-School Closures	146.8	78.4	90.3	138.5	193.2
	Elimination	223.9	86.8	164.3	212.0	277.6
UMIC						
Influenza-2009-X	**No Closures***†	2.3	0.8	1.7	2.2	2.7
	Reactive-Business/Sustained-School Closures	7.8	18.8	1.8	2.3	3.0
	Reactive-Business/Reactive-School Closures	3.3	3.6	1.8	2.3	3.0
	Elimination	75.6	46.5	5.6	95.0	109.1
Influenza-1957-X	**No Closures***†	7.1	10.2	3.1	4.3	6.5
	Reactive-Business/Sustained-School Closures	38.4	38.0	3.6	7.8	77.8
	Reactive-Business/Reactive-School Closures	11.2	9.1	3.6	8.7	17.1
	Elimination	107.7	28.8	100.7	111.5	122.2
Influenza-1918-X	No Closures	364.4	330.5	97.9	205.8	608.5
	Reactive-Business/Sustained-School Closures	247.2	147.9	152.5	195.6	299.6
	Reactive-Business/Reactive-School Closures*†	135.7	83.2	95.1	117.3	145.9
	Elimination	384.9	229.2	201.7	308.9	514.4
Covid-Omicron-X	**No Closures***	49.8	48.8	14.9	29.2	67.9
	Reactive-Business/Sustained-School Closures	76.5	49.5	30.8	80.4	105.8
	Reactive-Business/Reactive-School Closures†	50.6	40.3	23.2	38.7	65.6
	Elimination	117.7	44.0	97.2	123.8	141.9
Covid-Delta-X	No Closures	425.2	293.7	153.0	404.4	634.9
	Reactive-Business/Sustained-School Closures	422.9	267.4	191.9	370.5	608.3
	Reactive-Business/Reactive-School Closures*†	359.4	250.8	157.6	289.5	522.5
	Elimination	444.8	227.0	260.8	410.4	588.3
Covid-Wildtype-X	**No Closures***	124.9	116.9	31.4	78.4	194.1
	Reactive-Business/Sustained-School Closures	141.5	87.0	90.3	116.4	170.4
	Reactive-Business/Reactive-School Closures†	94.7	66.3	48.4	79.4	118.8
	Elimination	166.6	80.3	113.2	149.7	207.6
HIC						
Influenza-2009-X	**No Closures***†	1.9	0.9	1.2	1.8	2.4
	Reactive-Business/Sustained-School Closures	2.6	4.2	1.3	1.8	2.5
	Reactive-Business/Reactive-School Closures	2.2	2.0	1.3	1.8	2.5
	Elimination	48.9	23.6	43.0	55.6	63.5
Influenza-1957-X	**No Closures***†	5.5	7.5	2.7	4.1	5.9
	Reactive-Business/Sustained-School Closures	14.6	14.5	3.0	5.3	30.9
	Reactive-Business/Reactive-School Closures	8.2	6.6	3.0	5.3	14.0
	Elimination	62.9	13.7	56.9	63.2	69.5
Influenza-1918-X	No Closures	143.7	198.5	44.0	67.4	117.0
	Reactive-Business/Sustained-School Closures	85.8	60.8	56.6	74.0	96.1
	Reactive-Business/Reactive-School Closures*†	67.9	33.6	47.3	66.1	84.0
	Elimination	118.1	53.9	89.9	103.8	125.6
Covid-Omicron-X	**No Closures***	54.4	48.7	19.2	34.3	74.5
	Reactive-Business/Sustained-School Closures	63.5	41.4	40.1	55.5	79.0
	Reactive-Business/Reactive-School Closures†	46.7	34.2	25.0	36.6	56.8
	Elimination	86.7	26.4	73.1	82.5	95.1
Covid-Delta-X	No Closures	431.1	307.1	127.5	403.5	681.3
	Reactive-Business/Sustained-School Closures	360.1	274.8	122.3	257.3	571.9
	Reactive-Business/Reactive-School Closures*	288.4	230.2	112.1	188.2	429.6
	Elimination†	309.8	213.2	136.6	235.5	428.7
Covid-Wildtype-X	No Closures*	96.2	100.5	27.6	48.6	135.5

continued on next page

continued from previous page

Income Group / Disease	Closure Strategy	Mean	SD	Q_1	Q_2	Q_3
	Reactive-Business/Sustained-School Closures	77.8	59.4	46.5	61.5	87.3
	Reactive-Business/Reactive-School Closures†	56.4	34.8	34.7	49.5	70.2
	Elimination	90.0	35.6	71.0	82.7	100.4

Table S5: Summary statistics of projected socioeconomic losses (expressed as a percentage of annual GDP) under different closure strategies, for each disease and country-income group. The closure strategies with the two lowest means (bold), lowest median (*) and lowest upper quartile (†) are indicated. Distributions are shown in main text Figure 2.

Income Group / Disease	Closure Strategy	Mean	SD	Q_1	Q_2	Q_3
LLMIC						
Influenza-2009-X	No Closures	2.3	2.7	1.3	1.6	2.1
	Reactive-Business/Sustained-School Closures	1.6	0.9	1.2	1.5	1.8
	Reactive-Business/Reactive-School Closures	1.5	0.5	1.2	1.4	1.7
	Elimination	1.9	2.6	1.0	1.3	1.8
Influenza-1957-X	No Closures	6.4	9.3	1.9	2.7	6.0
	Reactive-Business/Sustained-School Closures	3.3	4.3	1.7	2.2	3.1
	Reactive-Business/Reactive-School Closures	2.4	2.1	1.6	2.0	2.6
	Elimination	5.5	9.1	1.3	2.0	4.4
Influenza-1918-X	No Closures	552.2	340.7	207.9	583.3	823.0
	Reactive-Business/Sustained-School Closures	388.6	264.3	135.1	345.7	603.4
	Reactive-Business/Reactive-School Closures	320.3	276.9	91.4	182.4	532.7
	Elimination	612.3	335.4	335.3	613.8	895.6
Covid-Omicron-X	No Closures	48.8	39.6	15.1	36.0	77.5
	Reactive-Business/Sustained-School Closures	41.8	37.5	11.6	26.9	65.5
	Reactive-Business/Reactive-School Closures	35.5	34.4	9.7	20.8	51.8
	Elimination	37.6	35.2	9.9	24.0	56.2
Covid-Delta-X	No Closures	274.5	165.7	140.7	275.5	374.1
	Reactive-Business/Sustained-School Closures	241.0	165.5	92.0	234.6	343.7
	Reactive-Business/Reactive-School Closures	213.4	157.5	71.3	196.5	316.1
	Elimination	228.9	156.2	96.3	218.4	326.9
Covid-Wildtype-X	No Closures	95.2	72.2	29.6	88.3	142.9
	Reactive-Business/Sustained-School Closures	70.0	64.3	17.7	46.8	109.6
	Reactive-Business/Reactive-School Closures	49.5	50.0	13.4	28.2	71.2
	Elimination	73.0	62.8	19.3	57.9	109.7
UMIC						
Influenza-2009-X	No Closures	1.9	0.8	1.4	1.7	2.3
	Reactive-Business/Sustained-School Closures	1.8	0.7	1.3	1.7	2.2
	Reactive-Business/Reactive-School Closures	1.8	0.7	1.3	1.7	2.2
	Elimination	1.6	0.7	1.1	1.4	1.9
Influenza-1957-X	No Closures	6.3	9.7	2.6	3.7	5.8
	Reactive-Business/Sustained-School Closures	3.8	2.4	2.4	3.3	4.5
	Reactive-Business/Reactive-School Closures	3.6	1.7	2.4	3.3	4.4
	Elimination	3.5	4.8	1.8	2.6	3.8
Influenza-1918-X	No Closures	342.4	310.4	91.9	193.4	571.8
	Reactive-Business/Sustained-School Closures	166.7	133.5	81.5	112.4	208.0
	Reactive-Business/Reactive-School Closures	100.6	69.3	72.6	85.3	100.0
	Elimination	260.1	215.9	85.6	185.9	380.0
Covid-Omicron-X	No Closures	45.2	45.2	12.8	26.4	61.9
	Reactive-Business/Sustained-School Closures	38.2	40.8	11.7	20.7	48.4
	Reactive-Business/Reactive-School Closures	32.2	35.4	10.8	17.9	37.5
	Elimination	33.7	36.1	10.3	19.5	42.4
Covid-Delta-X	No Closures	386.7	270.1	138.7	363.5	574.9
	Reactive-Business/Sustained-School Closures	333.4	261.3	103.4	273.8	509.0
	Reactive-Business/Reactive-School Closures	280.5	238.8	81.6	203.1	426.2
	Elimination	323.7	228.3	138.8	283.1	463.6
Covid-Wildtype-X	No Closures	113.2	107.1	28.0	71.0	175.6
	Reactive-Business/Sustained-School Closures	73.0	81.2	19.9	39.1	92.0
	Reactive-Business/Reactive-School Closures	46.6	50.6	17.1	28.4	52.2
	Elimination	74.6	68.6	23.2	51.3	105.1
HIC						
Influenza-2009-X	No Closures	1.6	0.8	1.0	1.5	2.1
	Reactive-Business/Sustained-School Closures	1.6	0.8	1.0	1.5	2.1
	Reactive-Business/Reactive-School Closures	1.6	0.8	1.0	1.5	2.1
	Elimination	1.2	0.7	0.7	1.0	1.5
Influenza-1957-X	No Closures	5.0	7.2	2.3	3.6	5.4
	Reactive-Business/Sustained-School Closures	3.4	1.8	2.2	3.2	4.4
	Reactive-Business/Reactive-School Closures	3.5	1.8	2.2	3.4	4.7
	Elimination	2.4	1.4	1.4	2.2	3.1
Influenza-1918-X	No Closures	135.6	187.1	41.8	63.7	110.5
	Reactive-Business/Sustained-School Closures	60.2	54.4	34.1	49.0	68.7
	Reactive-Business/Reactive-School Closures	53.8	29.1	37.0	52.4	67.6
	Elimination	53.3	50.4	28.0	39.3	57.8
Covid-Omicron-X	No Closures	50.0	45.2	17.4	31.5	68.8
	Reactive-Business/Sustained-School Closures	39.4	37.7	15.4	23.6	49.4
	Reactive-Business/Reactive-School Closures	31.5	30.1	14.0	20.3	36.6
	Elimination	27.9	29.8	11.3	16.9	31.1
Covid-Delta-X	No Closures	393.8	281.0	118.4	367.2	618.3
	Reactive-Business/Sustained-School Closures	302.2	254.7	82.5	204.7	492.3
	Reactive-Business/Reactive-School Closures	233.3	212.8	70.2	136.1	359.0
	Elimination	228.9	203.7	64.9	157.4	336.6
Covid-Wildtype-X	No Closures	87.9	92.0	25.2	44.7	123.6
	Reactive-Business/Sustained-School Closures	47.2	51.8	18.9	29.4	51.9
	Reactive-Business/Reactive-School Closures	31.3	25.7	17.5	25.3	36.2
	Elimination	33.3	32.6	13.6	22.2	41.1

Table S6: Summary statistics of projected VLYL (expressed as a percentage of annual GDP) under different closure strategies, for each disease and country-income group. Distributions are shown in Figure S7.

Income Group / Disease	Closure Strategy	Mean	SD	Q_1	Q_2	Q_3
LLMIC						
Influenza-2009-X	No Closures	0.3	0.2	0.2	0.3	0.3
	Reactive-Business/Sustained-School Closures	3.4	6.3	0.2	0.4	4.9
	Reactive-Business/Reactive-School Closures	5.3	7.2	0.2	0.4	9.5
	Elimination	37.3	19.4	30.4	40.9	50.0
Influenza-1957-X	No Closures	0.8	0.8	0.4	0.5	0.8
	Reactive-Business/Sustained-School Closures	5.4	7.2	0.5	4.3	6.9
	Reactive-Business/Reactive-School Closures	9.2	8.9	0.5	7.0	15.0
	Elimination	44.3	14.9	36.9	45.0	53.5
Influenza-1918-X	No Closures	30.3	19.9	10.6	31.0	45.7
	Reactive-Business/Sustained-School Closures	28.9	18.3	13.9	26.3	41.3
	Reactive-Business/Reactive-School Closures	45.0	23.3	27.2	41.8	61.9
	Elimination	70.8	20.4	55.3	70.8	86.0
Covid-Omicron-X	No Closures	6.4	4.6	2.2	4.9	11.0
	Reactive-Business/Sustained-School Closures	8.7	6.1	4.6	7.7	12.1
	Reactive-Business/Reactive-School Closures	14.2	8.7	7.9	13.3	18.1
	Elimination	32.1	20.2	13.7	32.2	48.4
Covid-Delta-X	No Closures	40.9	20.7	21.8	46.8	57.3
	Reactive-Business/Sustained-School Closures	41.9	19.7	24.3	45.9	57.3
	Reactive-Business/Reactive-School Closures	55.2	18.6	43.3	56.8	67.0
	Elimination	66.4	17.9	54.4	64.2	77.6
Covid-Wildtype-X	No Closures	14.7	9.9	4.8	14.8	23.5
	Reactive-Business/Sustained-School Closures	18.3	10.8	10.4	16.7	24.9
	Reactive-Business/Reactive-School Closures	35.0	15.1	24.6	34.7	44.9
	Elimination	47.1	16.4	35.8	46.8	58.0
UMIC						
Influenza-2009-X	No Closures	0.2	0.1	0.2	0.2	0.3
	Reactive-Business/Sustained-School Closures	0.7	1.6	0.2	0.2	0.3
	Reactive-Business/Reactive-School Closures	1.1	3.0	0.2	0.2	0.3
	Elimination	26.6	17.3	2.4	32.2	39.4
Influenza-1957-X	No Closures	0.5	0.5	0.3	0.4	0.5
	Reactive-Business/Sustained-School Closures	3.2	3.7	0.4	0.7	5.2
	Reactive-Business/Reactive-School Closures	5.4	5.9	0.4	2.0	10.8
	Elimination	37.5	11.5	33.0	38.5	44.3
Influenza-1918-X	No Closures	16.8	15.8	4.4	9.1	28.3
	Reactive-Business/Sustained-School Closures	13.3	7.8	8.1	11.2	16.3
	Reactive-Business/Reactive-School Closures	19.8	9.3	14.1	18.2	24.4
	Elimination	49.8	12.0	41.0	48.5	57.6
Covid-Omicron-X	No Closures	4.0	3.6	1.5	2.3	5.2
	Reactive-Business/Sustained-School Closures	6.6	4.5	2.8	6.1	9.1
	Reactive-Business/Reactive-School Closures	10.4	7.6	4.1	9.5	15.0
	Elimination	32.0	16.4	16.4	37.1	44.5
Covid-Delta-X	No Closures	37.8	24.5	12.8	39.0	59.3
	Reactive-Business/Sustained-School Closures	38.2	21.7	18.6	35.1	56.7
	Reactive-Business/Reactive-School Closures	47.0	20.3	31.0	46.5	63.3
	Elimination	61.6	15.6	50.4	61.3	72.4
Covid-Wildtype-X	No Closures	11.2	10.0	2.9	6.8	18.3
	Reactive-Business/Sustained-School Closures	13.3	8.2	7.7	11.1	17.3
	Reactive-Business/Reactive-School Closures	23.3	11.8	15.1	22.0	30.9
	Elimination	37.4	13.1	28.7	38.6	46.3
HIC						
Influenza-2009-X	No Closures	0.2	0.1	0.1	0.2	0.2
	Reactive-Business/Sustained-School Closures	0.3	0.7	0.1	0.2	0.2
	Reactive-Business/Reactive-School Closures	0.5	1.7	0.1	0.2	0.2
	Elimination	27.8	14.4	23.2	31.3	36.8
Influenza-1957-X	No Closures	0.4	0.3	0.3	0.4	0.5
	Reactive-Business/Sustained-School Closures	2.1	2.4	0.3	0.4	4.3
	Reactive-Business/Reactive-School Closures	4.2	5.4	0.3	0.4	9.3
	Elimination	35.3	9.1	30.9	35.3	39.8
Influenza-1918-X	No Closures	7.1	10.3	1.8	3.1	5.9
	Reactive-Business/Sustained-School Closures	6.5	4.1	4.2	6.2	8.0
	Reactive-Business/Reactive-School Closures	11.9	7.3	4.9	12.7	15.5
	Elimination	38.5	7.9	33.6	37.8	42.5
Covid-Omicron-X	No Closures	4.1	3.7	1.6	2.4	5.2
	Reactive-Business/Sustained-School Closures	7.0	4.0	4.3	7.0	9.0
	Reactive-Business/Reactive-School Closures	12.1	7.4	6.3	13.0	16.7
	Elimination	35.2	12.0	29.0	37.2	42.3
Covid-Delta-X	No Closures	37.0	26.7	9.3	35.8	61.6
	Reactive-Business/Sustained-School Closures	34.2	23.2	14.5	25.1	54.6
	Reactive-Business/Reactive-School Closures	42.6	20.8	27.8	39.2	57.9
	Elimination	55.3	15.7	43.0	51.6	65.9
Covid-Wildtype-X	No Closures	8.0	8.7	2.3	3.7	11.0
	Reactive-Business/Sustained-School Closures	9.4	6.0	6.2	8.3	11.3
	Reactive-Business/Reactive-School Closures	17.9	9.7	13.1	17.6	23.6
	Elimination	34.3	10.0	29.1	35.0	40.0

Table S7: Summary statistics of projected GDPL (expressed as a percentage of annual GDP) under different closure strategies, for each disease and country-income group. Distributions are shown in Figure S8.

Income Group / Disease	Closure Strategy	Mean	SD	Q_1	Q_2	Q_3
LLMIC						
Influenza-2009-X	No Closures	0.3	0.1	0.3	0.3	0.4
	Reactive-Business/Sustained-School Closures	50.0	61.9	0.3	0.4	115.6
	Reactive-Business/Reactive-School Closures	3.1	5.2	0.3	0.4	4.1
	Elimination	103.5	49.7	98.4	116.8	133.9
Influenza-1957-X	No Closures	0.4	0.2	0.3	0.4	0.4
	Reactive-Business/Sustained-School Closures	77.6	61.8	0.4	104.0	128.5
	Reactive-Business/Reactive-School Closures	8.9	13.7	0.4	4.5	9.7
	Elimination	122.4	33.2	112.4	125.2	141.8
Influenza-1918-X	No Closures	13.3	8.0	5.1	14.4	19.9
	Reactive-Business/Sustained-School Closures	124.7	38.3	112.5	130.5	149.9
	Reactive-Business/Reactive-School Closures	74.2	43.9	39.4	75.9	108.0
	Elimination	141.0	20.9	126.0	139.3	157.1
Covid-Omicron-X	No Closures	1.0	0.1	0.9	1.0	1.1
	Reactive-Business/Sustained-School Closures	43.6	50.2	4.2	14.6	89.0
	Reactive-Business/Reactive-School Closures	18.3	18.6	5.6	12.1	24.2
	Elimination	75.7	58.5	8.0	93.9	128.2
Covid-Delta-X	No Closures	1.1	0.1	1.0	1.1	1.2
	Reactive-Business/Sustained-School Closures	76.6	54.4	9.2	88.7	123.4
	Reactive-Business/Reactive-School Closures	61.2	43.2	20.8	58.5	93.7
	Elimination	99.9	52.7	49.2	120.6	137.4
Covid-Wildtype-X	No Closures	0.8	0.1	0.7	0.8	0.9
	Reactive-Business/Sustained-School Closures	90.7	48.4	52.6	104.4	126.4
	Reactive-Business/Reactive-School Closures	62.3	35.5	32.9	60.6	88.4
	Elimination	103.8	39.5	77.7	113.5	131.3
UMIC						
Influenza-2009-X	No Closures	0.2	0.0	0.2	0.2	0.2
	Reactive-Business/Sustained-School Closures	5.3	17.4	0.2	0.2	0.2
	Reactive-Business/Reactive-School Closures	0.4	0.6	0.2	0.2	0.2
	Elimination	47.4	29.9	1.7	60.6	69.0
Influenza-1957-X	No Closures	0.2	0.1	0.2	0.2	0.2
	Reactive-Business/Sustained-School Closures	31.5	34.4	0.2	1.3	67.9
	Reactive-Business/Reactive-School Closures	2.1	3.6	0.2	1.7	2.7
	Elimination	66.7	17.7	63.4	69.5	75.6
Influenza-1918-X	No Closures	5.2	4.5	1.5	3.1	8.7
	Reactive-Business/Sustained-School Closures	67.2	20.6	64.3	71.9	78.3
	Reactive-Business/Reactive-School Closures	15.3	13.9	3.5	11.1	23.0
	Elimination	75.0	9.3	68.5	74.5	80.6
Covid-Omicron-X	No Closures	0.6	0.1	0.5	0.6	0.6
	Reactive-Business/Sustained-School Closures	31.7	32.9	1.8	6.2	67.4
	Reactive-Business/Reactive-School Closures	8.0	10.0	2.3	4.9	9.2
	Elimination	52.0	30.8	20.1	68.0	75.1
Covid-Delta-X	No Closures	0.7	0.1	0.6	0.7	0.7
	Reactive-Business/Sustained-School Closures	51.4	30.5	18.8	65.7	75.0
	Reactive-Business/Reactive-School Closures	31.9	22.7	11.2	30.0	48.5
	Elimination	59.5	27.0	57.7	70.2	76.6
Covid-Wildtype-X	No Closures	0.5	0.1	0.4	0.5	0.5
	Reactive-Business/Sustained-School Closures	55.2	26.0	46.6	64.9	72.4
	Reactive-Business/Reactive-School Closures	24.8	18.0	10.4	21.0	37.0
	Elimination	54.6	21.8	37.4	62.3	70.7
HIC						
Influenza-2009-X	No Closures	0.1	0.0	0.1	0.1	0.1
	Reactive-Business/Sustained-School Closures	0.6	3.5	0.1	0.1	0.1
	Reactive-Business/Reactive-School Closures	0.1	0.1	0.1	0.1	0.1
	Elimination	19.9	9.9	17.7	23.1	26.0
Influenza-1957-X	No Closures	0.1	0.0	0.1	0.1	0.1
	Reactive-Business/Sustained-School Closures	9.1	11.9	0.1	0.1	22.9
	Reactive-Business/Reactive-School Closures	0.5	0.8	0.1	0.1	0.9
	Elimination	25.3	5.4	23.3	25.5	27.7
Influenza-1918-X	No Closures	1.0	1.2	0.3	0.5	0.9
	Reactive-Business/Sustained-School Closures	19.1	11.5	0.7	24.2	26.7
	Reactive-Business/Reactive-School Closures	2.2	2.7	0.7	1.2	2.4
	Elimination	26.4	3.9	24.1	26.1	28.3
Covid-Omicron-X	No Closures	0.2	0.0	0.2	0.2	0.3
	Reactive-Business/Sustained-School Closures	17.2	12.7	1.3	24.2	27.2
	Reactive-Business/Reactive-School Closures	3.1	2.6	1.7	2.7	3.8
	Elimination	23.5	9.0	21.9	26.3	28.9
Covid-Delta-X	No Closures	0.3	0.1	0.2	0.3	0.3
	Reactive-Business/Sustained-School Closures	23.7	9.3	23.8	26.4	28.6
	Reactive-Business/Reactive-School Closures	12.5	7.8	5.6	12.0	19.0
	Elimination	25.6	6.8	24.4	26.7	29.1
Covid-Wildtype-X	No Closures	0.2	0.1	0.2	0.2	0.2
	Reactive-Business/Sustained-School Closures	21.2	9.4	21.3	24.0	26.2
	Reactive-Business/Reactive-School Closures	7.1	5.8	2.5	5.8	11.2
	Elimination	22.5	6.9	20.2	24.0	26.7

Table S8: Summary statistics of projected VSYL (expressed as a percentage of annual GDP) under different closure strategies, for each disease and country-income group. Distributions are shown in Figure S9.

Income Group / Disease	Closure Strategy	Decremental VLYL	Incremental GDPL + VSYL
LLMIC			
Influenza-2009-X	**No Closures*†**	0.0 (0.0; 0.0)	0.0 (0.0; 0.0)
	Reactive-Business/Sustained-School Closures	0.7 (0.0; 0.4)	52.7 (0.0; 121.5)
	Reactive-Business/Reactive-School Closures	0.8 (0.0; 0.4)	7.8 (0.0; 14.3)
	Elimination	0.4 (0.0; 0.7)	140.1 (132.0; 182.0)
Influenza-1957-X	**No Closures*†**	0.0 (0.0; 0.0)	0.0 (0.0; 0.0)
	Reactive-Business/Sustained-School Closures	3.1 (0.0; 2.9)	81.8 (0.0; 135.7)
	Reactive-Business/Reactive-School Closures	4.0 (0.0; 3.5)	17.0 (0.0; 23.0)
	Elimination	0.9 (-0.0; 1.8)	165.6 (150.6; 192.1)
Influenza-1918-X	No Closures	0.0 (0.0; 0.0)	0.0 (0.0; 0.0)
	Reactive-Business/Sustained-School Closures	163.5 (6.5; 303.9)	109.9 (91.9; 137.2)
	Reactive-Business/Reactive-School Closures*†	231.8 (12.4; 419.3)	75.5 (34.8; 112.1)
	Elimination	-60.1 (-232.7; 89.2)	168.1 (146.1; 190.2)
Covid-Omicron-X	**No Closures*†**	0.0 (0.0; 0.0)	0.0 (0.0; 0.0)
	Reactive-Business/Sustained-School Closures	7.0 (1.3; 9.6)	44.9 (2.9; 92.6)
	Reactive-Business/Reactive-School Closures	13.3 (3.4; 19.2)	25.1 (4.9; 34.8)
	Elimination	11.2 (2.7; 19.3)	100.4 (7.5; 171.6)
Covid-Delta-X	**No Closures**	0.0 (0.0; 0.0)	0.0 (0.0; 0.0)
	Reactive-Business/Sustained-School Closures	33.5 (4.8; 60.2)	76.6 (5.9; 124.0)
	Reactive-Business/Reactive-School Closures*†	61.0 (15.9; 102.0)	74.5 (23.3; 118.6)
	Elimination	45.6 (10.8; 89.7)	124.3 (55.5; 175.5)
Covid-Wildtype-X	**No Closures*†**	0.0 (0.0; 0.0)	0.0 (0.0; 0.0)
	Reactive-Business/Sustained-School Closures	25.2 (3.4; 41.5)	93.5 (53.7; 131.1)
	Reactive-Business/Reactive-School Closures	45.7 (11.2; 72.5)	81.8 (45.0; 115.1)
	Elimination	22.2 (-1.0; 53.1)	135.4 (99.6; 172.7)
UMIC			
Influenza-2009-X	**No Closures*†**	0.0 (0.0; 0.0)	0.0 (0.0; 0.0)
	Reactive-Business/Sustained-School Closures	0.0 (0.0; 0.0)	5.6 (0.0; 0.0)
	Reactive-Business/Reactive-School Closures	0.0 (0.0; 0.0)	1.1 (0.0; 0.0)
	Elimination	0.3 (0.0; 0.5)	73.6 (3.8; 107.3)
Influenza-1957-X	**No Closures*†**	0.0 (0.0; 0.0)	0.0 (0.0; 0.0)
	Reactive-Business/Sustained-School Closures	2.6 (0.0; 1.2)	33.9 (0.0; 73.2)
	Reactive-Business/Reactive-School Closures	2.7 (0.0; 1.0)	6.8 (0.0; 12.9)
	Elimination	2.8 (0.1; 2.1)	103.4 (97.1; 117.8)
Influenza-1918-X	No Closures	0.0 (0.0; 0.0)	0.0 (0.0; 0.0)
	Reactive-Business/Sustained-School Closures	175.7 (0.0; 344.7)	58.4 (45.3; 75.7)
	Reactive-Business/Reactive-School Closures*†	241.8 (5.5; 448.4)	13.1 (1.5; 20.8)
	Elimination	82.3 (-56.1; 222.9)	102.9 (90.1; 116.2)
Covid-Omicron-X	**No Closures***	0.0 (0.0; 0.0)	0.0 (0.0; 0.0)
	Reactive-Business/Sustained-School Closures	7.0 (0.0; 9.8)	33.7 (1.0; 72.1)
	Reactive-Business/Reactive-School Closures†	13.0 (0.5; 19.3)	13.8 (1.4; 19.4)
	Elimination	11.5 (1.3; 20.6)	79.4 (31.1; 115.7)
Covid-Delta-X	No Closures	0.0 (0.0; 0.0)	0.0 (0.0; 0.0)
	Reactive-Business/Sustained-School Closures	53.4 (6.6; 95.3)	51.1 (5.4; 76.9)
	Reactive-Business/Reactive-School Closures*†	106.2 (24.0; 177.4)	40.5 (8.4; 66.9)
	Elimination	63.0 (-9.3; 160.6)	82.6 (64.3; 113.5)
Covid-Wildtype-X	**No Closures***	0.0 (0.0; 0.0)	0.0 (0.0; 0.0)
	Reactive-Business/Sustained-School Closures	40.1 (3.2; 65.7)	56.8 (46.4; 76.2)
	Reactive-Business/Reactive-School Closures†	66.6 (6.3; 115.3)	36.5 (16.6; 52.9)
	Elimination	38.6 (-5.2; 90.6)	80.3 (50.7; 105.6)
HIC			
Influenza-2009-X	**No Closures*†**	0.0 (0.0; 0.0)	0.0 (0.0; 0.0)
	Reactive-Business/Sustained-School Closures	0.0 (0.0; 0.0)	0.7 (0.0; 0.0)
	Reactive-Business/Reactive-School Closures	0.0 (0.0; 0.0)	0.3 (0.0; 0.0)
	Elimination	0.4 (0.0; 0.7)	47.4 (41.4; 62.4)
Influenza-1957-X	**No Closures*†**	0.0 (0.0; 0.0)	0.0 (0.0; 0.0)
	Reactive-Business/Sustained-School Closures	1.5 (0.0; 0.6)	10.7 (0.0; 26.9)
	Reactive-Business/Reactive-School Closures	1.4 (0.0; 0.4)	4.2 (0.0; 9.9)
	Elimination	2.6 (0.3; 2.5)	60.1 (54.0; 66.9)
Influenza-1918-X	No Closures	0.0 (0.0; 0.0)	0.0 (0.0; 0.0)
	Reactive-Business/Sustained-School Closures	75.4 (0.0; 42.8)	17.5 (0.0; 29.3)
	Reactive-Business/Reactive-School Closures*†	81.8 (0.0; 42.3)	6.0 (0.0; 11.9)
	Elimination	82.3 (3.2; 48.2)	56.8 (50.2; 65.2)
Covid-Omicron-X	**No Closures***	0.0 (0.0; 0.0)	0.0 (0.0; 0.0)
	Reactive-Business/Sustained-School Closures	10.7 (0.7; 16.5)	19.8 (0.6; 31.9)
	Reactive-Business/Reactive-School Closures†	18.6 (1.3; 29.6)	10.9 (3.9; 15.4)
	Elimination	22.1 (3.9; 35.0)	54.4 (47.7; 68.0)
Covid-Delta-X	No Closures	0.0 (0.0; 0.0)	0.0 (0.0; 0.0)
	Reactive-Business/Sustained-School Closures	91.6 (17.6; 147.7)	20.6 (12.4; 30.4)
	Reactive-Business/Reactive-School Closures*	160.5 (34.5; 261.5)	17.8 (2.2; 30.9)
	Elimination†	164.9 (33.1; 271.0)	43.6 (27.4; 60.7)

continued on next page

continued from previous page

Income Group / Disease	Closure Strategy	Decremental VLYL	Incremental GDPL + VSYL
Covid-Wildtype-X	No Closures*	0.0 (0.0; 0.0)	0.0 (0.0; 0.0)
	Reactive-Business/Sustained-School Closures	40.7 (2.0; 65.3)	22.3 (17.3; 29.9)
	Reactive-Business/Reactive-School Closures†	56.7 (2.4; 89.7)	16.8 (10.4; 23.2)
	Elimination	54.7 (6.2; 85.7)	48.5 (35.0; 61.0)

Table S9: Summary statistics (mean, (IQR)) of projected decremental VSYL and incremental GDPL + VSYL (expressed as a percentage of annual GDP) of switching from the No Closures strategy to alternative closure strategies, for each disease and country-income group. The closure strategies with the two lowest mean socioeconomic losses (bold), lowest median (*) and lowest upper quartile (†) are indicated. Distributions are shown in main text Figure 3.

Income Group / Disease	Closure Strategy	Preschool-Age	School-Age	Working-Age	Retired-Age
LLMIC					
Influenza-2009-X	No Closures	0.3 (0.2; 0.4)	0.4 (0.3; 0.6)	0.7 (0.5; 0.9)	0.2 (0.1; 0.3)
	Reactive-Business/Sustained-School Closures	0.3 (0.2; 0.4)	0.4 (0.3; 0.5)	0.6 (0.5; 0.8)	0.2 (0.1; 0.2)
	Reactive-Business/Reactive-School Closures	0.3 (0.2; 0.3)	0.4 (0.3; 0.4)	0.6 (0.4; 0.7)	0.1 (0.1; 0.2)
	Elimination	0.3 (0.2; 0.4)	0.3 (0.2; 0.5)	0.5 (0.3; 0.8)	0.1 (0.1; 0.2)
Influenza-1957-X	No Closures	0.2 (0.1; 0.3)	0.5 (0.4; 1.1)	1.5 (1.0; 3.3)	0.5 (0.3; 1.3)
	Reactive-Business/Sustained-School Closures	0.1 (0.1; 0.2)	0.4 (0.3; 0.5)	1.2 (0.9; 1.8)	0.4 (0.3; 0.7)
	Reactive-Business/Reactive-School Closures	0.1 (0.1; 0.2)	0.4 (0.3; 0.5)	1.1 (0.8; 1.5)	0.4 (0.3; 0.6)
	Elimination	0.2 (0.1; 0.3)	0.4 (0.3; 0.7)	1.1 (0.7; 2.4)	0.4 (0.2; 1.0)
Influenza-1918-X	No Closures	146.8 (56.1; 227.6)	135.4 (47.5; 189.1)	267.4 (96.4; 393.1)	4.4 (1.7; 7.9)
	Reactive-Business/Sustained-School Closures	109.3 (44.2; 179.1)	67.6 (26.7; 120.7)	150.8 (59.7; 287.3)	2.8 (1.1; 5.6)
	Reactive-Business/Reactive-School Closures	64.1 (29.5; 165.0)	34.9 (20.5; 111.7)	74.0 (40.3; 236.8)	1.6 (0.7; 4.6)
	Elimination	220.1 (139.7; 289.0)	121.6 (54.5; 186.3)	253.4 (111.8; 402.2)	4.6 (1.8; 8.4)
Covid-Omicron-X	No Closures	0.1 (0.1; 0.1)	3.0 (1.9; 3.5)	28.8 (10.4; 68.5)	3.4 (1.9; 5.4)
	Reactive-Business/Sustained-School Closures	0.1 (0.1; 0.1)	2.5 (1.4; 3.3)	20.6 (8.0; 57.0)	3.1 (1.8; 5.0)
	Reactive-Business/Reactive-School Closures	0.1 (0.1; 0.1)	2.2 (1.1; 3.0)	15.1 (6.5; 43.4)	2.8 (1.6; 4.7)
	Elimination	0.1 (0.1; 0.1)	2.3 (1.2; 3.1)	17.9 (6.7; 48.2)	3.0 (1.6; 4.9)
Covid-Delta-X	No Closures	0.1 (0.1; 0.1)	4.2 (3.4; 4.7)	253.1 (123.0; 342.0)	18.2 (11.4; 28.1)
	Reactive-Business/Sustained-School Closures	0.1 (0.1; 0.1)	3.5 (2.4; 4.3)	213.0 (76.3; 313.7)	16.8 (9.8; 26.9)
	Reactive-Business/Reactive-School Closures	0.1 (0.1; 0.1)	3.2 (2.1; 4.0)	176.6 (57.8; 288.1)	15.7 (9.3; 25.7)
	Elimination	0.1 (0.1; 0.1)	3.3 (2.2; 4.1)	197.1 (83.3; 295.6)	16.7 (9.9; 26.5)
Covid-Wildtype-X	No Closures	0.0 (0.0; 0.1)	1.8 (1.2; 2.2)	79.8 (23.9; 132.0)	5.8 (3.4; 9.4)
	Reactive-Business/Sustained-School Closures	0.0 (0.0; 0.1)	1.2 (0.7; 1.7)	39.8 (14.1; 99.5)	4.6 (2.6; 7.8)
	Reactive-Business/Reactive-School Closures	0.0 (0.0; 0.1)	0.9 (0.5; 1.4)	22.9 (10.5; 63.2)	3.8 (2.1; 6.6)
	Elimination	0.1 (0.0; 0.1)	1.3 (0.7; 1.7)	50.8 (15.6; 99.8)	4.9 (2.6; 8.4)
UMIC					
Influenza-2009-X	No Closures	0.1 (0.1; 0.2)	0.3 (0.2; 0.3)	0.8 (0.6; 1.0)	0.5 (0.3; 0.8)
	Reactive-Business/Sustained-School Closures	0.1 (0.1; 0.2)	0.3 (0.2; 0.3)	0.8 (0.6; 1.0)	0.5 (0.3; 0.8)
	Reactive-Business/Reactive-School Closures	0.1 (0.1; 0.2)	0.3 (0.2; 0.3)	0.8 (0.6; 1.0)	0.5 (0.3; 0.8)
	Elimination	0.1 (0.1; 0.2)	0.2 (0.2; 0.3)	0.6 (0.5; 0.9)	0.4 (0.2; 0.6)
Influenza-1957-X	No Closures	0.1 (0.1; 0.1)	0.3 (0.2; 0.4)	2.0 (1.4; 2.9)	1.3 (0.7; 2.4)
	Reactive-Business/Sustained-School Closures	0.1 (0.1; 0.1)	0.3 (0.2; 0.3)	1.8 (1.3; 2.4)	1.1 (0.7; 1.8)
	Reactive-Business/Reactive-School Closures	0.1 (0.1; 0.1)	0.3 (0.2; 0.3)	1.8 (1.3; 2.3)	1.1 (0.7; 1.8)
	Elimination	0.1 (0.1; 0.1)	0.2 (0.2; 0.3)	1.4 (1.0; 2.0)	0.9 (0.5; 1.6)
Influenza-1918-X	No Closures	32.2 (16.1; 84.1)	36.3 (17.4; 102.9)	117.1 (54.6; 351.0)	6.0 (2.5; 15.7)
	Reactive-Business/Sustained-School Closures	24.8 (16.4; 47.8)	17.7 (12.3; 30.0)	66.6 (45.8; 119.7)	3.4 (1.7; 6.7)
	Reactive-Business/Reactive-School Closures	15.6 (12.3; 21.4)	15.6 (12.8; 18.7)	50.2 (40.2; 62.3)	2.6 (1.5; 4.4)
	Elimination	48.3 (22.6; 95.8)	26.4 (12.6; 58.6)	98.8 (45.4; 209.8)	4.5 (1.9; 10.3)
Covid-Omicron-X	No Closures	0.1 (0.1; 0.1)	1.3 (0.7; 2.3)	15.9 (7.7; 43.2)	7.8 (3.9; 15.1)
	Reactive-Business/Sustained-School Closures	0.1 (0.1; 0.1)	0.9 (0.6; 1.8)	11.8 (7.1; 31.3)	6.9 (3.6; 13.4)
	Reactive-Business/Reactive-School Closures	0.1 (0.1; 0.1)	0.8 (0.6; 1.5)	9.9 (6.6; 22.7)	6.2 (3.3; 11.9)
	Elimination	0.1 (0.1; 0.1)	0.8 (0.5; 1.6)	11.1 (6.2; 26.9)	6.5 (3.2; 12.7)
Covid-Delta-X	No Closures	0.1 (0.1; 0.1)	2.9 (2.0; 3.5)	309.6 (101.1; 493.8)	49.2 (26.7; 87.2)
	Reactive-Business/Sustained-School Closures	0.1 (0.1; 0.1)	2.2 (1.3; 2.9)	221.3 (73.4; 433.3)	44.2 (23.0; 80.7)
	Reactive-Business/Reactive-School Closures	0.1 (0.1; 0.1)	1.9 (1.1; 2.6)	151.1 (56.1; 356.3)	39.0 (20.5; 72.9)
	Elimination	0.1 (0.1; 0.1)	2.1 (1.4; 2.7)	234.0 (106.2; 385.5)	43.7 (23.7; 78.0)
Covid-Wildtype-X	No Closures	0.0 (0.0; 0.0)	1.0 (0.5; 1.5)	52.3 (19.7; 149.3)	13.8 (6.6; 27.1)
	Reactive-Business/Sustained-School Closures	0.0 (0.0; 0.0)	0.5 (0.3; 0.9)	27.2 (14.1; 70.7)	9.9 (5.0; 19.7)

continued on next page

continued from previous page

Income Group / Disease	Closure Strategy	Preschool-Age	School-Age	Working-Age	Retired-Age
	Reactive-Business/Reactive-School Closures	0.0 (0.0; 0.0)	0.4 (0.3; 0.6)	19.4 (12.3; 35.9)	7.9 (4.2; 14.6)
	Elimination	0.0 (0.0; 0.0)	0.6 (0.4; 0.9)	37.8 (16.4; 83.1)	11.0 (5.3; 21.3)
HIC					
Influenza-2009-X	No Closures	0.1 (0.0; 0.1)	0.2 (0.1; 0.2)	0.7 (0.5; 0.9)	0.6 (0.3; 1.0)
	Reactive-Business/Sustained-School Closures	0.1 (0.0; 0.1)	0.1 (0.1; 0.2)	0.7 (0.5; 0.9)	0.6 (0.3; 1.0)
	Reactive-Business/Reactive-School Closures	0.1 (0.0; 0.1)	0.1 (0.1; 0.2)	0.7 (0.5; 0.9)	0.6 (0.3; 1.0)
	Elimination	0.1 (0.0; 0.1)	0.1 (0.1; 0.1)	0.4 (0.3; 0.6)	0.4 (0.2; 0.7)
Influenza-1957-X	No Closures	0.0 (0.0; 0.0)	0.2 (0.1; 0.2)	1.8 (1.3; 2.5)	1.6 (0.8; 2.7)
	Reactive-Business/Sustained-School Closures	0.0 (0.0; 0.0)	0.1 (0.1; 0.2)	1.6 (1.2; 2.1)	1.4 (0.7; 2.2)
	Reactive-Business/Reactive-School Closures	0.0 (0.0; 0.0)	0.2 (0.1; 0.2)	1.7 (1.2; 2.2)	1.4 (0.7; 2.3)
	Elimination	0.0 (0.0; 0.0)	0.1 (0.1; 0.1)	1.1 (0.7; 1.5)	0.9 (0.5; 1.5)
Influenza-1918-X	No Closures	7.9 (5.7; 12.9)	9.6 (5.7; 16.5)	41.6 (26.0; 75.7)	3.7 (1.6; 7.6)
	Reactive-Business/Sustained-School Closures	7.7 (5.5; 11.0)	6.2 (3.9; 9.0)	31.0 (20.7; 45.1)	2.6 (1.1; 4.5)
	Reactive-Business/Reactive-School Closures	7.0 (5.3; 9.1)	7.8 (4.7; 10.3)	33.1 (22.5; 44.0)	2.8 (1.2; 4.8)
	Elimination	8.1 (5.7; 12.3)	4.6 (3.0; 7.1)	24.0 (16.4; 36.4)	1.9 (0.9; 3.5)
Covid-Omicron-X	No Closures	0.0 (0.0; 0.1)	0.9 (0.4; 1.5)	16.3 (8.5; 41.3)	12.9 (6.8; 25.3)
	Reactive-Business/Sustained-School Closures	0.0 (0.0; 0.1)	0.5 (0.4; 1.0)	11.4 (7.7; 26.4)	11.2 (6.0; 20.8)
	Reactive-Business/Reactive-School Closures	0.0 (0.0; 0.0)	0.5 (0.4; 0.8)	9.3 (7.3; 18.0)	9.8 (5.4; 17.1)
	Elimination	0.0 (0.0; 0.1)	0.4 (0.3; 0.6)	7.8 (5.9; 15.3)	8.2 (4.3; 14.6)
Covid-Delta-X	No Closures	0.0 (0.0; 0.0)	1.8 (0.9; 2.3)	292.7 (73.6; 498.0)	69.5 (31.5; 126.7)
	Reactive-Business/Sustained-School Closures	0.0 (0.0; 0.0)	1.0 (0.5; 1.6)	140.9 (49.4; 392.9)	53.4 (26.1; 107.9)
	Reactive-Business/Reactive-School Closures	0.0 (0.0; 0.0)	0.8 (0.5; 1.4)	85.2 (42.4; 272.4)	43.8 (22.2; 88.3)
	Elimination	0.0 (0.0; 0.0)	0.8 (0.4; 1.3)	106.5 (38.9; 257.0)	42.1 (20.3; 82.8)
Covid-Wildtype-X	No Closures	0.0 (0.0; 0.0)	0.4 (0.2; 0.8)	28.4 (16.0; 89.4)	14.6 (7.1; 31.0)
	Reactive-Business/Sustained-School Closures	0.0 (0.0; 0.0)	0.2 (0.1; 0.3)	17.8 (12.4; 32.1)	10.4 (5.3; 18.9)
	Reactive-Business/Reactive-School Closures	0.0 (0.0; 0.0)	0.2 (0.2; 0.3)	15.6 (11.6; 21.3)	9.2 (4.8; 14.9)
	Elimination	0.0 (0.0; 0.0)	0.2 (0.1; 0.3)	13.7 (8.8; 25.4)	7.8 (3.8; 14.7)

Table S10: Summary statistics (median, (IQR)) of projected VLYL by age-group (expressed as a percentage of annual GDP) under different closure strategies, for each disease and country-income group. Distributions are shown in Figure S15.

Income Group / Disease	Closure Strategy	AFF	MIN	MAN	UTL	CON	RTH	TRA	ICT	PFT	PAO
LLMIC											
Influenza-2009-X	No Closures	0.0 (0.0; 0.0)	0.0 (0.0; 0.0)	0.0 (0.0; 0.0)	0.0 (0.0; 0.0)	0.0 (0.0; 0.0)	0.0 (0.0; 0.1)	0.0 (0.0; 0.0)	0.0 (0.0; 0.0)	0.0 (0.0; 0.1)	0.0 (0.0; 0.1)
	Reactive-Business/Sustained-School Closures	0.0 (0.0; 0.0)	0.0 (0.0; 0.1)	0.1 (0.0; 0.5)	0.0 (0.0; 0.1)	0.0 (0.0; 0.2)	0.1 (0.0; 0.8)	0.0 (0.0; 0.4)	0.0 (0.0; 0.0)	0.1 (0.0; 0.3)	0.1 (0.0; 0.2)
	Reactive-Business/Reactive-School Closures	0.1 (0.0; 1.4)	0.0 (0.0; 0.2)	0.1 (0.0; 0.8)	0.0 (0.0; 0.0)	0.0 (0.0; 0.3)	0.1 (0.0; 0.6)	0.1 (0.0; 0.8)	0.0 (0.0; 0.2)	0.1 (0.0; 0.6)	0.1 (0.0; 0.7)
	Elimination	3.3 (0.8; 6.1)	0.4 (0.0; 1.8)	5.2 (1.9; 9.8)	0.1 (0.0; 0.4)	2.3 (0.8; 4.5)	9.0 (3.5; 14.2)	2.9 (1.2; 4.9)	0.4 (0.1; 1.0)	1.6 (0.6; 3.1)	2.4 (1.2; 4.4)
Influenza-1957-X	No Closures	0.0 (0.0; 0.1)	0.0 (0.0; 0.1)	0.1 (0.0; 0.1)	0.0 (0.0; 0.0)	0.0 (0.0; 0.0)	0.1 (0.1; 0.2)	0.0 (0.0; 0.1)	0.0 (0.0; 0.0)	0.1 (0.0; 0.1)	0.1 (0.0; 0.1)
	Reactive-Business/Sustained-School Closures	0.0 (0.0; 0.1)	0.0 (0.0; 0.4)	0.3 (0.1; 0.9)	0.0 (0.0; 0.1)	0.2 (0.0; 0.4)	0.6 (0.1; 1.3)	0.3 (0.0; 0.7)	0.0 (0.0; 0.0)	0.2 (0.1; 0.5)	0.2 (0.1; 0.4)
	Reactive-Business/Reactive-School Closures	0.8 (0.1; 2.5)	0.1 (0.0; 0.7)	0.6 (0.1; 1.6)	0.0 (0.0; 0.0)	0.2 (0.0; 0.7)	0.6 (0.1; 1.3)	0.5 (0.1; 1.5)	0.1 (0.0; 0.4)	0.4 (0.1; 1.1)	0.5 (0.1; 1.3)
	Elimination	4.1 (2.0; 6.8)	0.7 (0.1; 2.3)	6.5 (3.3; 11.1)	0.2 (0.1; 0.5)	2.8 (1.4; 5.3)	10.7 (6.1; 15.7)	3.4 (1.9; 5.6)	0.6 (0.2; 1.2)	2.0 (1.0; 3.5)	2.9 (1.7; 5.0)
Influenza-1918-X	No Closures	2.3 (0.7; 5.1)	0.7 (0.1; 2.8)	2.2 (0.8; 5.0)	0.2 (0.1; 0.6)	0.6 (0.2; 1.4)	4.1 (1.5; 8.1)	1.7 (0.6; 3.5)	0.5 (0.1; 1.3)	2.5 (1.0; 5.6)	2.9 (1.1; 6.2)
	Reactive-Business/Sustained-School Closures	1.3 (0.5; 3.2)	0.8 (0.1; 4.0)	2.3 (1.0; 4.6)	0.2 (0.1; 0.6)	0.7 (0.3; 1.5)	3.9 (1.9; 7.2)	2.3 (1.1; 4.4)	0.3 (0.1; 0.8)	2.1 (1.0; 4.3)	2.2 (1.0; 4.6)
	Reactive-Business/Reactive-School Closures	4.6 (2.1; 8.3)	1.0 (0.2; 3.4)	4.7 (2.2; 9.1)	0.2 (0.1; 0.5)	1.9 (0.8; 4.0)	6.9 (3.0; 13.0)	3.2 (1.7; 5.8)	0.7 (0.2; 1.6)	2.8 (1.4; 5.5)	3.7 (2.0; 6.6)
	Elimination	6.6 (3.4; 11.3)	1.5 (0.3; 5.0)	9.2 (5.0; 15.4)	0.4 (0.2; 1.0)	3.6 (2.0; 6.8)	14.9 (9.0; 21.7)	5.0 (2.9; 8.4)	1.1 (0.4; 2.3)	4.7 (2.4; 8.1)	6.0 (3.6; 9.9)
Covid-Omicron-X	No Closures	0.6 (0.2; 1.4)	0.2 (0.0; 0.7)	0.5 (0.2; 1.2)	0.0 (0.0; 0.1)	0.2 (0.1; 0.4)	0.6 (0.3; 1.4)	0.3 (0.1; 0.6)	0.1 (0.0; 0.3)	0.5 (0.2; 1.1)	0.5 (0.2; 1.0)
	Reactive-Business/Sustained-School Closures	0.4 (0.2; 1.2)	0.3 (0.0; 1.2)	0.7 (0.3; 1.5)	0.1 (0.0; 0.2)	0.3 (0.1; 0.5)	1.1 (0.5; 1.9)	0.6 (0.3; 1.1)	0.1 (0.0; 0.3)	0.6 (0.3; 1.2)	0.6 (0.3; 1.1)
	Reactive-Business/Reactive-School Closures	1.5 (0.6; 3.1)	0.3 (0.1; 1.2)	1.4 (0.7; 2.7)	0.1 (0.0; 0.2)	0.5 (0.2; 1.2)	1.8 (0.9; 3.1)	0.9 (0.4; 1.8)	0.2 (0.1; 0.5)	0.9 (0.4; 1.8)	1.0 (0.6; 1.9)
	Elimination	2.6 (1.0; 5.3)	0.5 (0.1; 1.9)	3.4 (1.4; 7.7)	0.2 (0.1; 0.4)	1.6 (0.4; 3.7)	5.3 (1.9; 11.9)	2.1 (0.7; 4.3)	0.4 (0.1; 0.9)	1.6 (0.8; 3.0)	2.0 (1.0; 3.7)
Covid-Delta-X	No Closures	4.4 (1.4; 8.9)	1.1 (0.2; 4.6)	3.8 (1.6; 7.7)	0.3 (0.1; 0.9)	1.1 (0.4; 2.4)	5.4 (2.3; 9.2)	2.1 (0.9; 3.9)	0.8 (0.2; 2.0)	3.8 (1.6; 7.4)	3.6 (1.6; 6.7)
	Reactive-Business/Sustained-School Closures	3.4 (1.1; 7.7)	1.4 (0.2; 5.8)	3.8 (1.8; 7.6)	0.4 (0.1; 0.9)	1.2 (0.5; 2.4)	5.6 (2.9; 9.2)	2.9 (1.6; 4.9)	0.6 (0.2; 1.7)	3.5 (1.6; 6.9)	3.4 (1.7; 6.2)
	Reactive-Business/Reactive-School Closures	6.1 (3.0; 10.8)	1.5 (0.3; 5.1)	6.4 (3.3; 11.1)	0.4 (0.1; 0.9)	2.3 (1.2; 4.5)	9.0 (5.0; 13.8)	3.6 (2.0; 6.0)	1.0 (0.4; 2.3)	4.3 (2.2; 7.8)	4.7 (2.7; 8.0)
	Elimination	7.0 (3.6; 11.9)	1.6 (0.3; 5.5)	8.4 (4.5; 14.0)	0.5 (0.2; 1.1)	3.1 (1.6; 6.1)	12.1 (7.2; 18.2)	4.4 (2.5; 7.2)	1.1 (0.4; 2.4)	4.8 (2.6; 8.4)	5.3 (3.3; 8.8)
Covid-Wildtype-X	No Closures	1.2 (0.4; 2.9)	0.3 (0.1; 1.5)	1.1 (0.4; 2.6)	0.1 (0.0; 0.3)	0.3 (0.1; 0.8)	1.7 (0.7; 3.6)	0.7 (0.3; 1.6)	0.2 (0.1; 0.7)	1.2 (0.4; 2.7)	1.2 (0.5; 2.6)
	Reactive-Business/Sustained-School Closures	0.7 (0.3; 1.9)	0.5 (0.1; 2.7)	1.5 (0.7; 3.0)	0.2 (0.1; 0.4)	0.5 (0.2; 1.0)	2.6 (1.4; 4.3)	1.6 (0.8; 2.9)	0.1 (0.0; 0.5)	1.3 (0.6; 2.6)	1.3 (0.7; 2.4)
	Reactive-Business/Reactive-School Closures	3.8 (1.8; 6.6)	0.8 (0.1; 2.7)	4.0 (2.0; 7.3)	0.2 (0.1; 0.4)	1.7 (0.8; 3.4)	5.9 (2.9; 10.0)	2.6 (1.4; 4.5)	0.5 (0.2; 1.2)	2.2 (1.1; 3.9)	2.7 (1.5; 4.8)
	Elimination	4.2 (2.1; 7.5)	0.9 (0.2; 3.0)	6.2 (3.2; 10.6)	0.3 (0.1; 0.6)	2.6 (1.3; 5.0)	9.8 (5.3; 15.0)	3.4 (1.9; 5.8)	0.7 (0.2; 1.4)	2.7 (1.4; 4.8)	3.5 (2.1; 5.8)
UMIC											
Influenza-2009-X	No Closures	0.0 (0.0; 0.0)	0.0 (0.0; 0.0)	0.0 (0.0; 0.0)	0.0 (0.0; 0.0)	0.0 (0.0; 0.0)	0.0 (0.0; 0.1)	0.0 (0.0; 0.0)	0.0 (0.0; 0.0)	0.0 (0.0; 0.1)	0.0 (0.0; 0.1)
	Reactive-Business/Sustained-School Closures	0.0 (0.0; 0.0)	0.0 (0.0; 0.0)	0.0 (0.0; 0.0)	0.0 (0.0; 0.0)	0.0 (0.0; 0.0)	0.0 (0.0; 0.1)	0.0 (0.0; 0.0)	0.0 (0.0; 0.0)	0.0 (0.0; 0.1)	0.0 (0.0; 0.1)
	Reactive-Business/Reactive-School Closures	0.0 (0.0; 0.0)	0.0 (0.0; 0.0)	0.0 (0.0; 0.0)	0.0 (0.0; 0.0)	0.0 (0.0; 0.0)	0.0 (0.0; 0.1)	0.0 (0.0; 0.0)	0.0 (0.0; 0.0)	0.0 (0.0; 0.1)	0.1 (0.0; 0.1)
	Elimination	0.7 (0.1; 1.7)	0.2 (0.0; 0.8)	4.8 (0.4; 7.6)	0.4 (0.1; 0.8)	2.6 (0.2; 4.4)	7.5 (0.4; 11.5)	2.7 (0.3; 4.1)	0.5 (0.0; 0.8)	2.2 (0.2; 3.5)	2.6 (0.2; 4.2)
Influenza-1957-X	No Closures	0.0 (0.0; 0.0)	0.0 (0.0; 0.0)	0.0 (0.0; 0.1)	0.0 (0.0; 0.0)	0.0 (0.0; 0.0)	0.1 (0.0; 0.1)	0.0 (0.0; 0.0)	0.0 (0.0; 0.0)	0.1 (0.0; 0.1)	0.1 (0.1; 0.1)
	Reactive-Business/Sustained-School Closures	0.0 (0.0; 0.0)	0.0 (0.0; 0.2)	0.1 (0.0; 0.6)	0.0 (0.0; 0.2)	0.0 (0.0; 0.4)	0.2 (0.1; 1.0)	0.1 (0.0; 0.6)	0.0 (0.0; 0.0)	0.2 (0.1; 0.5)	0.1 (0.1; 0.3)
	Reactive-Business/Reactive-School Closures	0.1 (0.0; 0.7)	0.0 (0.0; 0.3)	0.3 (0.0; 1.3)	0.0 (0.0; 0.1)	0.1 (0.0; 0.6)	0.3 (0.1; 0.8)	0.2 (0.0; 1.4)	0.0 (0.0; 0.3)	0.2 (0.1; 1.4)	0.2 (0.1; 1.3)
	Elimination	1.2 (0.6; 2.3)	0.4 (0.1; 1.2)	6.7 (4.6; 9.4)	0.6 (0.3; 1.1)	3.8 (2.2; 5.3)	10.1 (6.9; 13.7)	3.5 (2.5; 4.9)	0.6 (0.4; 0.9)	3.0 (2.0; 4.4)	3.5 (2.5; 5.2)
Influenza-1918-X	No Closures	0.3 (0.1; 1.0)	0.2 (0.1; 0.7)	1.1 (0.5; 2.9)	0.3 (0.1; 0.8)	0.4 (0.2; 0.9)	1.6 (0.7; 4.4)	0.7 (0.3; 1.9)	0.2 (0.1; 0.7)	1.6 (0.7; 4.5)	2.0 (0.9; 5.4)
	Reactive-Business/Sustained-School Closures	0.2 (0.1; 0.4)	0.3 (0.1; 1.4)	1.4 (0.8; 2.2)	0.4 (0.2; 0.8)	0.6 (0.4; 0.9)	1.9 (1.2; 3.0)	1.2 (0.7; 2.2)	0.1 (0.1; 0.2)	1.5 (0.9; 2.4)	1.4 (0.8; 2.3)
	Reactive-Business/Reactive-School Closures	1.0 (0.5; 2.0)	0.4 (0.1; 1.2)	2.4 (1.5; 3.9)	0.2 (0.1; 0.5)	1.2 (0.7; 1.9)	2.4 (1.3; 4.4)	2.1 (1.4; 3.1)	0.5 (0.3; 0.8)	2.5 (1.7; 3.7)	2.7 (1.8; 3.9)
	Elimination	1.6 (0.8; 3.2)	0.7 (0.2; 1.8)	8.1 (5.8; 11.2)	0.9 (0.5; 1.6)	4.4 (2.8; 6.0)	12.3 (8.7; 16.4)	4.3 (3.2; 6.1)	0.9 (0.6; 1.3)	4.7 (3.2; 6.9)	5.6 (3.8; 7.9)

continued on next page

continued from previous page

Income Group / Disease	Closure Strategy	AFF	MIN	MAN	UTL	CON	RTH	TRA	ICT	PFT	PAO
Covid-Omicron-X	No Closures	0.1 (0.1; 0.3)	0.1 (0.0; 0.2)	0.3 (0.2; 0.7)	0.1 (0.0; 0.2)	0.1 (0.1; 0.2)	0.4 (0.2; 0.8)	0.2 (0.1; 0.4)	0.1 (0.0; 0.2)	0.4 (0.3; 0.9)	0.4 (0.2; 0.8)
	Reactive-Business/Sustained-School Closures	0.1 (0.0; 0.2)	0.1 (0.0; 0.6)	0.7 (0.3; 1.3)	0.2 (0.1; 0.4)	0.3 (0.1; 0.6)	0.9 (0.4; 1.6)	0.6 (0.2; 1.1)	0.1 (0.0; 0.1)	0.7 (0.4; 1.3)	0.6 (0.3; 1.0)
	Reactive-Business/Reactive-School Closures	0.4 (0.1; 1.0)	0.2 (0.1; 0.5)	1.3 (0.5; 2.2)	0.1 (0.1; 0.3)	0.6 (0.2; 1.1)	1.3 (0.6; 2.3)	0.9 (0.3; 1.7)	0.2 (0.1; 0.4)	1.2 (0.5; 2.2)	1.2 (0.5; 2.1)
	Elimination	0.9 (0.4; 2.0)	0.4 (0.1; 1.1)	5.5 (2.5; 8.6)	0.5 (0.3; 1.0)	2.8 (1.1; 4.9)	8.0 (3.1; 12.7)	3.0 (1.5; 4.6)	0.5 (0.3; 0.9)	2.8 (1.7; 4.2)	3.1 (1.8; 4.8)
Covid-Delta-X	No Closures	1.2 (0.5; 3.1)	0.7 (0.2; 2.3)	4.2 (1.5; 7.7)	1.0 (0.4; 2.3)	1.4 (0.5; 2.8)	5.1 (2.0; 9.1)	2.3 (0.9; 3.9)	0.9 (0.3; 1.8)	5.9 (2.2; 10.6)	5.7 (2.2; 9.8)
	Reactive-Business/Sustained-School Closures	1.0 (0.4; 2.6)	1.0 (0.3; 3.2)	4.2 (2.1; 7.4)	1.1 (0.5; 2.2)	1.4 (0.8; 2.7)	5.3 (3.0; 8.8)	3.1 (2.0; 4.9)	0.7 (0.2; 1.5)	5.1 (2.4; 9.5)	4.7 (2.2; 8.9)
	Reactive-Business/Reactive-School Closures	1.8 (0.9; 3.7)	0.9 (0.3; 2.6)	6.5 (4.1; 9.6)	1.0 (0.5; 2.1)	2.9 (1.7; 4.5)	8.4 (5.1; 12.2)	3.7 (2.5; 5.5)	1.0 (0.6; 1.8)	5.9 (3.5; 9.7)	6.1 (3.6; 9.9)
	Elimination	2.3 (1.1; 4.4)	1.1 (0.4; 3.1)	9.3 (6.6; 13.0)	1.4 (0.8; 2.7)	4.6 (2.8; 6.5)	12.9 (9.0; 17.5)	4.8 (3.5; 6.7)	1.3 (0.8; 2.1)	7.5 (4.9; 11.1)	7.5 (5.1; 11.0)
Covid-Wildtype-X	No Closures	0.3 (0.1; 0.7)	0.2 (0.0; 0.6)	0.8 (0.3; 2.1)	0.2 (0.1; 0.6)	0.3 (0.1; 0.7)	1.1 (0.5; 2.8)	0.5 (0.2; 1.2)	0.2 (0.1; 0.5)	1.2 (0.5; 3.0)	1.2 (0.5; 3.1)
	Reactive-Business/Sustained-School Closures	0.2 (0.1; 0.4)	0.3 (0.1; 1.3)	1.3 (0.7; 2.4)	0.4 (0.2; 0.8)	0.6 (0.3; 0.9)	2.0 (1.2; 3.1)	1.4 (0.8; 2.4)	0.1 (0.1; 0.2)	1.4 (0.8; 2.4)	1.2 (0.7; 2.3)
	Reactive-Business/Reactive-School Closures	1.0 (0.4; 2.0)	0.4 (0.1; 1.2)	3.2 (1.9; 5.1)	0.3 (0.2; 0.7)	1.6 (0.9; 2.6)	4.0 (2.0; 6.6)	2.3 (1.5; 3.5)	0.5 (0.3; 0.8)	2.6 (1.7; 3.9)	2.8 (1.7; 4.3)
	Elimination	1.2 (0.6; 2.3)	0.5 (0.2; 1.3)	6.0 (3.9; 8.8)	0.7 (0.4; 1.3)	3.2 (1.9; 4.9)	8.8 (5.6; 12.8)	3.4 (2.3; 4.9)	0.6 (0.4; 1.0)	3.5 (2.3; 5.4)	3.9 (2.6; 5.8)
HIC											
Influenza-2009-X	No Closures	0.0 (0.0; 0.0)	0.0 (0.0; 0.0)	0.0 (0.0; 0.0)	0.0 (0.0; 0.0)	0.0 (0.0; 0.0)	0.0 (0.0; 0.0)	0.0 (0.0; 0.0)	0.0 (0.0; 0.0)	0.0 (0.0; 0.1)	0.0 (0.0; 0.1)
	Reactive-Business/Sustained-School Closures	0.0 (0.0; 0.0)	0.0 (0.0; 0.0)	0.0 (0.0; 0.0)	0.0 (0.0; 0.0)	0.0 (0.0; 0.0)	0.0 (0.0; 0.0)	0.0 (0.0; 0.0)	0.0 (0.0; 0.0)	0.0 (0.0; 0.1)	0.0 (0.0; 0.1)
	Reactive-Business/Reactive-School Closures	0.0 (0.0; 0.0)	0.0 (0.0; 0.0)	0.0 (0.0; 0.0)	0.0 (0.0; 0.0)	0.0 (0.0; 0.0)	0.0 (0.0; 0.0)	0.0 (0.0; 0.0)	0.0 (0.0; 0.0)	0.0 (0.0; 0.1)	0.0 (0.0; 0.1)
	Elimination	0.3 (0.1; 0.6)	0.0 (0.0; 0.1)	4.7 (2.7; 7.1)	0.3 (0.2; 0.5)	3.3 (1.9; 4.3)	8.1 (5.3; 10.8)	2.5 (1.6; 3.3)	0.7 (0.4; 1.0)	3.4 (2.1; 4.6)	3.8 (2.4; 5.2)
Influenza-1957-X	No Closures	0.0 (0.0; 0.0)	0.0 (0.0; 0.0)	0.0 (0.0; 0.1)	0.0 (0.0; 0.0)	0.0 (0.0; 0.0)	0.1 (0.0; 0.1)	0.0 (0.0; 0.0)	0.0 (0.0; 0.0)	0.1 (0.1; 0.1)	0.1 (0.1; 0.1)
	Reactive-Business/Sustained-School Closures	0.0 (0.0; 0.0)	0.0 (0.0; 0.0)	0.1 (0.0; 0.4)	0.0 (0.0; 0.1)	0.0 (0.0; 0.4)	0.1 (0.0; 0.8)	0.0 (0.0; 0.6)	0.0 (0.0; 0.0)	0.1 (0.1; 0.7)	0.1 (0.1; 0.2)
	Reactive-Business/Reactive-School Closures	0.0 (0.0; 0.2)	0.0 (0.0; 0.0)	0.1 (0.0; 1.0)	0.0 (0.0; 0.0)	0.0 (0.0; 0.6)	0.1 (0.0; 0.7)	0.0 (0.0; 1.1)	0.0 (0.0; 0.4)	0.1 (0.1; 1.9)	0.1 (0.1; 1.5)
	Elimination	0.4 (0.2; 0.7)	0.1 (0.0; 0.2)	5.8 (4.0; 8.2)	0.4 (0.3; 0.6)	3.9 (3.0; 4.8)	9.6 (7.5; 12.2)	2.9 (2.2; 3.7)	0.9 (0.7; 1.1)	4.0 (3.1; 5.2)	4.6 (3.4; 5.9)
Influenza-1918-X	No Closures	0.0 (0.0; 0.1)	0.0 (0.0; 0.1)	0.3 (0.2; 0.7)	0.1 (0.0; 0.2)	0.1 (0.1; 0.3)	0.5 (0.3; 1.0)	0.2 (0.1; 0.4)	0.1 (0.1; 0.3)	0.8 (0.4; 1.6)	0.7 (0.4; 1.4)
	Reactive-Business/Sustained-School Closures	0.0 (0.0; 0.1)	0.0 (0.0; 0.1)	0.7 (0.3; 1.2)	0.2 (0.1; 0.3)	0.5 (0.2; 0.6)	1.1 (0.7; 1.6)	0.7 (0.3; 1.1)	0.1 (0.0; 0.1)	1.2 (0.8; 1.7)	0.7 (0.5; 1.0)
	Reactive-Business/Reactive-School Closures	0.2 (0.1; 0.5)	0.0 (0.0; 0.1)	1.4 (0.6; 2.2)	0.1 (0.1; 0.2)	0.8 (0.3; 1.2)	1.2 (0.6; 2.0)	1.4 (0.4; 1.9)	0.6 (0.2; 0.8)	2.7 (1.3; 3.6)	2.2 (1.1; 3.2)
	Elimination	0.4 (0.2; 0.7)	0.1 (0.0; 0.2)	6.2 (4.4; 8.7)	0.5 (0.3; 0.7)	4.0 (3.2; 5.0)	10.1 (8.0; 12.8)	3.1 (2.4; 3.9)	1.0 (0.7; 1.2)	4.6 (3.7; 5.9)	5.2 (4.0; 6.5)
Covid-Omicron-X	No Closures	0.0 (0.0; 0.1)	0.0 (0.0; 0.0)	0.3 (0.2; 0.7)	0.1 (0.0; 0.1)	0.1 (0.1; 0.3)	0.4 (0.2; 0.8)	0.2 (0.1; 0.3)	0.1 (0.1; 0.2)	0.7 (0.4; 1.5)	0.5 (0.3; 1.0)
	Reactive-Business/Sustained-School Closures	0.0 (0.0; 0.1)	0.0 (0.0; 0.1)	0.8 (0.4; 1.4)	0.2 (0.1; 0.3)	0.5 (0.2; 0.7)	1.2 (0.6; 1.7)	0.8 (0.4; 1.2)	0.1 (0.1; 0.2)	1.4 (0.8; 2.0)	0.7 (0.4; 1.1)
	Reactive-Business/Reactive-School Closures	0.2 (0.1; 0.4)	0.0 (0.0; 0.1)	1.5 (0.7; 2.5)	0.1 (0.1; 0.2)	0.9 (0.4; 1.3)	1.6 (0.9; 2.5)	1.2 (0.5; 1.9)	0.5 (0.2; 0.8)	2.5 (1.1; 3.6)	2.0 (0.9; 3.1)
	Elimination	0.4 (0.2; 0.7)	0.1 (0.0; 0.2)	5.6 (3.6; 8.3)	0.4 (0.3; 0.7)	3.8 (2.4; 4.9)	9.4 (6.5; 12.4)	3.0 (2.1; 3.9)	0.9 (0.6; 1.2)	4.4 (3.3; 5.7)	4.7 (3.3; 6.3)
Covid-Delta-X	No Closures	0.4 (0.1; 1.0)	0.1 (0.0; 0.4)	3.5 (1.1; 7.2)	0.7 (0.2; 1.5)	1.5 (0.4; 3.1)	5.2 (1.5; 9.1)	1.9 (0.6; 3.6)	1.3 (0.4; 2.6)	8.7 (2.5; 16.2)	6.7 (1.9; 11.4)
	Reactive-Business/Sustained-School Closures	0.2 (0.1; 0.7)	0.1 (0.0; 0.5)	3.3 (1.5; 6.3)	0.6 (0.3; 1.3)	1.3 (0.8; 2.7)	4.6 (2.6; 8.3)	2.8 (1.8; 4.2)	0.7 (0.3; 1.9)	5.7 (2.8; 13.4)	4.3 (1.9; 9.7)
	Reactive-Business/Reactive-School Closures	0.6 (0.3; 1.1)	0.1 (0.0; 0.4)	5.4 (3.2; 8.4)	0.6 (0.3; 1.1)	3.1 (1.9; 4.4)	7.9 (4.8; 11.2)	3.1 (2.1; 4.4)	1.3 (0.9; 2.2)	6.9 (4.6; 12.2)	6.5 (4.2; 10.4)
	Elimination	0.6 (0.4; 1.2)	0.1 (0.0; 0.4)	7.9 (5.6; 11.4)	0.8 (0.5; 1.3)	4.8 (3.8; 6.0)	12.3 (9.7; 15.6)	4.0 (3.0; 5.3)	1.5 (1.1; 2.3)	8.3 (5.7; 12.6)	7.9 (5.8; 11.2)
Covid-Wildtype-X	No Closures	0.1 (0.0; 0.2)	0.0 (0.0; 0.1)	0.4 (0.2; 1.2)	0.1 (0.0; 0.3)	0.2 (0.1; 0.5)	0.6 (0.3; 1.7)	0.2 (0.1; 0.7)	0.2 (0.1; 0.4)	1.0 (0.6; 2.9)	0.8 (0.5; 2.3)
	Reactive-Business/Sustained-School Closures	0.0 (0.0; 0.1)	0.0 (0.0; 0.2)	1.0 (0.5; 1.7)	0.2 (0.1; 0.3)	0.5 (0.3; 0.7)	1.6 (1.0; 2.3)	1.2 (0.7; 1.8)	0.1 (0.1; 0.2)	1.6 (1.1; 2.3)	0.9 (0.6; 1.5)

continued on next page

continued from previous page

Income Group / Disease	Closure Strategy	AFF	MIN	MAN	UTL	CON	RTH	TRA	ICT	PFT	PAO
	Reactive-Business/Reactive-School Closures	0.3 (0.1; 0.6)	0.0 (0.0; 0.2)	2.4 (1.3; 3.8)	0.2 (0.1; 0.3)	1.4 (0.8; 2.2)	2.9 (1.5; 5.0)	1.7 (1.1; 2.4)	0.7 (0.4; 0.9)	3.2 (2.2; 4.2)	2.9 (1.9; 4.0)
	Elimination	0.4 (0.2; 0.7)	0.1 (0.0; 0.2)	5.4 (3.6; 7.9)	0.4 (0.3; 0.6)	3.6 (2.5; 4.6)	8.9 (6.5; 11.6)	2.8 (2.1; 3.7)	0.9 (0.6; 1.2)	4.3 (3.2; 5.5)	4.6 (3.3; 6.0)

Table S11: Summary statistics (median, (IQR)) of projected GDPL by aggregate economic sector (expressed as a percentage of annual GDP) under different closure strategies, for each disease and country-income group. AFF = Agriculture, Forestry, Fishing, MIN = Mining, MAN = Manufacturing, UTL = Utilities, CON = Construction, RTH = Retail, Hospitality, TRA = Transport, ICT = IT, Telecommunications, PFT = Finance, Professional, Technical, PAO = Public Administration, Other Services. Distributions are shown in Figure S16.

5 Code & Future Work

The code and data to reproduce this analysis are available on GitHub[18]. However, there is ongoing work to further develop the daedalus model as a pandemic planning tool:

- The daedalus R package[110] is currently under development as an open-source tool for pandemic projections, with associated data and scenario comparison packages;
- DAEDALUS Explore[111] is an interactive dashboard tool, based on the daedalus R package, that acts as an accessible interface for decision-makers.

References

[1] Jackson C, Mangtani P, Hawker J, Olowokure B, Vynnycky E. The effects of school closures on influenza outbreaks and pandemics: systematic review of simulation studies. *PloS one* 2014; **9**: e97297.

[2] Lee VJ, Lye DC, Wilder-Smith A. Combination strategies for pandemic influenza response-a systematic review of mathematical modeling studies. *BMC medicine* 2009; **7**: 1-8.

[3] Longini Jr IM, Nizam A, Xu S, et al. Containing pandemic influenza at the source. *Science* 2005; **309**: 1083-7.

[4] Bolton K, McCaw J, Moss R, et al. Likely effectiveness of pharmaceutical and non-pharmaceutical interventions for mitigating influenza virus transmission in Mongolia. *Bulletin of the World Health Organization* 2012; **90**: 264-71.

[5] Milne GJ, Baskaran P, Halder N, Karl S, Kelso J. Pandemic influenza in Papua New Guinea: a modelling study comparison with pandemic spread in a developed country. *BMJ open* 2013; **3**: e002518.

[6] Handel A, Miller JC, Ge Y, Fung ICH. If long-term suppression is not possible, how do we minimize mortality for COVID-19 and other emerging infectious disease outbreaks? *MedRxiv* 2020: 2020-03.

[7] Dobson A, Ricci C, Boucekkine R, et al. Balancing economic and epidemiological interventions in the early stages of pathogen emergence. *Science Advances* 2023; **9**: eade6169.

[8] Nowak SA, Nascimento de Lima P, Vardavas R. Optimal non-pharmaceutical pandemic response strategies depend critically on time horizons and costs. *Scientific Reports* 2023; **13**: 2416.

[9] Pisaneschi G, Tarani M, Di Donato G, Landi A, Laurino M, Manfredi P. Optimal social distancing in epidemic control: cost prioritization, adherence and insights into preparedness principles. *Scientific Reports* 2024; **14**: 4365.

[10] Doyle NJ, Cumming F, Thompson RN, Tildesley MJ. When should lockdown be implemented? Devising cost-effective strategies for managing epidemics amid vaccine uncertainty. *PLOS Computational Biology* 2024; **20**: e1012010.

[11] Halder N, Kelso JK, Milne GJ. Cost-effective strategies for mitigating a future influenza pandemic with H1N1 2009 characteristics. *PLoS One* 2011; **6**: e22087.

[12] Kelso JK, Halder N, Postma MJ, Milne GJ. Economic analysis of pandemic influenza mitigation strategies for five pandemic severity categories. *BMC public health* 2013; **13**: 1-17.

[13] Kelso JK, Halder N, Milne GJ. Vaccination strategies for future influenza pandemics: a severity-based cost effectiveness analysis. *BMC infectious diseases* 2013; **13**: 1-13.

[14] Milne GJ, Halder N, Kelso JK. The cost effectiveness of pandemic influenza interventions: a pandemic severity based analysis. *PloS one* 2013; **8**: e61504.

[15] Haw DJ, Forchini G, Doohan P, et al. Optimizing social and economic activity while containing SARS-CoV-2 transmission using DAEDALUS. *Nature Computational Science* 2022; **2**: 223-33.

[16] Johnson R, Djaafara B, Haw D, et al. The societal value of SARS-CoV-2 booster vaccination in Indonesia. *Vaccine* 2023; **41**: 1885-91.

[17] Johnson R, Carnalla M, Basto-Abreu A, et al. Promoting healthy populations as a pandemic preparedness strategy: a simulation study from Mexico. *The Lancet Regional Health–Americas* 2024; **30**.

[18] Doohan P. daedalus_mfp; 2025. Available from: https://github.com/jameel-institute/daedalus_mfp.

[19] Walker PG, Whittaker C, Watson OJ, et al. The impact of COVID-19 and strategies for mitigation and suppression in low-and middle-income countries. *Science* 2020; **369**: 413-22.

[20] Hausmann R, Schetter U. Horrible trade-offs in a pandemic: Poverty, fiscal space, policy, and welfare. *World Development* 2022; **153**: 105819.

[21] Barnett-Howell Z, Watson OJ, Mobarak AM. The benefits and costs of social distancing in high-and low-income countries. *Transactions of the Royal Society of Tropical Medicine and Hygiene* 2021; **115**: 807-19.

[22] The World Bank. The World by Income and Region; 2023. Available from: https://datatopics.worldbank.org/world-development-indicators/the-world-by-income-and-region.html.

[23] The United Nations. World Population Prospects; 2019. Available from: https://population.un.org/wpp/.

[24] The World Health Organization. Global Health Observatory; 2025. Available from: https://apps.who.int/gho/data/node.home.

[25] The United Nations. International Standard Industrial Classification of All Economic Activities; 2008. Available from: https://unstats.un.org/unsd/publication/seriesm/seriesm_4rev4e.pdf.

[26] The Organisation for Economic Co-operation and Development. Trade in Employment; 2021. Available from: https://www.oecd.org/en/data/datasets/trade-in-employment.html.

[27] The International Labour Organization. Statistics on Employment; 2025. Available from: https://ilostat.ilo.org/topics/employment/.

[28] The Organisation for Economic Co-operation and Development. Input-Output Tables; 2021. Available from: https://www.oecd.org/en/data/datasets/input-output-tables.html.

[29] Béraud G, Kazmercziak S, Beutels P, et al. The French connection: the first large population-based contact survey in France relevant for the spread of infectious diseases. *PloS one* 2015; **10**: e0133203.

[30] Prem K, Zandvoort Kv, Klepac P, et al. Projecting contact matrices in 177 geographical regions: an update and comparison with empirical data for the COVID-19 era. *PLoS computational biology* 2021; **17**: e1009098.

[31] Prem K, Cook AR, Jit M. Projecting social contact matrices in 152 countries using contact surveys and demographic data. *PLoS computational biology* 2017; **13**: e1005697.

[32] Mossong J, Hens N, Jit M, et al. Social contacts and mixing patterns relevant to the spread of infectious diseases. *PLoS medicine* 2008; **5**: e74.

[33] Mehand MS, Al-Shorbaji F, Millett P, Murgue B. The WHO R&D Blueprint: 2018 review of emerging infectious diseases requiring urgent research and development efforts. *Antiviral research* 2018; **159**: 63.

[34] Fraser C, Donnelly CA, Cauchemez S, et al. Pandemic potential of a strain of influenza A (H1N1): early findings. *science* 2009; **324**: 1557-61.

[35] Vynnycky E, Edmunds W. Analyses of the 1957 (Asian) influenza pandemic in the United Kingdom and the impact of school closures. *Epidemiology & Infection* 2008; **136**: 166-79.

[36] Ferguson NM, Cummings DA, Cauchemez S, et al. Strategies for containing an emerging influenza pandemic in Southeast Asia. *Nature* 2005; **437**: 209-14.

[37] Lyngse FP, Mortensen LH, Denwood MJ, et al. SARS-CoV-2 Omicron VOC transmission in Danish households. *MedRxiv* 2021: 2021-12.

[38] Liu Y, Rocklöv J. The reproductive number of the Delta variant of SARS-CoV-2 is far higher compared to the ancestral SARS-CoV-2 virus. *Journal of travel medicine* 2021; **28**: taab124.

[39] Billah MA, Miah MM, Khan MN. Reproductive number of coronavirus: A systematic review and meta-analysis based on global level evidence. *PloS one* 2020; **15**: e0242128.

[40] Mills CE, Robins JM, Lipsitch M. Transmissibility of 1918 pandemic influenza. *Nature* 2004; **432**: 904-6.

[41] Byambasuren O, Cardona M, Bell K, Clark J, McLaws ML, Glasziou P. Estimating the extent of asymptomatic COVID-19 and its potential for community transmission: systematic review and meta-analysis. *Official Journal of the Association of Medical Microbiology and Infectious Disease Canada* 2020; **5**: 223-34.

[42] Balcan D, Hu H, Goncalves B, et al. Seasonal transmission potential and activity peaks of the new influenza A (H1N1): a Monte Carlo likelihood analysis based on human mobility. *BMC medicine* 2009; **7**: 1-12.

[43] Li B, Deng A, Li K, et al. Viral infection and transmission in a large, well-traced outbreak caused by the SARS-CoV-2 Delta variant. *Nature communications* 2022; **13**: 460.

[44] Knock ES, Whittles LK, Lees JA, et al. The 2020 SARS-CoV-2 epidemic in England: key epidemiological drivers and impact of interventions. *MedRxiv* 2021: 2021-01.

[45] Cheng AC, Kotsimbos T, Reynolds A, et al. Clinical and epidemiological profile of patients with severe H1N1/09 pandemic influenza in Australia and New Zealand: an observational cohort study. *BMJ open* 2011; **1**: e000100.

[46] Iuliano AD. Trends in disease severity and health care utilization during the early Omicron variant period compared with previous SARS-CoV-2 high transmission periods—United States, December 2020–January 2022. *MMWR Morbidity and mortality weekly report* 2022; **71**.

[47] Guan Wj, Ni Zy, Hu Y, et al. Clinical characteristics of coronavirus disease 2019 in China. *New England journal of medicine* 2020; **382**: 1708-20.

[48] Carrat F, Vergu E, Ferguson NM, et al. Time lines of infection and disease in human influenza: a review of volunteer challenge studies. *American journal of epidemiology* 2008; **167**: 775-85.

[49] Ma Q, Liu J, Liu Q, et al. Global percentage of asymptomatic SARS-CoV-2 infections among the tested population and individuals with confirmed COVID-19 diagnosis: a systematic review and meta-analysis. *JAMA network open* 2021; **4**: e2137257-7.

[50] Reed C, Angulo FJ, Swerdlow DL, et al. Estimates of the prevalence of pandemic (H1N1) 2009, United States, April–July 2009. *Emerging infectious diseases* 2009; **15**: 2004.

[51] Napoli C, Fabiani M, Rizzo C, et al. Assessment of human influenza pandemic scenarios in Europe. *Eurosurveillance* 2015; **20**: 1-10.

[52] Nyberg T, Ferguson NM, Nash SG, et al. Comparative analysis of the risks of hospitalisation and death associated with SARS-CoV-2 omicron (B. 1.1. 529) and delta (B. 1.617. 2) variants in England: a cohort study. *The lancet* 2022; **399**: 1303-12.

[53] Sheikh A, McMenamin J, Taylor B, Robertson C. SARS-CoV-2 Delta VOC in Scotland: demographics, risk of hospital admission, and vaccine effectiveness. *The Lancet* 2021; **397**: 2461-2.

[54] Verity R, Okell LC, Dorigatti I, et al. Estimates of the severity of coronavirus disease 2019: a model-based analysis. *The Lancet infectious diseases* 2020; **20**: 669-77.

[55] Donaldson LJ, Rutter PD, Ellis BM, et al. Mortality from pandemic A/H1N1 2009 influenza in England: public health surveillance study. *Bmj* 2009; **339**.

[56] McDonald J. Asian influenza in Great Britain 1957-58. *Proceedings of the Royal Society of Medicine* 1958; **51**: 1016-8.

[57] Taubenberger JK, Morens DM. 1918 Influenza: the mother of all pandemics. *Revista Biomedica* 2006; **17**: 69-79.

[58] Diekmann O, Heesterbeek JAP, Metz JAJ. On the definition and the computation of the basic reproduction ratio R 0 in models for infectious diseases in heterogeneous populations. *Journal of mathematical biology* 1990; **28**: 365-82.

[59] Van den Driessche P, Watmough J. Reproduction numbers and sub-threshold endemic equilibria for compartmental models of disease transmission. *Mathematical biosciences* 2002; **180**: 29-48.

[60] Ritchie H. Google Mobility Trends: How has the pandemic changed the movement of people around the world? *Our World in Data* 2020. Https://ourworldindata.org/covid-mobility-trends.

[61] Roser M. What is the COVID-19 Stringency Index? *Our World in Data* 2021. Https://ourworldindata.org/metrics-explained-covid19-stringency-index.

[62] Zhang P, Wang T, Xie SX. Meta-analysis of several epidemic characteristics of COVID-19. *Journal of data science: JDS* 2020; **18**: 536.

[63] Mathieu E, Ritchie H, Rodés-Guirao L, et al. Coronavirus (COVID-19) Deaths. *Our World in Data* 2020. Https://ourworldindata.org/covid-deaths.

[64] Wang H, Paulson KR, Pease SA, et al. Estimating excess mortality due to the COVID-19 pandemic: a systematic analysis of COVID-19-related mortality, 2020–21. *The Lancet* 2022; **399**: 1513-36.

[65] Delignette-Muller ML, Dutang C. fitdistrplus: An R package for fitting distributions. *Journal of statistical software* 2015; **64**: 1-34.

[66] Sun K, Wang W, Gao L, et al. Transmission heterogeneities, kinetics, and controllability of SARS-CoV-2. *Science* 2021; **371**: eabe2424.

[67] Ng Y. Evaluation of the effectiveness of surveillance and containment measures for the first 100 patients with COVID-19 in Singapore—January 2–February 29, 2020. *MMWR Morbidity and mortality weekly report* 2020; **69**.

[68] Whitty C, Atherton F, McBride M, et al. Technical report on the COVID-19 pandemic in the UK. *Department of Public Health and Social Care* 2022: 169-83.

[69] McAloon C, Collins Á, Hunt K, et al. Incubation period of COVID-19: a rapid systematic review and meta-analysis of observational research. *BMJ open* 2020; **10**: e039652.

[70] Auranen K, Shubin M, Erra E, et al. Efficacy and effectiveness of case isolation and quarantine during a growing phase of the COVID-19 epidemic in Finland. *Scientific reports* 2023; **13**: 298.

[71] Ali ST, Yeung A, Shan S, et al. Serial intervals and case isolation delays for coronavirus disease 2019: a systematic review and meta-analysis. *Clinical Infectious Diseases* 2022; **74**: 685-94.

[72] Fraser C, Riley S, Anderson RM, Ferguson NM. Factors that make an infectious disease outbreak controllable. *Proceedings of the National Academy of Sciences* 2004; **101**: 6146-51.

[73] Klinkenberg D, Fraser C, Heesterbeek H. The effectiveness of contact tracing in emerging epidemics. *PloS one* 2006; **1**: e12.

[74] Peak CM, Childs LM, Grad YH, Buckee CO. Comparing nonpharmaceutical interventions for containing emerging epidemics. *Proceedings of the National Academy of Sciences* 2017; **114**: 4023-8.

[75] Mathieu E, Ritchie H, Rodés-Guirao L, et al. Coronavirus (COVID-19) Testing. *Our World in Data* 2020. Https://ourworldindata.org/coronavirus-testing.

[76] Russell TW, Golding N, Hellewell J, et al. Reconstructing the early global dynamics of under-ascertained COVID-19 cases and infections. *BMC medicine* 2020; **18**: 332.

[77] The World Bank. World Bank Open Data; 2021. Available from: https://data.worldbank.org/indicator/SH.MED.BEDS.ZS.

[78] The World Health Organization. European Health Information Gateway; 2024. Available from: https://gateway.euro.who.int/en/indicators/hfa_542-6210-bed-occupancy-rate-acute-care-hospitals-only/.

[79] Bagust A, Place M, Posnett JW. Dynamics of bed use in accommodating emergency admissions: stochastic simulation model. *Bmj* 1999; **319**: 155-8.

[80] Bayati M, Noroozi R, Ghanbari-Jahromi M, Jalali FS. Inequality in the distribution of Covid-19 vaccine: a systematic review. *International journal for equity in health* 2022; **21**: 122.

[81] Mathieu E, Ritchie H, Rodés-Guirao L, et al. Coronavirus (COVID-19) Vaccinations. *Our World in Data* 2020. Https://ourworldindata.org/covid-vaccinations.

[82] Hogan AB, Winskill P, Watson OJ, et al. Within-country age-based prioritisation, global allocation, and public health impact of a vaccine against SARS-CoV-2: A mathematical modelling analysis. *Vaccine* 2021; **39**: 2995-3006.

[83] Flaxman S, Mishra S, Gandy A, et al. Estimating the effects of non-pharmaceutical interventions on COVID-19 in Europe. *Nature* 2020; **584**: 257-61.

[84] Wu S, Neill R, De Foo C, et al. Aggressive containment, suppression, and mitigation of covid-19: lessons learnt from eight countries. *bmj* 2021; **375**.

[85] Kung S, Hills T, Kearns N, Beasley R. New Zealand's COVID-19 elimination strategy and mortality patterns. *The Lancet* 2023; **402**: 1037-8.

[86] Dickens BL, Koo JR, Lim JT, et al. Modelling lockdown and exit strategies for COVID-19 in Singapore. *The Lancet Regional Health–Western Pacific* 2020; **1**.

[87] Forman R, Mossialos E. The EU response to COVID-19: from reactive policies to strategic Decision-Making. *Journal of Common Market Studies* 2021; **59**: 56.

[88] Keeling MJ, Hill EM, Gorsich EE, et al. Predictions of COVID-19 dynamics in the UK: Short-term forecasting and analysis of potential exit strategies. *PLoS computational biology* 2021; **17**: e1008619.

[89] Shimul SN, Hussain M, Faisel AJ, Hamid SA, Sultana N, Kuddus MA. Impact of alternative Non-Pharmaceutical Interventions strategies for controlling COVID-19 outbreak in Bangladesh: A modeling study. *Plos one* 2024; **19**: e0293863.

[90] Caldwell JM, de Lara-Tuprio E, Teng TR, et al. Understanding COVID-19 dynamics and the effects of interventions in the Philippines: A mathematical modelling study. *The Lancet Regional Health–Western Pacific* 2021; **14**.

[91] Perez-Guzman PN, Chanda SL, Schaap A, et al. Pandemic burden in low-income settings and impact of limited and delayed interventions: A granular modelling analysis of COVID-19 in Kabwe, Zambia. *International journal of infectious diseases* 2024; **147**: 107182.

[92] Lee K. Working from home as an economic and social change: A review. *Labour Economics* 2023; **85**: 102462.

[93] Khawar L, Donovan B, Peeling RW, Guy RJ, McGregor S. Elimination and eradication goals for communicable diseases: a systematic review. *Bulletin of the World Health Organization* 2023; **101**: 649.

[94] Badan Pusat Statistik [Central Bureau of Statistics]. PDB Menurut Lapangan Usaha Seri 2010 [GDP by Industry 2010 Series]; 2025. Available from: https://www.bps.go.id/id/statistics-table/2/NjUjMg==/-2010-version-gdp-at-2010-version.html.

[95] Office for National Statistics. Monthly gross domestic product by gross value added; 2025. Available from: https://www.ons.gov.uk/economy/grossdomesticproductgdp/datasets/monthlygrossdomesticproductbygrossvalueadded.

[96] Australian Bureau of Statistics. Australian System of National Accounts; 2024. Available from: https://www.abs.gov.au/statistics/economy/national-accounts/australian-system-national-accounts/latest-release.

[97] Office for National Statistics. Business insights and impact on the UK economy; 2025. Available from: https://www.ons.gov.uk/economy/economicoutputandproductivity/output/datasets/businessinsightsandimpactontheukeconomy.

[98] Gottlieb C, Grobovšek J, Poschke M, Saltiel F. Working from home in developing countries. *European Economic Review* 2021; **133**: 103679.

[99] Sittimart M, Rattanavipapong W, Mirelman AJ, et al. An overview of the perspectives used in health economic evaluations. *Cost effectiveness and resource allocation* 2024; **22**: 41.

[100] The Global Fund . Results Report 2024; 2024. Available from: https://www.theglobalfund.org/media/14794/core_2024-results_report_en.pdf.

[101] Ananthapavan J, Moodie M, Milat AJ, Carter R. Systematic review to update 'value of a statistical life'estimates for Australia. *International journal of environmental research and public health* 2021; **18**: 6168.

[102] Robinson LA, Sullivan R, Shogren JF. Do the benefits of COVID-19 policies exceed the costs? Exploring uncertainties in the age–VSL relationship. *Risk Analysis* 2021; **41**: 761-70.

[103] Masterman CJ, Viscusi WK. The income elasticity of global values of a statistical life: stated preference evidence. *Journal of Benefit-Cost Analysis* 2018; **9**: 407-34.

[104] U S Department of Transportation. Departmental Guidance on Valuation of a Statistical Life in Economic Analysis; 2025. Available from: https://www.transportation.gov/office-policy/transportation-policy/revised-departmental-guidance-on-valuation-of-a-statistical-life-in-economic-analysis.

[105] Yarrow N, Masood E, Afkar R. Estimates of COVID-19 impacts on learning and earning in Indonesia: How to turn the tide. World Bank, Washington, DC; 2020.

[106] National Economic and Development Authority. COVID-19 Pandemic to Cost PHP 41.4T for the Next 40 Years. *Technical Report* 2021.

[107] Psacharopoulos G, Collis V, Patrinos HA, Vegas E. The COVID-19 cost of school closures in earnings and income across the world. *Comparative Education Review* 2021; **65**: 271-87.

[108] National Audit Office. Education Recovery in Schools in England. *Technical Report* 2023.

[109] de Bruijn AG, Meeter M. Catching up after COVID-19: do school programs for remediating pandemic-related learning loss work? In: Frontiers in Education. vol. 8 Frontiers Media SA; 2023. p. 1298171.

[110] Gupte P, Doohan P, Johnson R, et al.. daedalus: Model Health, Social, and Economic Costs of a Pandemic;. Available from: https://github.com/jameel-institute/daedalus.

[111] Mears D, Gupte P, Russell E, et al.. DAEDALUS Explore; 2025. Available from: https://daedalus.jameel-institute.org/.